Evaluation of the feasibility of a managed aquifer recharge through irrigation canals in the Lower Diguillín River basin, Chile

By

Luis Alegría Olivera

Thesis
Submitted to Flinders University
for the degree of Master of Science (Groundwater Hydrology)

Master of Science (Groundwater Hydrology)

Flinders University

5th July 2022

Table of Contents

Abstract

One of the many sustainable management practices of water resources is the so-called managed aquifer recharge (MAR) method. This technique, apart from injecting water into the system, includes a variety of short-term and long-term benefits for the community. Globally, a series of real case studies have been carried out to evaluate the efficiency of MAR techniques, however in Chile it is still relatively unknown to ordinary people. An efficient MAR design consists of maximizing the storage gain with the least amount of injected water and minimize the losses through downstream discharge. Within the methodologies to develop a MAR, there is the recharge through irrigation canals, where Chile comes to play a fundamental role due to its extensive portfolio of unlined canals for agricultural purposes. In this study, different MAR designs were examined using the irrigation canals at the Lower Diguillín River Basin (LDRB) located at Southcentral Chile, through the construction of a numerical model using Flopy (MODFLOW) and the processing of water balance outcomes of the shallow aquifer for each established scenario, with the objective of defining the most efficient MAR design for the LDRB. As a result, it is obtained that the maximum annual volume of an efficient recharge lies between $5x10^5$ m^3 and $9x10^5$ m^3, which represents around 2.5% and 11.2% of the total annual inflows for the same period.

Declaration

I certify that this thesis does not incorporate without acknowledgment any material previously submitted for a degree or diploma in any university; and that to the best of my knowledge and belief it does not contain any material previously published or written by another person except where due reference is made in the text.

Signed.....Luis Alegría Olivera.....

Date.....03 Jul 2022.....

Acknowledgements

First, I would like to thank to my family for their constant support in my personal decisions and for being the spark that keeps me constantly awake.

Secondly, I am going to share my thanks to the two main professors involved, who have supported me during this stage, either constantly or diffusely, in person or by video call, in English or Spanish. These two characters would be at first my thesis supervisor, Okke Batelaan, who has been constantly supporting and guiding me during the preparation of this work. And second, but not least, thank to Jose Luis Arumí for his disposition and motivation towards this project, who also gave me the pass to be a part of it.

Of course, I must give my sincere thanks to Flinders University and all its faculty, for giving me the opportunity to enter their house of study and fulfill one of my dreams since I started focusing my studies on Earth Sciences. This whole stage has been a tremendous personal experience, that has led me to learn and know fundamental aspects for my personal development and has also given me the motivation to continue along the same line of study.

Finally, I would like to thank everyone who supported me directly or indirectly at this stage, whether it be my girlfriend, colleagues, friends, distant relatives, pets, neighbours, unknown people, and all those who have given me good vibes.

List of Figures

List of Tables

1 INTRODUCTION

According to recent climate projections, it is known that central-southern Chile is considered a hot spot for having future water security issues (Prudhomme et al., 2017) and its facing the most prolonged sequence of dry years since 2010, known as the Mega Drought (Garreaud et al., 2017), which reveals a rainfall decrease of about 20 to 40% influenced by both climate change and anthropogenic factors (Boisier et al., 2016; Garreaud et al., 2017, 2020). In addition, temperature is sightly increasing towards the north, in about 3-4°C above the historical baseline (Vicuña et al., 2011). These changes are even more intensified when groundwater recharge and streamflows depend on snow melting during dry season (Barnett et al., 2005).

In Chile, the economy is based on extracting natural resources to mainly market them abroad, being water one of the major ones due to the previous Water Code that remained in place until 2021, allowing this resource to be treated as an economic good (Donoso, 2006). Today, there is a new water code, released in 2022, that puts the prioritisation of human water consumption and sanitation, effective water use, and conservation of water resources at the forefront. Even so, the balanced management of this resource remains an issue that needs to be addressed.

Since agriculture acts as the major water consumptive industry, representing around 80% of the total freshwater consumption from the extraction of both surface and groundwater sources (DGA, 2016), it plays a fundamental role in the territory. Although it is known that nations practicing agriculture as their main industry are widely affected by drought due to its high sensitivity to climate variations (Howden et al., 2007), there are different solutions to reduce the impacts associated with this, either by implementing technology to increase irrigation efficiency (Pfeiffer et al., 2014) or by going directly to the availability and well driven administration of the natural resource.

One of the many sustainable management practices of water resources is the so-called managed aquifer recharge (MAR) method, which, beyond the basic concept of introducing intentionally more water than would naturally occur into the subsurface for further recovery and favourable use (Dillon, 2005), it includes a variety of benefits both short- and long-term, as well as a wide range of implementation methods that have already been tested in real case studies at different geographical locations worldwide, and therefore, in different climatic, geological and social conditions (Bonilla Valverde et al., 2018; Dillon et al., 2020; Sprenger et al., 2017).

In Chile, MAR has not been widely implemented yet and to date it is still unknown to most water users, however, there has been a progressive interest from the scientific community and public institutions in educating the population and in developing risk-based guidelines to assess groundwater users (Page et al., 2020), in order to reduce uncertainties and rapidly promote the use of these measures that ensure sustainable groundwater management and increase national water security over time (Dillon et al., 2020).

Given the decline in surface water flows and groundwater levels throughout the studied area, the most affected have been low-income farmers who generally sustain their economy by pumping the shallow aquifer, especially during summer season. From this, the National Commission of Irrigation (CNR, based on its initials in Spanish) in conjunction with the local water user communities have decided to start a detailed work of the basin and its response to MAR, giving rise to this investigation in parallel, which has different scopes and limitations, but use the same available information.

This study will focus on the lower area of the Diguillín River basin (LDRB), which represents a common agricultural site with a wide range of irrigation unlined canals. These canals have already been tested since 2012 onwards by the CNR for MAR during winter seasons, but there is still no detailed study of the effectiveness of this technique and quantification of recharge in space and time. One of the most usual mechanisms to quantify water systems and predict different scenarios when a new management practice is established is by carrying out numerical models so that both the feasibility and the optimal design for its implementation can be assisted, in such a way that short- and long-term consequences on groundwater supply, groundwater-dependent ecosystems and aquifer sustainability can be assess (Kourakos et al., 2019).

Currently there are different types of software to generate numerical models and work with their results. In general, the industry uses Graphical User Interfaces (GUI's) to design, modify, run and post-process a MODFLOW model (Harbaugh, 2005) because they are very intuitive to work with. However, this study follows another path to develop a numerical model, which is by working directly with the MODFLOW input and output scripts, programmatically, using a Python package called FloPy (Bakker et al., 2016). This tool may be more cumbersome and archaic in the first instance, but in the long run it has many benefits, it is very powerful and has a greater degree of flexibility while working with complex models.

2 HYPOTHESIS

The execution of a managed aquifer recharge (MAR) through irrigation canals in the Lower Diguillin River basin (LDRB) is feasible as long as there is complete control over the activation time of these canals and the areas to be activated. Otherwise, there is a risk of generating potential groundwater outcrops in sites where the piezometric level is close enough to the surface and, in addition, without careful management of these irrigation canals, it is likely that the water infiltrated into the subsoil will not accumulate in the shallow aquifer but will be discharged downstream towards the Itata river.

3 OBJECTIVE

The main objective of this study is to determine whether the implementation of a MAR through irrigation canals is feasible or not, given the hydrogeological conditions of the Lower Diguillín River basin.

3.1 Specific objectives

To achieve the main objective, the following specific objectives are being proposed.

- Elaborate a conceptual model of the groundwater system at the Lower Diguillín River basin
  - Use available background information.
  - Define geological units, boundary conditions, aquifer layers and groundwater flow.
  - Determine groundwater outcrop zones.
  - Determine groundwater recharge sources of the basin
- Stablish the water balance of the groundwater system
  - Estimate direct recharge
  - Estimate water balance using MODFLOW (FloPy)
- Estimate the maximum feasible volume of annual recharge introduced into the shallow aquifer
  - Assess the aquifer response to different MAR scenarios.
  - Analyse the water balance at different sites of interest to identify potential impacts.

4 BACKGROUND INFORMATION

The information available to carry out this study includes public and private reports from previous years, provided by the National Irrigation Commission, where the hydrogeological characterization is described at different scales than the one needed for this project, using both regional and local extensions, with different scopes and objectives. Despite this limitation, these reports allow a good understanding and conceptualization of the groundwater and surface water system in the LDRB area. The main results to be used in this work are indicated below.

HYDROGEOLOGICAL STUDY OF THE ITATA RIVER BASIN, AQUATERRA INGENIEROS LIMITADA (DECEMBER 2011).

The main objective of this work is the development of a conceptual hydrogeological model of the aquifer system in the Itata river basin. It incorporates a description of each hydrogeological unit of the basin based on surface geology and geomorphology, stratigraphic information from 286 well profiles and a geophysical survey with 353 gravimetric stations located along 9 surface profiles. The domain of a large hydrogeological unit with horizontal and vertical variations in its permeability is proposed, defining two sub-units. Given the type of sedimentary deposits present in the area, permeability is subject to variations from medium to low. According to the geophysical method used, the basement depths vary between 500 to 1000 m in the central zone, but they propose a more exhaustive and accurate analysis to get reliable information.

In addition, this report includes a water table contour map generated from the measurement of 204 static levels carried out during August 2011 in deep wells distributed along the studied area. Some of these wells were also used to analyse stratigraphic profiles and recorded pumping tests to get information on hydraulic properties of the aquifer (s) involved. Also, this was used to define areas of groundwater-surface water interaction.

There is also a compilation of data from 26 pluviometric stations and 17 fluviometric stations distributed throughout the area, with monthly variations dated for period 1941/42 - 2010/11. This information was analysed based on their length and quality, to later fill in the missing information by using basic statistics. Regarding the diffuse recharge used in this work, they propose a value of 0.27 l/s/ha based on a simplified hydrologic simulation using irrigation zones, superficial water flux, dams and pumping wells. Finally, this work includes an evaluation of water use over time based on the water rights of consumers.

HYDROGEOLOGICAL STUDY OF GROUNDWATER AVAILABILITY IN SOUTHEAST AREA OF BULNES, GFC INGENIEROS CONSULTORES LTDA (SEPTEMBER 2013).

This study comprises a hydrogeological characterization of a site located 14 km south of the city of Bulnes, to determine if there is sufficient availability of groundwater to install a natural gas combined cycle thermoelectric plant. This report describes the local geology of the area, the

compilation of information obtained from 29 deep wells, including static levels and extraction flows. In addition, there is information on granted water rights, stratigraphic description of wells, transmissivity analysis of the aquifer, estimation of the potential specific storage within the aquifer and a geophysical study using the electromagnetic transient method (TEM, based on its initials in Spanish) to define the basement depth.

The interpretation of the geophysical study indicates that the basement is located between 129 m and 206 m depth, underlying a sedimentary package formed by layers of different granulometry, composed of gravel, sand and clay. Apart from the collected information, 2 deep wells were carried out, including pumping tests to estimate hydraulic properties of the aquifer and hydro-stratigraphic descriptions.

CONCEPTUAL AND NUMERICAL MODEL FOR EXTRACTION OPTIMIZATION AND LONG-TERM AWARENESS, GEOHIDROLOGÍA CONSULTORES (MARCH 2014).

This study includes the hydrogeological characterization carried out in the previous report, but also including the conceptualization of the water system and implementation of a numerical model using MODFLOW-USG code and Groundwater Vistas 6 platform to process the output files.

It provides an analysis of the transmissivity of the aquifer, using information described by Aquaterra (2011) and data collected from pumping tests in deep drilled wells. In addition to this, there is a hydraulic conductivity estimation based on the type of sediments and hydrogeological units. Also, hydrochemical and isotopic measurements on main rivers, streams and groundwater were applied to characterize the nature of available water. In general, samples show that there is a predominant bicarbonate Ca-Na and bicarbonate Ca-Mg type of water around the studied area, either in surface or subsurface.

Monthly precipitation and streamflow were updated until 2013 with public information from the General Water Directorate (DGA, based on its initials in Spanish) stations. Regarding water consumption in the area, previous works were reviewed and updated, linking databases with water rights granted by the DGA. Out of a total of 120 wells observed, the total flow granted corresponds to 1,463 l/s, to which a factor was assigned depending on the type of use given to the resource, finally leaving a total consumption of 530 l/s in the studied area.

This work includes an estimate of surface recharge, which involves percolation by excess irrigation, percolation by precipitation, infiltration from irrigation channels and from natural watercourses. For this, a simplified hydrological model was applied, including a mass balance in different irrigation sectors based on irrigation demands, precipitation and irrigation flow rights. Also, the report includes a lateral recharge and discharge analysis, based on the Darcy’s law applied to the edges of the studied area.

The calibration of the numerical model developed in this report is based on a manual process of trial and error, but also using PEST (Doherty, 2005) estimator to adjust hydraulic conductivity values. This section includes a verification of the model's mass balance error, the residual statistics, the simulated water levels and flows versus the observed ones, and finally a comparison between water contour lines obtained in the present study to those delivered by Aquaterra in 2011.

ANALYSIS AND APPLICATION OF THE AQUIFER DELIMITATION AND SECTORIZATION METHODOLOGY IN THE ÑUBLE PROVINCE, VIII REGION, SUBTERRANEA SPA (OCTOBER 2015).

This project is composed of two stages, in the first the methodology imposed by the S.I.T N ° 341 study is examined in detail, relevant information is compiled exhaustively, the methodology is applied detailing each procedure and the areas of the geophysical campaign are shown. The second stage consists of implementing geophysical prospection to define different aquifer layers more precisely. 81 TEM stations and 141 gravimetric stations were performed where the interpreted results indicate that the shallow unsaturated zone has an approximate thickness of 40 m and resistivity values between 30 to 400 ohm-m, indicating the presence of gravel, clay and sand deposits with variations in saturation. In addition, there is a main aquifer with resistivity values ranging between 5 and 60 ohm-m, composed of clastic deposits, sands and clays. This aquifer is subject to permeability variations and confining variations depending on the overlaying layer. Finally, the impermeable basement is interpreted when values of resistivity are higher than 500 ohm-m, reaching maximum depths of 500 m.

DIAGNOSIS OF AQUIFER RECHARGE THROUGH CANALS, DIGUILLÍN RIVER, CON POTENCIAL CONSULTORES (APRIL 2021)

This work consists of the diagnosis of aquifer recharge through channels in the Diguillín River in collaboration with the National Irrigation Commission. It includes the presentation of field work, analysis and results, and the guidelines for future activities related to further steps to evaluate the MAR project.

The most relevant information obtained from this report are the permeability tests performed on the surface soil, which can be correlated to the hydraulic properties of the irrigation canals. The rest of the information gathered in this study is related to other scopes, therefore, it is discarded to elaborate the conceptual hydrogeological model.

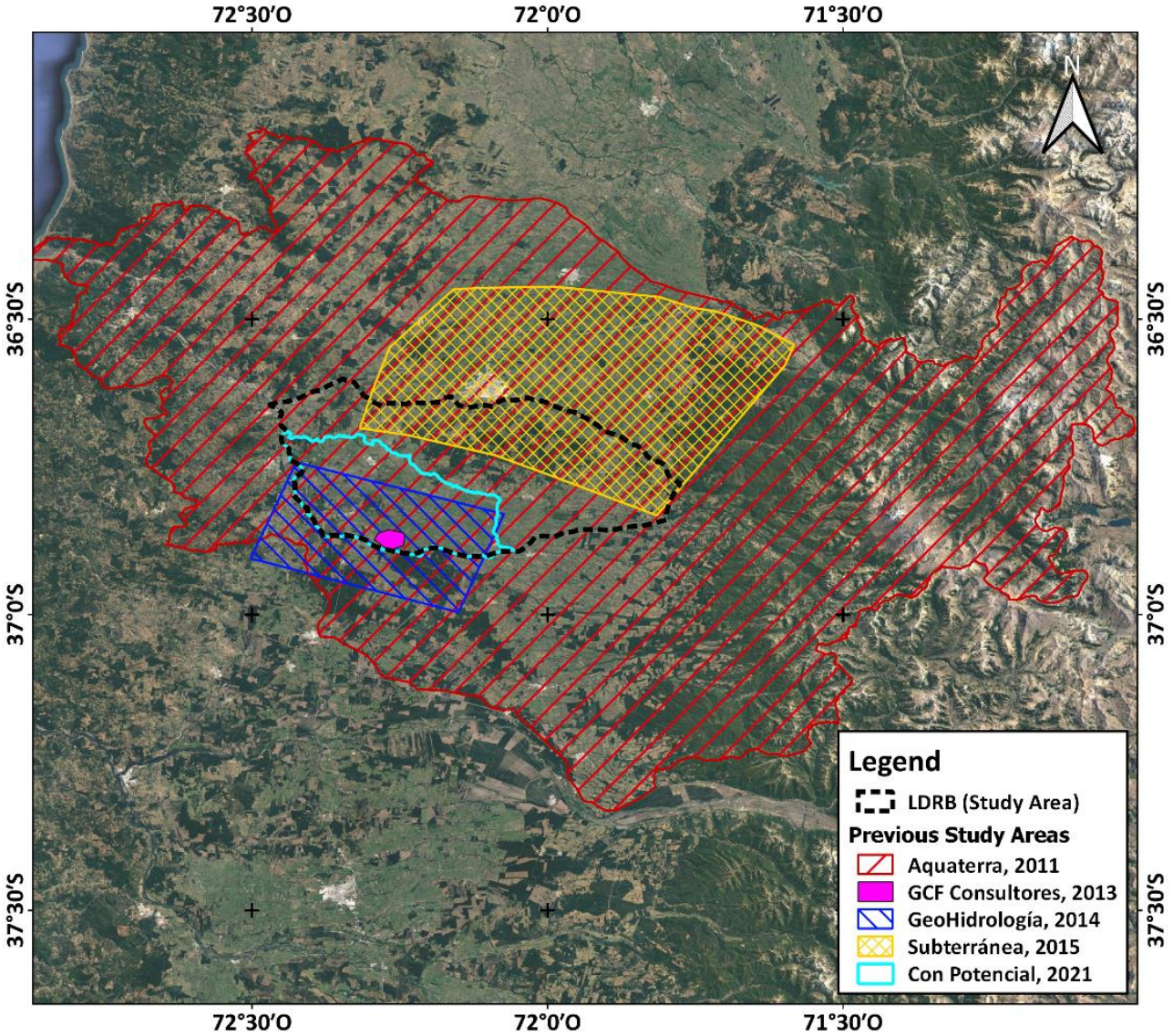

Figure 4-1 Previous studies location

5 Conceptualisation

5.1 The study area

The study area is located between 36°30'S, 37°00'S and 71°30'W, 72°30'W in Central Chile, involving several sub-sub basins of the Itata River regional basin. The Itata River basin is the largest water system of the region and like most of these in this area, it begins to the east, on the southwestern slopes of the Nevados de Chillán volcanic complex, where processes such as snow-melting, mountain-block recharge, geothermal springs contribution and groundwater-surface water interactions occur. These processes have been outlined by different authors in detail (Arumí, 2014; Markovich et al., 2019; Muñoz et al., 2016; Zúñiga et al., 2012), but remains an overly broad and complex focus of study.

Downward of the eastern main mountain range, towards the Pacific Ocean, the basin enters the geomorphological unit called Central Depression, into an area with a homogeneous slope, until it meets the Itata River, remarkably close to the Cordillera de la Costa Mountain range, which acts as a hydraulic barrier in a regional scale. The flat area of the basin, where this project is being developed, comprises most of the agricultural zone in the region due to its topographic, geologic and hydrogeologic conditions, which in this case are favourable for the extraction of both surface and groundwater.

The study area is located near the city of Bulnes, approximately 70 km east of the city of Concepción and 30 km southwest of the city of Chillán. It comprises a surface of 1400 km^2, with approximately 60 km long (east to west direction) and 30 km wide (north-south direction), limited to the west by the Itata river, to the south by the Diguillín river and to the north by the Chillán river. Hereafter, for simplicity, the study area will be referred to as LDRB, representing the initials for the "Lower Diguillín River basin".

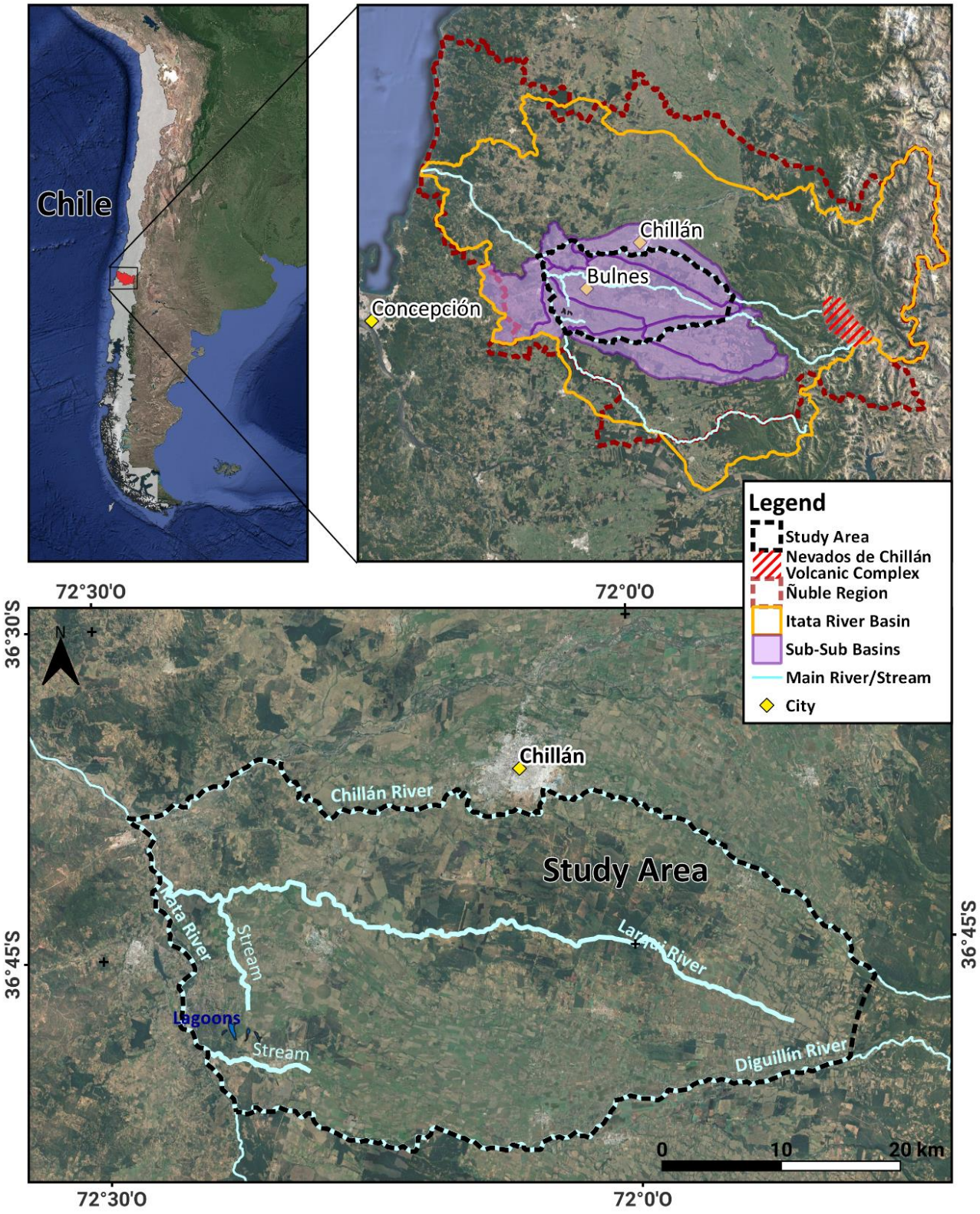

Figure 5-1 Study area

5.2 Geomorphology

The LDRB is in the geomorphological unit called Central Depression, which is bounded to the east by the Andes Mountains and to the west by the Coastal Mountains. These regional units are mostly distributed in a N-S direction along the country, with the highest elevation occurring in the Andes mountains, being this a snow accumulation point during winter and usually where the main rivers begin to flow.

The Central Depression is considered a regional sedimentary basin filled up with materials coming from the erosion of the Andes and Coastal Mountains. It consists of a wide plain with about 150 m asl of average height, characterized by presenting an undulated surface with rivers channelled in sectors of greater depth. The maximum range of this unit around the studied area is 40 km, where it has a gentle slope towards the west.

5.3 Geology

The subsurface geology of the LDRB consists mainly of unconsolidated continental (fluvial, fluvioglacial, glacial and lake) deposits ranging ages from the Pliocene to the Holocene, associated to La Montaña and Mininco Formations, respectively, as well as current fluvial deposits (Gajardo, 1981). In addition, to the west there is a massive intrusive rock of tonalite-granodiorite composition from the Paleozoic, outcropping through a regional inferred fault with NNW trend. These intrusive rocks are part of the Coastal Mountains and belong to the Coastal Batholith described by Hervé (1977). Towards the east, the study area is limited by the outcropping volcano-sedimentary rocks raised in the foothills, which are in contact with the rocks of the Mininco formation.

Despite not being strictly in the study area, it is important to mention the Volcanic Complex Nevados de Chillán, because most of the rocks present in the region are the result of the volcanic activity of this complex throughout history.

5.3.1 Rock units

5.3.1.1 La Montaña Formation (Pleistocene - - Holocene)

This unit was first defined by Muñoz Cristi in 1960 as the "Tills of La Montaña Formation". It is made up of a series of morrenic and alluvial deposits of little compaction and uniform composition, represented by lenticular banks of clays and unconsolidated fine sands, with red to reddish-brown and chaotic in shape. It contains fragments of basaltic and granitic volcanic rocks, of different degrees of rounding and in different states of alteration. The size of these sediments varies between 7 to 40 cm in average diameter, existing in some areas particles of up to 5 m.

In this sedimentary set there are intercalations of volcanic ash well stratified, which would correspond to lagoon deposits. The age of this unit has been assigned to the Quaternary.

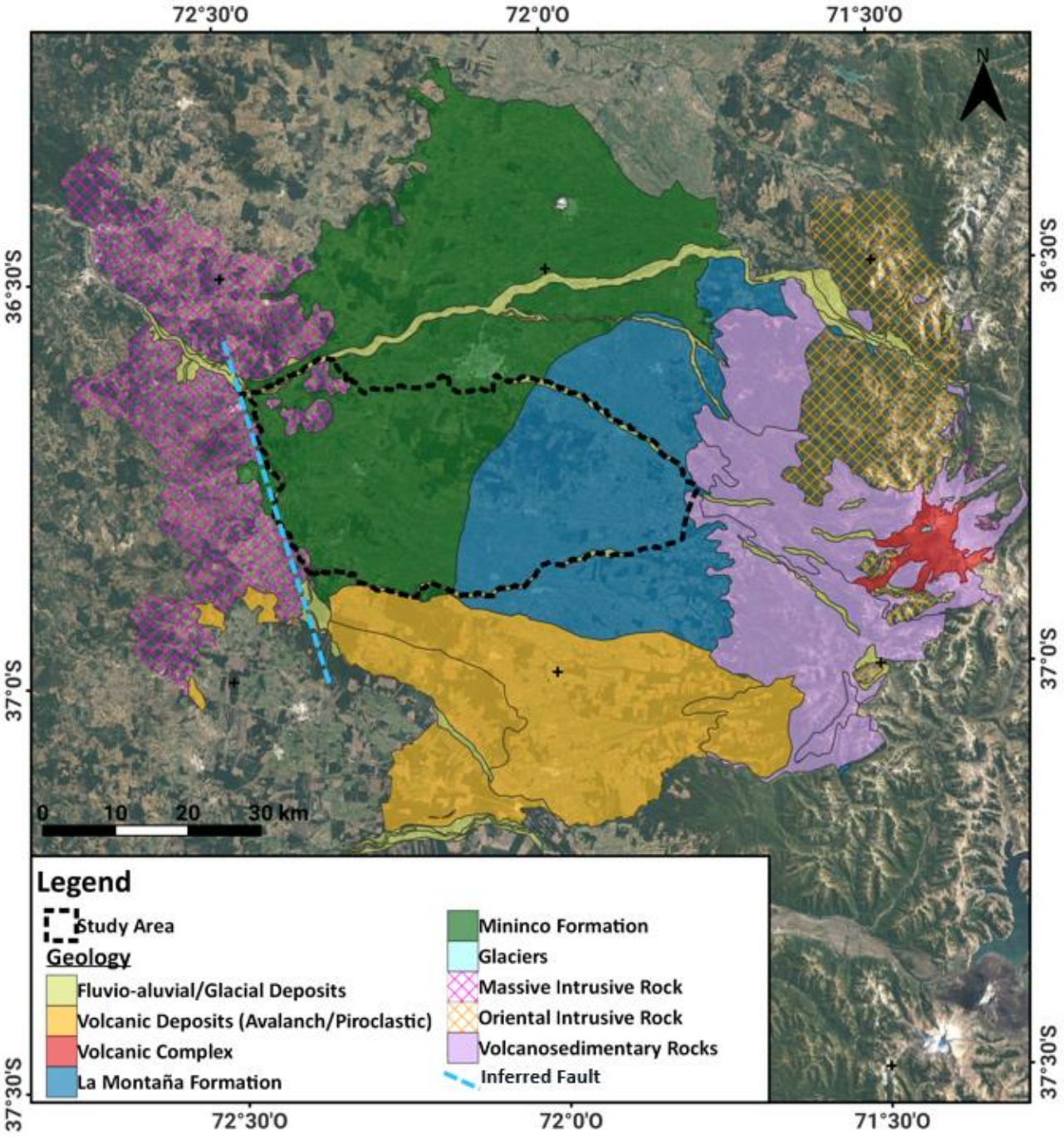

Figure 5-2 Geological Map

5.3.1.2 Mininco Formation (Pliocene – Quaternary)

This unit was also defined by Muñoz Cristi in 1960. It is distributed in the Central Depression and its major outcrops are observed in the valleys of the rivers and estuaries, or currently in anthropogenic cuts made by roads, paths, or railways. It comprises lagoon and fluvial sediments, represented by tobaceous sandstones, limolites and conglomerates, with intercalations of clays and tuffs. The contribution is mainly andesitic in the sandstones, also finding ashes in the matrix.

The age of this unit has been assigned to the Quaternary, but sedimentation might have started during the Pliocene.

5.3.1.3 Stratovolcanoes and volcanic complexes

In the Ñuble region, this unit is represented by the Nevados de Chillán Volcanic Complex, which is composed of black to gray-reddish slag-type andesitic lava flows and andesitic-basaltic lava. It includes a series of inactive slag volcanic cones composed of porphytic andesitic lava with pumps and lapilli, from Pleistocene to Holocene age, plus an active cone that is frequently pulling fine pyroclastic material outward.

5.3.2 Non-consolidated deposits

5.3.2.1 Colluvial deposits

These deposits are located on the edges of steeply sloping hills, mostly without vegetation, distributed along the valleys of glacial origin. Sediments of colluvial origin are very immature and are usually composed by monomictic and angular fragments of rocks, coming from the highest parts of the hills. These sediments have irregular fan shapes due to the collapse of the hill, produced by gravitational instability or saturation of water. In general, these sediments constitute key areas where rainfall can infiltrate the soil, thus allowing the storage of a large amount of water depending on the size and wideness of the deposits.

5.3.2.2 Fuvio - Alluvial deposits

These deposits include non-consolidated material represented by blocks, gravels and sands, constituting the main filling of rivers and streams. They can be rather current or old, differing by the location and activity of the respective channels. In general, the permeability of these sediments ranges in the order of 1 m/day.

5.3.2.3 Pyroclastic deposits

These deposits are usually associated with lake deposits where they mix with clayed sands. They usually form terraced levels of sediments. In this case, this type of deposit is associated with the volcanic activity of the Nevados de Chillán complex throughout its active period.

5.3.2.4 Glaciers, Tills, Fluvio-glaciers and Lake-glaciers deposits

The materials that make up these deposits are well stratified, poorly selected and immature, with clasts of block size, gravel and sands, encompassed in a sandy-clayed matrix.

Fluvio-glacial deposits usually form multiple levels of discontinuous terraces on the banks of the main water channels, attached to the slopes of the valleys, allowing a good development of soil and vegetation, which is usually used for agriculture, livestock or for the implementation of houses and towns.

Deposits of glacial origin are partially dismembered by erosion and covered by river deposits. Major moraines can be observed, associated with an ancient glaciation, while small moraines are

associated to current glaciers, which usually cover the high peaks of the main mountains or volcanoes.

Till deposits of more than 100 m of thickness characterize the area, giving a typical morphology of soft hills, composed of clastic angular volcanic material lying in a sandy matrix of yellowish gray and reddish colors. These deposits relate to the last glacial period or during its retreat stage.

5.3.3 Structures

The main regional structure recognized in the study area is the NNW trending fault that allows the rise of the Coastal Mountain Range, just on the western edge of the LDRB, established as the domain for this project. This structure along with others of similar characteristics in the surrounding regions, are responsible for the large sedimentary accumulations that exist to the east of the Coastal Mountain Range, causing rivers, such as the Itata, to make their way through notoriously narrow valleys.

5.4 Hydrogeology

This chapter includes the hydrogeological characterization of the study area, where the definition of the hydrogeological units is presented, an estimate of precipitations, evapotranspiration and direct recharge is delivered, the hydraulic properties obtained from pumping tests, the characteristic piezometric curves of the area and the main direction of the groundwater flow, pumping extraction flows, surface and groundwater level fluctuations and the interaction between these two.

5.4.1 Hydro-stratigraphic units

The sedimentary aquifer system of the LDRB is build up by a complex arrangement of Pliocene and Holocene age sediments with a total thickness that reaches about 250 meters in some areas. Even though there is limited information about the extension and distribution of this aquifer system and its local variations in the type of sediment present, there are studies and previous reports that help to understand the system, which will be detailed below.

Based on the stratigraphic description of some deep wells drilled up to a maximum depth of 100 meters, GFC Consultores (2013) defines two main hydrogeological formations, the first and shallow formation has an approximate thickness of 30 meters, originated from fluvial sediments consisting in pebbles, gravels, sands and a significant number of clays. At greater depth, a sedimentary stratum is described with coarser particles and intercalations of fines in a smaller proportion. As a complement, using the Electromagnetic Transient geophysics method (TEM), GFC Consultores (2013) also points out that the deep aquifer could reach depths much bigger than those already evaluated, of up to 200 meters.

Another similar characterization occurs in Aquaterra (2011), where they define the existence of a large aquifer unit in the region, of phreatic type and variations in its degree of permeability. Using geophysical information obtained from a gravimetric method, the authors propose that the basal rock is located at depths of up to 1000 meters, however, not necessarily the aquifers of the area reach this depth, because there is a higher clay content in depth that limit the existence of usable hydrogeological units.

Moreover, there is information gathered in field which allows to establish the presence of an impermeable layer constituted by volcanic tuff in the northern part of the study area, which keeps the two main aquifers disconnected and generates certain degrees of confinement along the area, where deep wells have been drilled.

Considering the above and the scope of this study, the site where the MAR project will be carried out has 2 main hydro-stratigraphic units, limited by a third one that has less hydrogeological information available, but is recognised as acting as a hydraulic barrier of very low permeability. The shallow and top unit consists of a 20 meters thickness layer with medium to high

permeabilities and a spatial continuity that covers the entire study area. The deeper unit has a thickness of about 200 meters, also distributed continuously in the study area and reporting medium to low permeability compared to the top unit. However, the groundwater yield of this aquifer is much higher than the yield observed for the shallow aquifer. Finally, the unit that separates the two aforementioned units has approximately 5 metres thickness and an extremely low permeability acting as an aquitard.

Given the lack of information within the study area, there is a high uncertainty regarding the connection between the two main aquifers in the complete extension of the LDRB but considering the principle of simplicity defined by Barnet (2012), it is established that the top aquifer is unconfined to its full extent, and the deeper aquifer and aquitard are completely confined.

5.4.2 Rainfall

The LDRB is under the influence of a Mediterranean climate and has at least two months of dry weather with water deficit. Humidity conditions are high in winter, but in summer it decreases considerably (Aquaterra, 2011). The study area is characterized by a high climatic variability between the summer and winter period; however, these variations have been exacerbated in the last decade due to Climate Change (Vicuña et al., 2011) and the so-called Mega Drought (Garreaud et al., 2020).

To characterize the most representative precipitation series of the study area, the nearest meteorological stations of the DGA (General Directorate of Water) were used. In total, 6 meteorological stations were chosen, of which only the Chillán Viejo station presents a complete record from 1980 to 2020. The gaps observed in the rest of the stations were completed using the meteorological estimator that best fits the observed data. To select the most accurate estimator for the area, the simulated values of each estimator were compared with the observed data for each meteorological station separately. The result of this analysis is shown in Table 5-1 and the description of the most accurate estimators for this area is detailed below.

- **CR2MET v2**: Product developed by researchers from the Science Centre of Climate and Resilience (CR)2 (Boisier et al., 2018), based on data from atmospheric reanalysis and local topography and pluviometry data.
- **RF-MEP v2**: Product developed especially for Chile through the application of the Random Forest based MErging Procedure algorithm (Baez-Villanueva et al., 2020). This algorithm allows merging gridded precipitation products with precipitation measurements in pluviometers and topography data

Table 5-1 Pearson correlation coefficient for meteorological estimators.

	Pearson Coefficient				
Estimator / Station	Diguillín	Chillancito	Mayulermo	Nueva Aldea	Pemuco
CR2MET_v2	0,98	0,96	0,98	0,97	0,96
RFMEP_v2	0,99	0,98	0,98	0,98	0,98
ERA5	0,97	0,96	0,97	0,97	0,96
CHIRPS_v2	0,93	0,92	0,93	0,92	0,92

From Table 5-1 we can see that the best correlation occurs with estimator RFMEP_v2. Given that this estimator does not have simulated values for the first ten years of analysis, the gaps of information in the Mayulermo station during the first ten years were filled with CR2MET_v2, which has the second-best correlation, and the rest of the missing data was filled by using the simulated values of RFMEP_v2.

Figure 5-3 shows the rainfall time series obtained by averaging the filled data of the 6 meteorological stations and compares it with the simulated values of CR2MET_v2 and RFMEP_v2. The average annual rainfall using the monthly average series is 1279 mm.

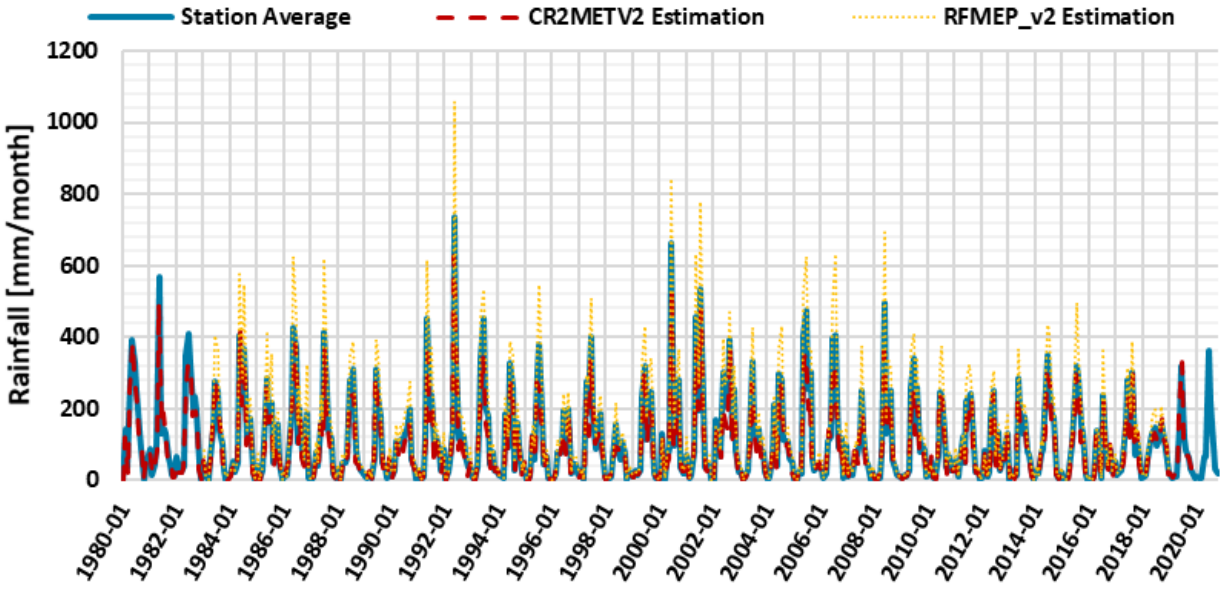

Figure 5-3 Monthly time-series of rainfall.

5.4.3 Evapotranspiration

There are no specific studies estimating evapotranspiration in the study area, however, given the dense vegetative cover, high temperatures during summer and the extensive land use for agriculture and monocultures across the area, it is expected that this value covers a large part of the water balance in the LDRB.

This document will follow the procedure proposed by the FAO Irrigation and drainage paper 56 (Allen et al., 1998), to calculate reference and crop evapotranspiration from meteorological data and crop coefficients.

5.4.3.1 Reference evapotranspiration (rET)

Over the last decades, different methodologies proposed by a wide range of scientists and specialists have emerged to estimate reference evapotranspiration, however, the method that is currently recommended as sole standard is the FAO Penman-Monteith method, due to its great ability to predict rET in different places and climates, as well as allowing its application when there is scarce information.

Reference evapotranspiration refers to the rate of evapotranspiration from a reference surface that contains unlimited availability of water to be eventually evaporated or transpired. Consequently, when there is low vegetative density, water is lost mainly by evaporation from the surface, while if there is dense vegetation, the surface is almost completely covered, so transpiration becomes the main process of water loss. This same effect occurs seasonally with the change in crop size.

Locally, estimates of reference evapotranspiration are available at the Centre for Climate and Resilience Research $(CR)^2$ website. These estimates are an average of 2 different sources of rET at a catchment-scale (Alvarez-Garreton et al., 2018):

- The first rET is based only on surface temperature data, and follows the formulae proposed by Hargreaves and Samani (1985), using CR2MET/Tmax and CR2MET/Tmin to generate a gridded rET estimate.
- The second rET data is obtained from the MODIS PET product (MOD16 collection 5; Mu et al., 2005), which includes leaf area index and fractional photo synthetically active radiation, land cover type 2, albedo, and daily meteorological reanalysis data. This is calculated following the Penman–Monteith approach (Howell and Evett, 2001).

From this, a reference evapotranspiration time series is obtained for a specific polygonal area. The closest polygon to the LDRB that can be selected in the $(CR)^2$ website represents the sub-catchment of the Larqui River (detailed in Figure 5-4). This covers a large part of the studied area and based on the parameters used to estimate the rET, it can be ensured that both the area within the estimated polygon and outside are closely the same, so it represents a good estimate for this study.

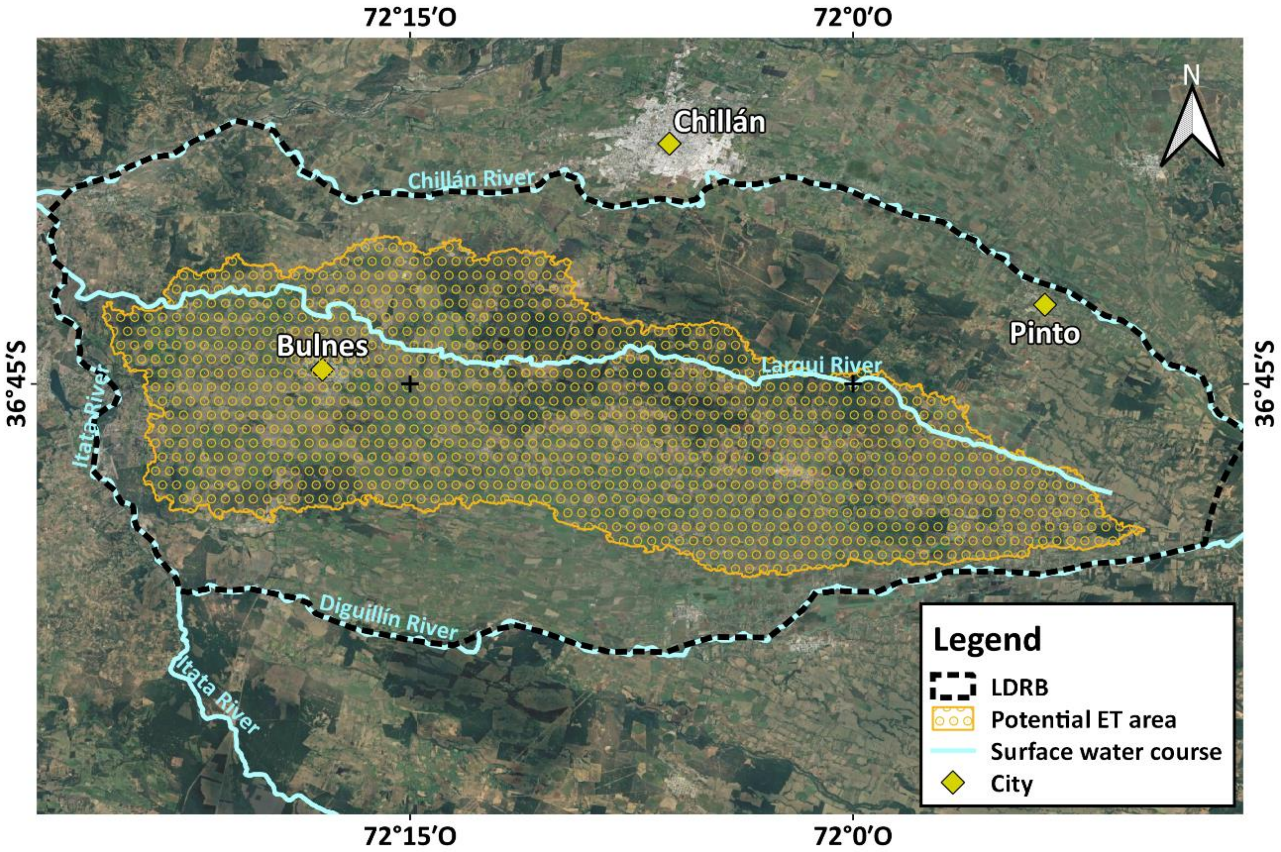

Figure 5-4 Reference (potential) evapotranspiration estimation area.

The following graph shows the monthly estimates of reference evapotranspiration assigned for the LDRB presenting values that vary between 40 and 200 mm approximately. The rET series is also cyclical, with the highest values occurring between November and March, while the lowest values occur during winter stage, between May and August. The average rET for the LDRB is 112 mm per month.

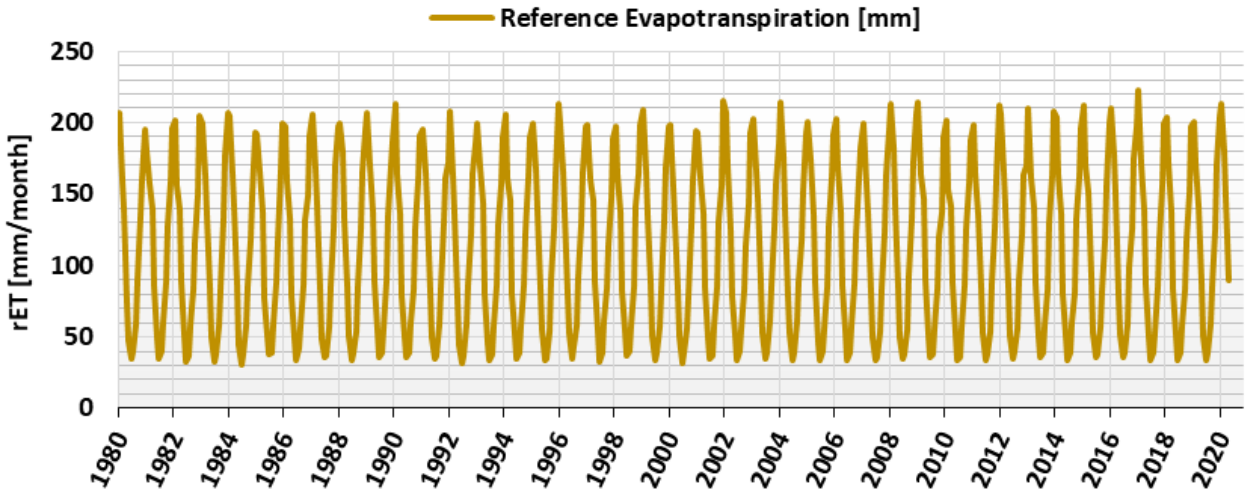

Figure 5-5 Monthly time-series of reference evapotranspiration.

5.4.3.2 Crop evapotranspiration cET

To adjust the monthly time series of reference evapotranspiration to more representative series of the study area, it is necessary to apply an appropriate crop coefficient to the LDRB. This crop coefficient (Kc) implicitly integrates the characteristics of the crops within the basin, differentiating them from the reference grass used for rET estimation. The 4 characteristics that are included in the coefficient have to do with crop height, albedo of the crop-soul surface, canopy resistance and evaporation from soil (Allen et al., 1998).

The way crop evapotranspiration is determined is by multiplying the representative crop coefficient by the reference evapotranspiration: cET = Kc x rET. In this case, the most common and abundant type of crops are cereals and alfalfa, and there is also a large area covered by exotic plantations of eucalyptus and pines (ODEPA/INE, 2019). According to the data of the FAO Guidelines and other studies (Allen et al., 1998; Alves et al., 2013), these types of crops have a total average value of Kc equal to 0,8.

To calculate the crop evapotranspiration of the LDRB, the reference evapotranspiration time series is multiplied by 0.75, resulting in the monthly time series of evapotranspiration shown in Figure 5-6.

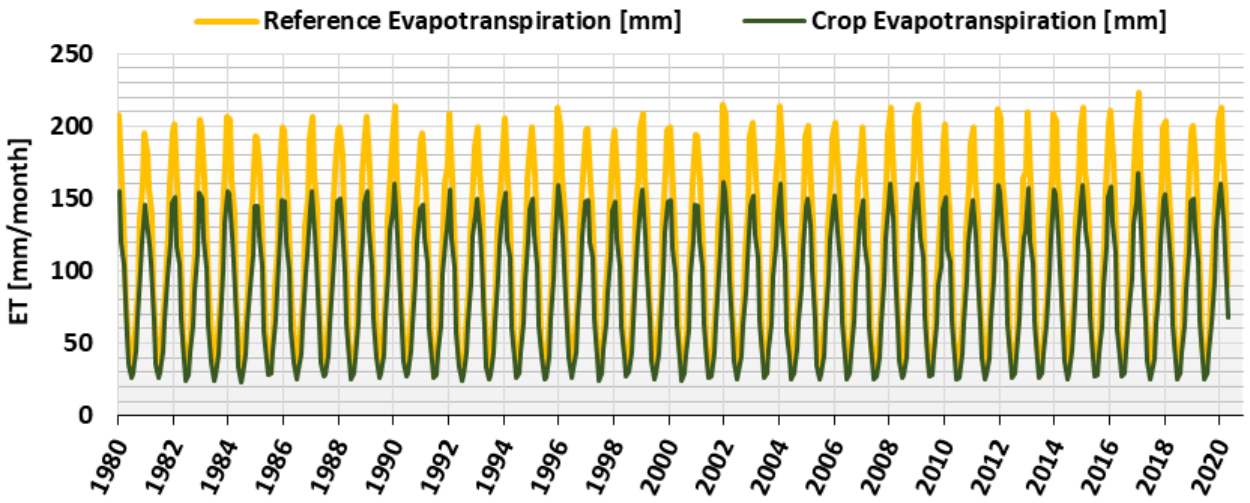

Figure 5-6 Monthly time-series of reference and crop evapotranspiration.

5.4.4 Distributed Recharge

Since there are no diligent works in the LDRB to estimate the distributed recharge produced by rainfall, this study estimates a monthly recharge series by means of a simplified water balance, using the series of precipitations occurring in the LDRB and the previously estimated evapotranspiration.

The methodology used is a simple difference between fallen rainfall along the basin and the calculated evapotranspiration: R = P – ET. The monthly recharge time series obtained from this balance is shown in the Figure 5-7. For comparison, this figure also shows the estimated recharge from a precipitation factor equal to 0.4.

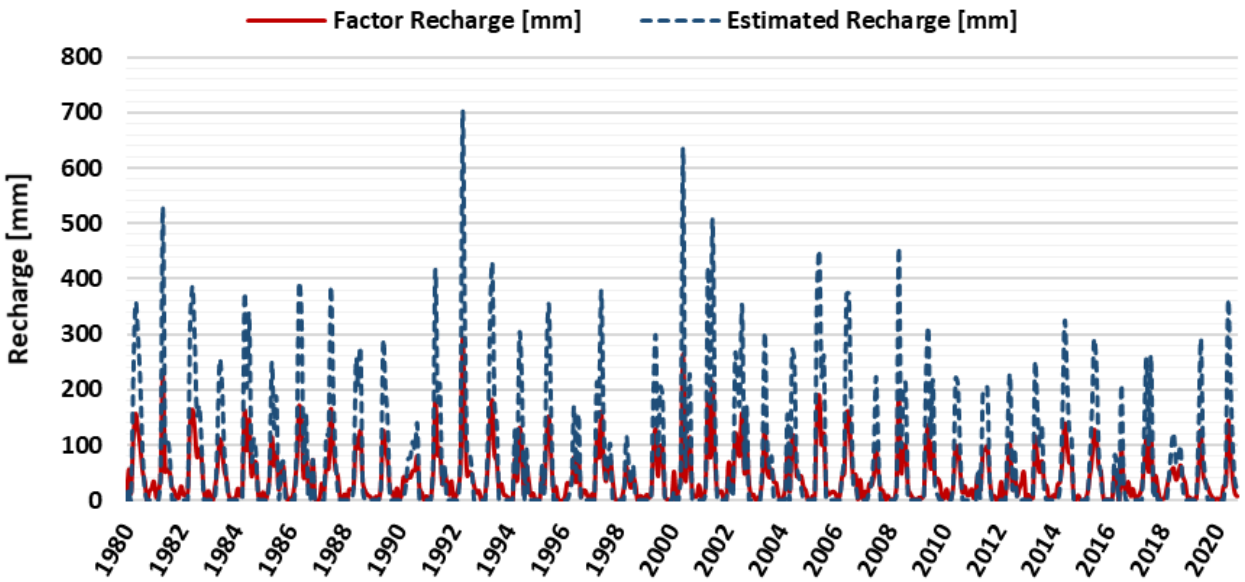

Figure 5-7 Monthly time-series of distributed recharge in LDRB.

5.4.5 Hydraulic properties

The most comprehensive overview of hydraulic properties within the aquifer system is provided by Aquaterra (2011) and Con Potencial (2021). The first gives a detailed description of the deeper aquifer, while the second delivers a more specific study about the shallow aquifer properties. In total, there are 87 hydraulic conductivity measures in the study area obtained from pumping tests and 21 obtained from surface infiltration methods. The pumping test points are located throughout the extent of the site and represent both the confined aquifer and the unconfined aquifer, while the infiltration tests points are specifically located in the south centre side of the LDRB, where most of the irrigation canals are placed.

Since these two methodologies for obtaining hydraulic conductivity values differ considerably, they will not be used together. Values of hydraulic conductivity estimated by pumping tests will be used to assign the hydraulic parameters of the different aquifers in the study area, while those estimated through Porchet infiltration tests will be used to assign a representative value of permeability to the impervious irrigation canals used for the application of MAR within the basin.

In the following figure we can see the spatial distribution of all hydraulic conductivity measuring points and the type of test from which they were interpreted

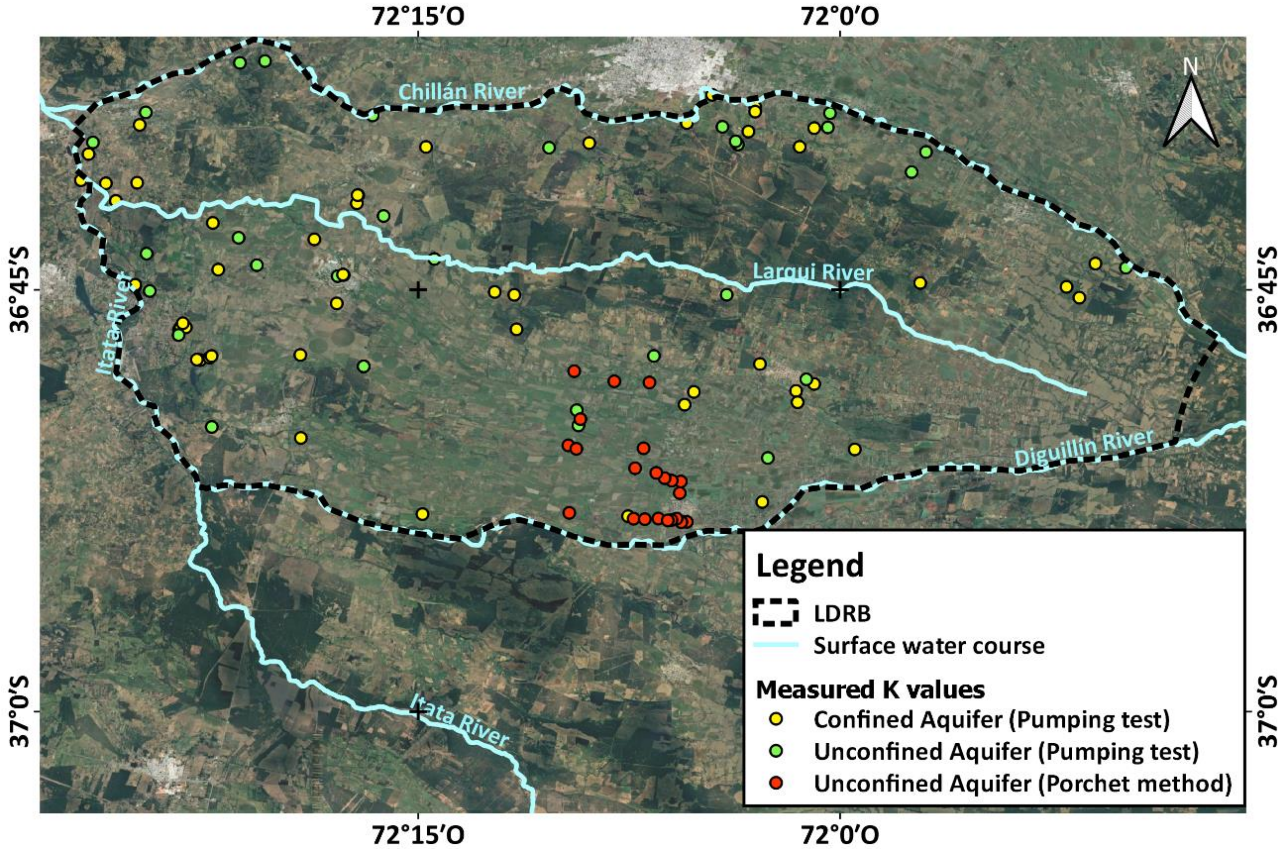

Figure 5-8 Hydraulic conductivity measured points.

Most measures are representing hydraulic conductivity of the deep confined aquifer (Table 5-2), which presents a range of values that go from 0.01 to 3.8 m/d, with a geometric mean of 0.3 m/d. As for the unconfined aquifer, the range of values is slightly higher, going from 0.5 to 30.3 m/d, and a geometric mean equal to 4 m/d.

Table 5-2 Hydraulic conductivity [m/d] values of hydrogeological units

Hydrogeological Unit	Count	Min	25%	Geometric Mean	Median	75%	Max
Unconfined Aquifer	35	0.5	2.4	4.0	4.3	6.0	30.3
Confined Aquifer	52	0.01	0.1	0.3	0.2	0.6	3.8

The difference in hydraulic conductivity between both aquifers is about an order of magnitude. The values observed in the Figure 5-9 are consistent with the physical characteristics of each hydrogeological unit. In general, deposits located on shallow surfaces are less compact or cemented, and are also affected by erosion, which could be generating greater permeability. On the other side, greater depths imply on greater compaction levels, which induces in lower permeabilities.

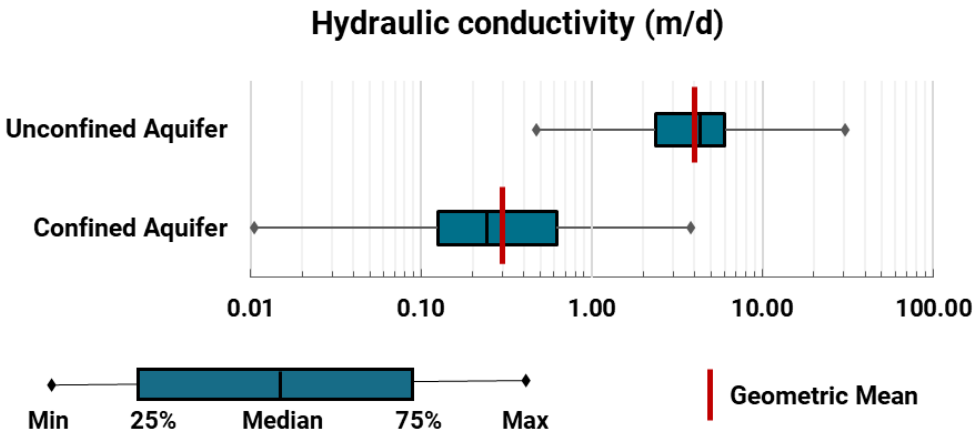

Figure 5-9 Hydraulic conductivity (K) box plot of hydrogeological units.

As mentioned above, it is important to make the difference between these values interpreted from pumping tests and the following values obtained from infiltration Porchet tests (Figure 5-10). These tests provide slightly higher values than the unconfined aquifer pumping results. This difference is due to the type of test being used, the methodology implemented by the samplers to obtain them and the low spatial representativity of these types of tests compared with hydraulic pumping tests.

The values obtained with Porchet tests vary between 3.1 and 73 m/d, with a geometric mean of 11 m/s.

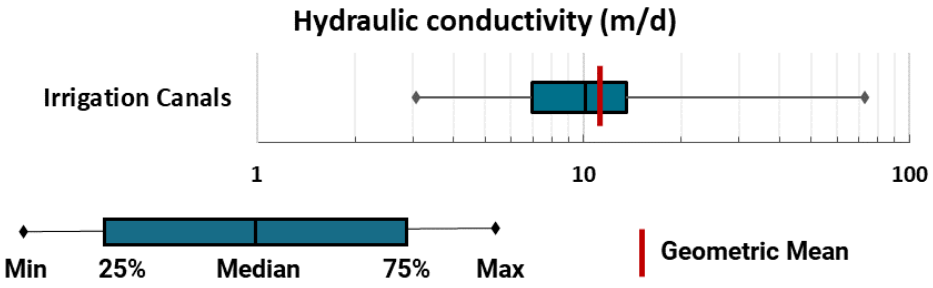

Figure 5-10 Hydraulic conductivity (K) box plot of irrigation canals.

These values are still representative of the unconfined aquifer, however, being local tests that cover only the first meter of deposits, they will be used to represent the permeability of the impervious irrigation channels rather than the shallow unconfined aquifer itself.

5.4.6 Groundwater potentiometric surfaces and flow system

As in most of the Chilean territory, the flow of groundwater goes from east to west, starting at the highest peaks of the Andes Mountain range, and “ending” its course down towards the Pacific Ocean. The origin of these waters is mainly from glacial melting or produced by rainfall, which infiltrates through fractured volcanic rocks of the highest regions or through sedimentary deposits located in the central depression, after having moved as surface water.

Groundwater levels in unconfined aquifers tends to follow the shape of the topography, therefore, in most elevated zones of the continent, where there is a greater topographic slope, the level of groundwater also presents itself with a greater hydraulic gradient, while as we move towards the west, the topography flattens considerably as does the observed hydraulic gradient.

Since there are two main lateral groundwater recharge mechanisms, it is possible to define two main groundwater flows. The first relates to a shallow flow through a surface unconfined aquifer composed of poorly consolidated deposits, while the other one represents a more regional flow, moving through a deeper confined aquifer composed by compacted geological deposits, with variations in the level of confinement and its groundwater recharge coming mainly from mountain block recharge MBR processes (Markovich et al., 2019).

To the west, the system encounters poorly permeable granitic rocks from the coastal mountain range, acting as a hydraulic barrier, where both groundwater and surface waters make their way through regional structural weaknesses, forming alluvial valleys that allow the passage of water resources going from the central depression to the Pacific Ocean.

There is a study conducted by Aquaterra in 2011 mentioned in the background information, where a hydrogeological characterization of the Itata river regional basin is performed. In this, the

piezometric curves of that year were constructed, where regional trends of groundwater flow can be observed and allows us to visualize the different flow directions within the basin. In Figure 5-11 we can see a representation of these piezometric curves in the study area.

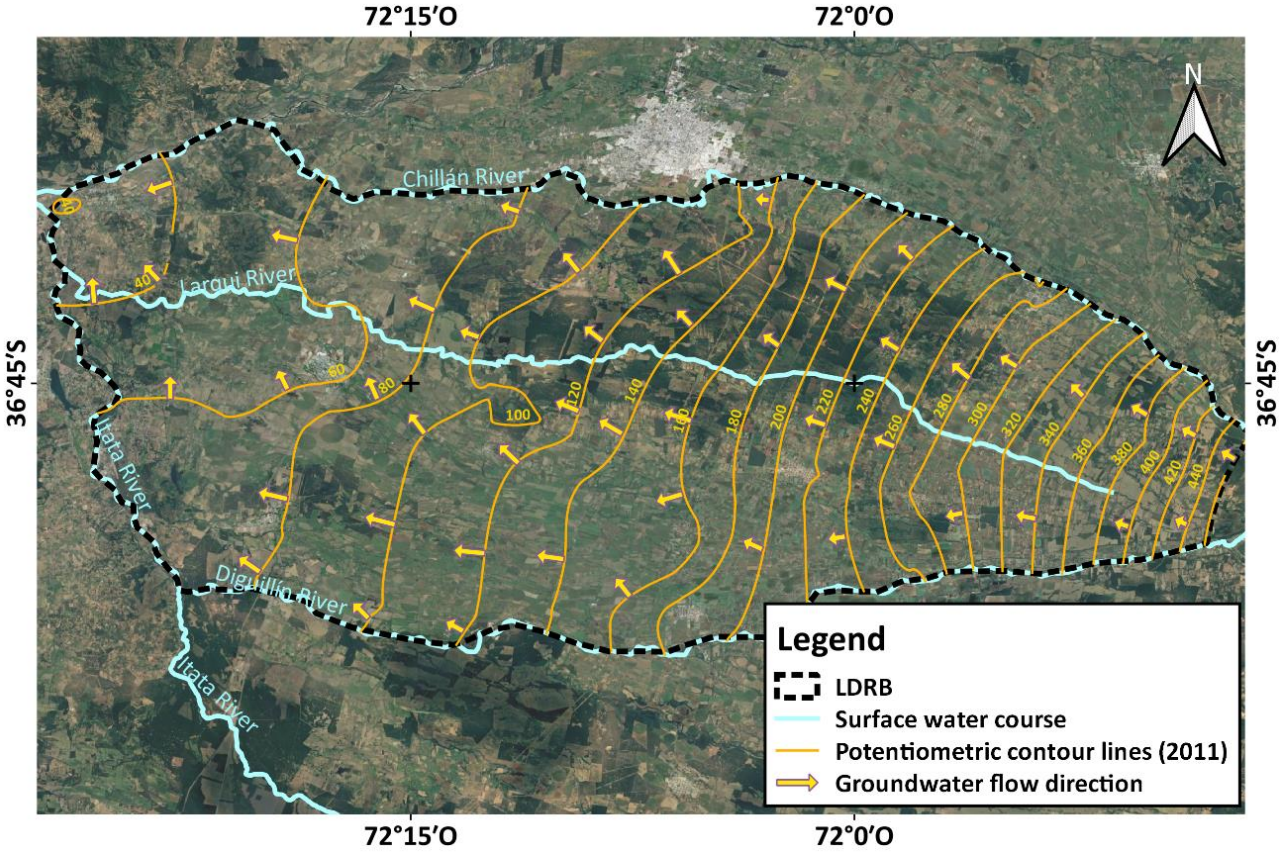

Figure 5-11 Potentiometric contour lines in year 2011

There is a direct relationship between the direction of surface rivers and the flow of groundwater. On the west side of the system, we can see that when groundwater meets the Itata river boundary, it varies its main east-west flow direction to a southeast-northwest flow direction, directing all the water of the aquifer system towards the conjunction of the Chillán and Itata rivers. On the other hand, in the potentiometric curves shown in the Figure 5-11, we can also see certain artifacts that alter the flow of groundwater, which is mainly due to artificial pumping extractions carried out during the measurement of water levels in 2011, causing local groundwater descents around the wells.

Also, there is a slight change in flow direction towards the north in the central part of the LDRB, which can be attributed to urban activities along the big city of Chillan, located just next to the basin.

5.4.7 Water level fluctuations

Fluctuations in water levels throughout the LDRB, whether in groundwater or surface water, are mainly conditioned by variations in climatic factors and by the exploitation of aquifers for agricultural irrigation. The most influential climatic factors, both for piezometric level fluctuations and river stage oscillations, are precipitation and glacier melting in the high mountain range.

Figure 5-12 shows the location of 6 gauging stations along the main rivers of the LDRB. These stations have irregular hourly to daily measurements of surface water level within the river. In addition, we can see that there is a groundwater level observation point in the study area, located in the most northeastern part of the basin. The seasonal variation of the potentiometric level at this observation point is shown in Figure 5-13.

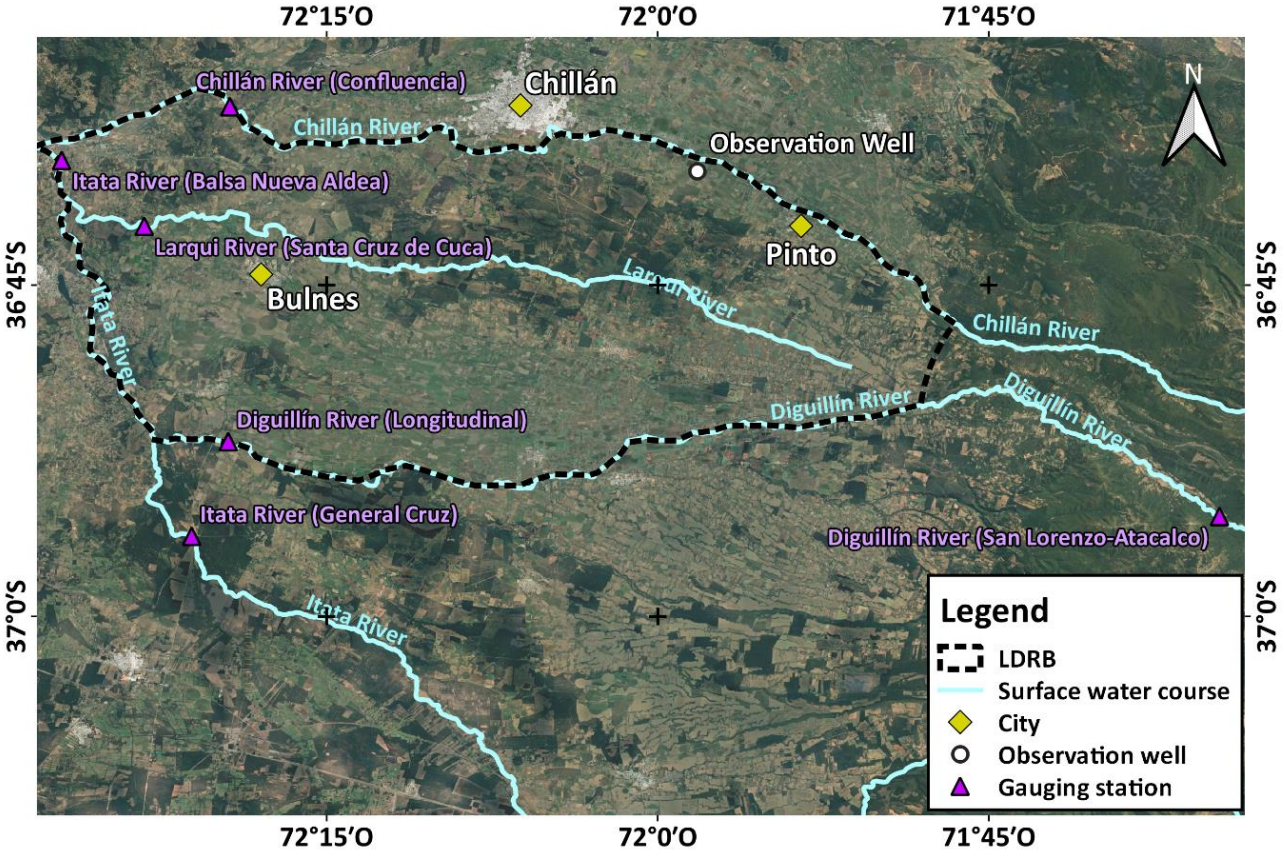

Figure 5-12 Gaugin stations and groundwater level observation point.

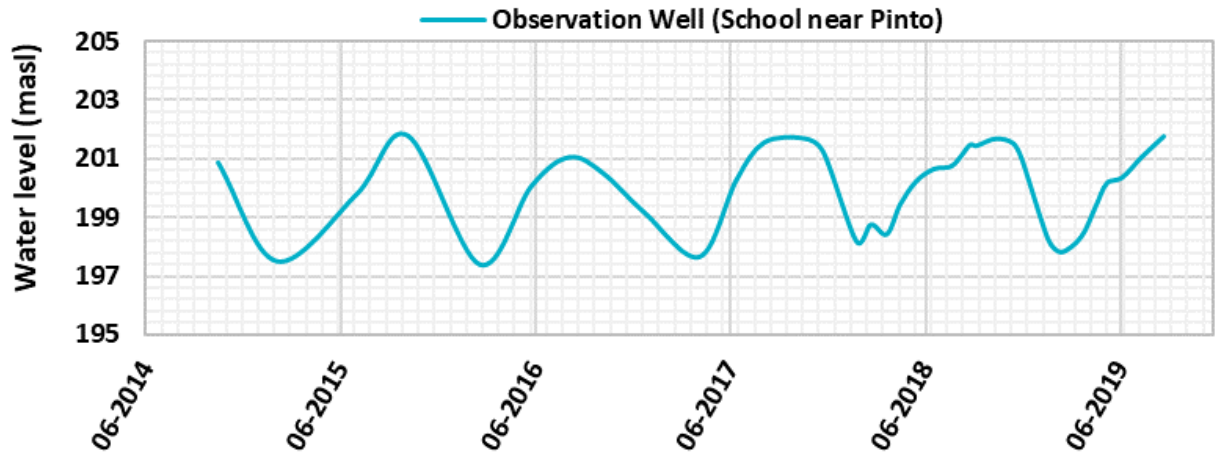

Figure 5-13 Water level variation **in 'School near Pinto' observation well.**

The water level in the observation well begins to drop in November and remains low during most of the summer months. From April to May, when the first rainfall occurs in the central-southern regions of Chile, the water level begins to rise again. This cyclical trend continues during the measured period (2014 - 2019), with minor differences observed between each year.

As for the variation in water level in rivers, there are 1 or 2 measurements along each river. Consequently, the variation in river stage along the entire length of the rivers is estimated from an average stage factor, obtained from the available data. Figure 5-14 shows the monthly time series for the stage factor applied to all rivers in the LDRB.

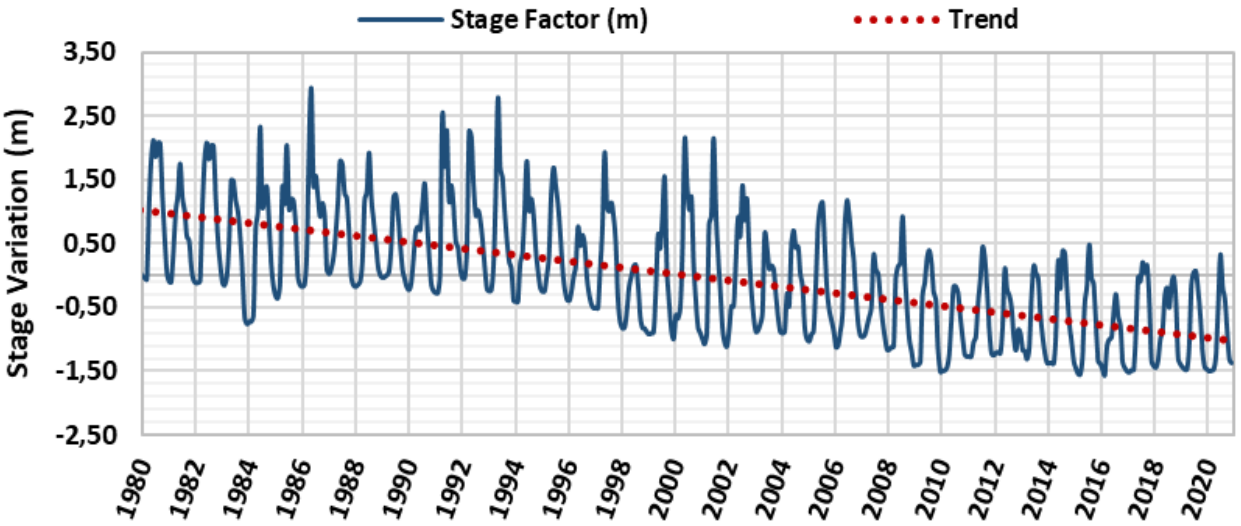

Figure 5-14 Monthly time-series for river stage factor.

In general, there is a downward trend in the water level of the river, which drops most sharply between 1994 and 2010, and then maintains a slight decrease until the last measure. In addition,

this level shows an annual cyclical behaviour that can be attributed to both precipitation and snowmelt occurring in the eastern high mountains.

5.4.8 Groundwater use

The main stress occurring on groundwater levels in the studied aquifer system is related to the extraction of water through pumping wells. The extracted groundwater is mainly used for agricultural and forestry irrigation within the area and, secondarily, for human consumption.

Within the LDRB there is a record of 556 pumping wells obtained from previous studies (Aquaterra, 2011; GFC Consultores, 2013; Con Potencial, 2021) and updated with information from the DGA, with a total flow of 6820 l/s granted to date as groundwater use rights. According to background information, the average use factor of these wells over the maximum usable flow is 0.6, giving a total average of 4092 l/s of groundwater extracted through these wells. In Figure 5-15 we can see the distribution of pumping wells within the study area.

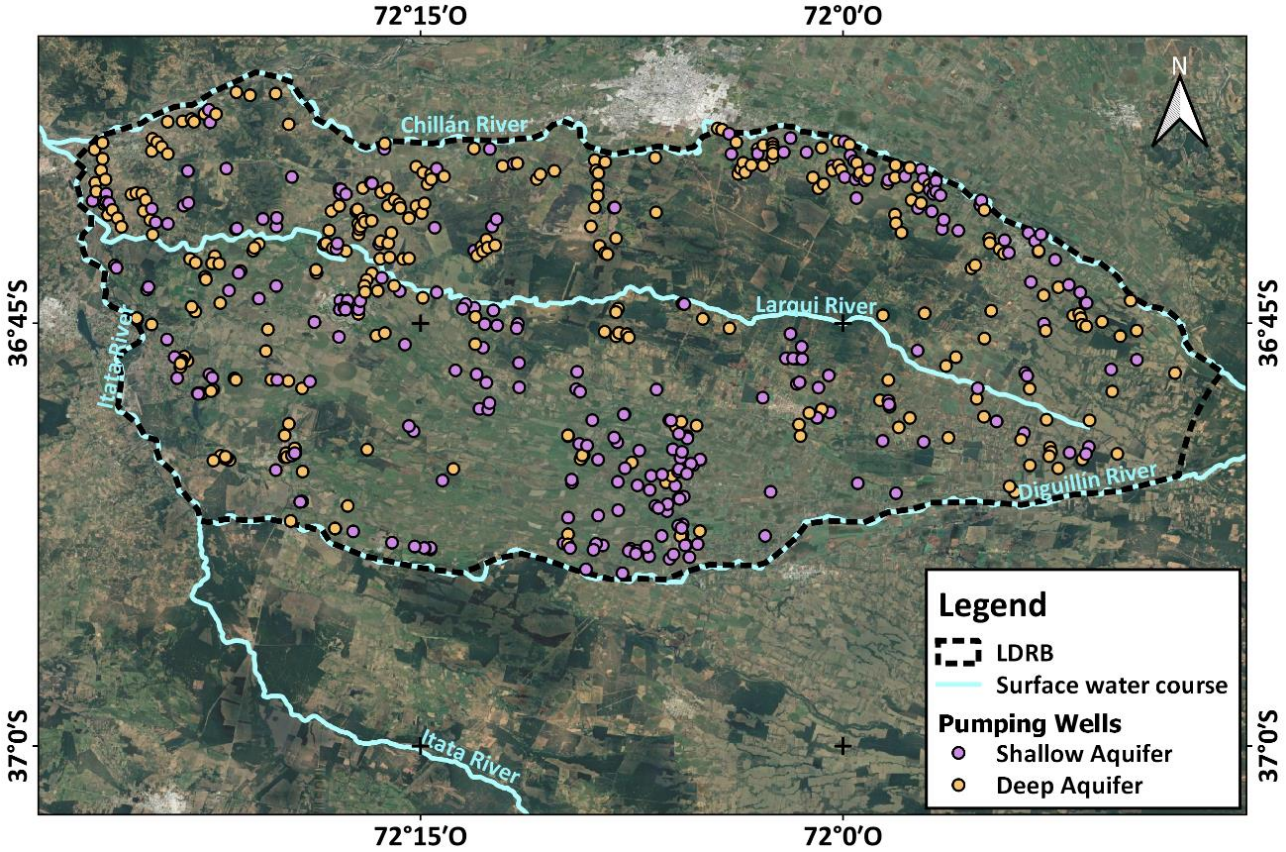

Figure 5-15 Distribution of pumping wells in the LDRB.

The distribution of wells is quite heterogeneous, covering the entire studied area, even so, there are some gaps without pumping wells, for example, in the centre of the watershed, north of the Larqui River, which can be attributed to the fact that this area is located at a higher geographical altitude.

There is also another area where there are not many pumping wells, in the south-central part of the basin, which is mainly because this area is irrigated with surface water obtained through irrigation canals rather than using groundwater.

It is important to note that the use of these wells varies seasonally according to climatic conditions, specifically rainfall, and the availability of surface water. During months when rainfall is high, irrigation decreases considerably, causing a decrease in the use of groundwater through pumping wells. Conversely, when rainfall is scarce, there is an increase in groundwater use. This variation is expressed as an annual curve that increases during summer and decreases in winter. The peak values of the curve are estimated based on the information gathered from well logs obtained from the DGA. Figure 5-16 shows the monthly variation curve of the usage factor during a complete hypothetical year.

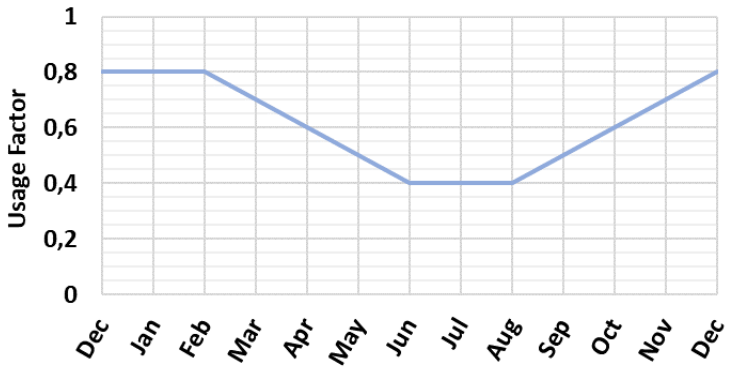

Figure 5-16 Pumping wells usage factor curve

The months with the highest usage factor are December, January and February, while those with the lowest usage are June, July and August (Figure 5-16).

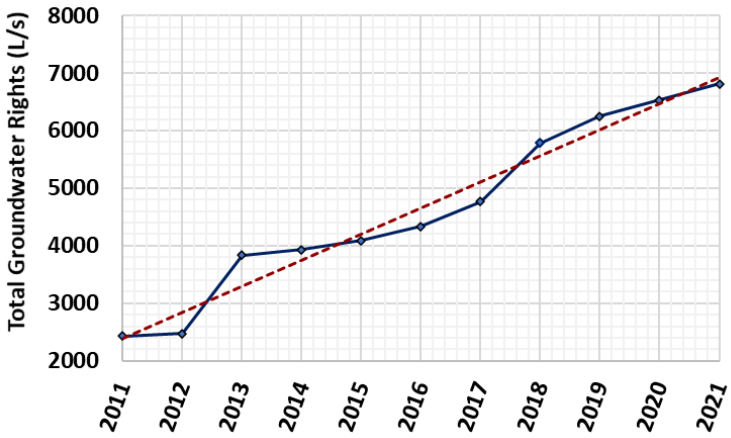

Figure 5-17 Annual groundwater rights (l/s) variation from period 2011 – 2021

From Figure 5-17 it is inferred that there is an increase in total groundwater rights granted between 2011 and 2021. On average, there is an 11% increase in total groundwater rights from year to

year, starting in 2011 with almost 2500 L/s and reaching near 7000 L/s by 2021. To extrapolate this to the years prior to 2011 where there is no detailed information, we use the same factor obtained previously, which gives us the yellow curve shown in Figure 5-18.

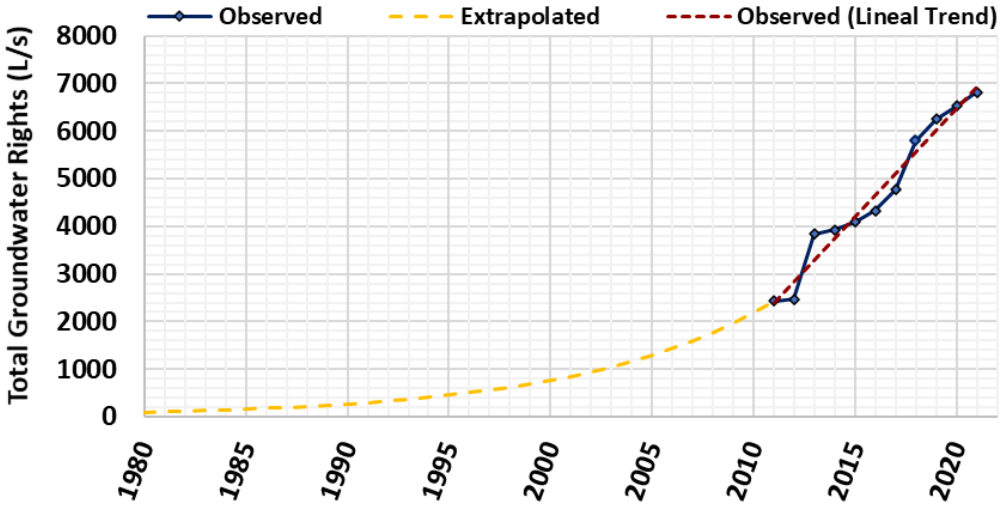

Figure 5-18 Estimated annual groundwater rights (l/s) for period 1980 – 2011

Consequently, putting together the estimated annual groundwater rights and the monthly usage factor shown in Figure 5-16, we obtain the transient series of the total groundwater extraction from the LDRB. Figure 5-19 shows the curves attained by including either an average usage factor or a usage factor that varies on a monthly basis.

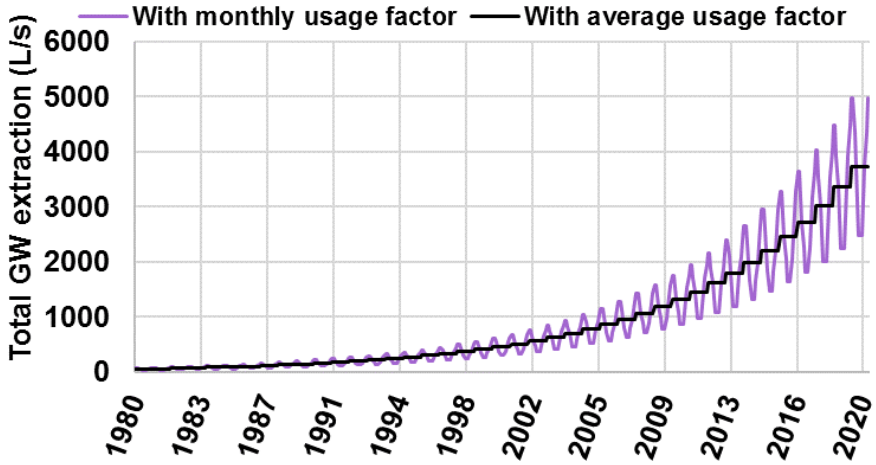

Figure 5-19 Total groundwater extraction time-series

5.4.9 Surface water and groundwater interaction

Many natural surfaces water bodies and artificial irrigation canals distributed along the study area are constantly interacting with groundwater contained in the shallow unconfined aquifer. The spatial distribution of each of these entities is shown in Figure 5-20 and detailed below.

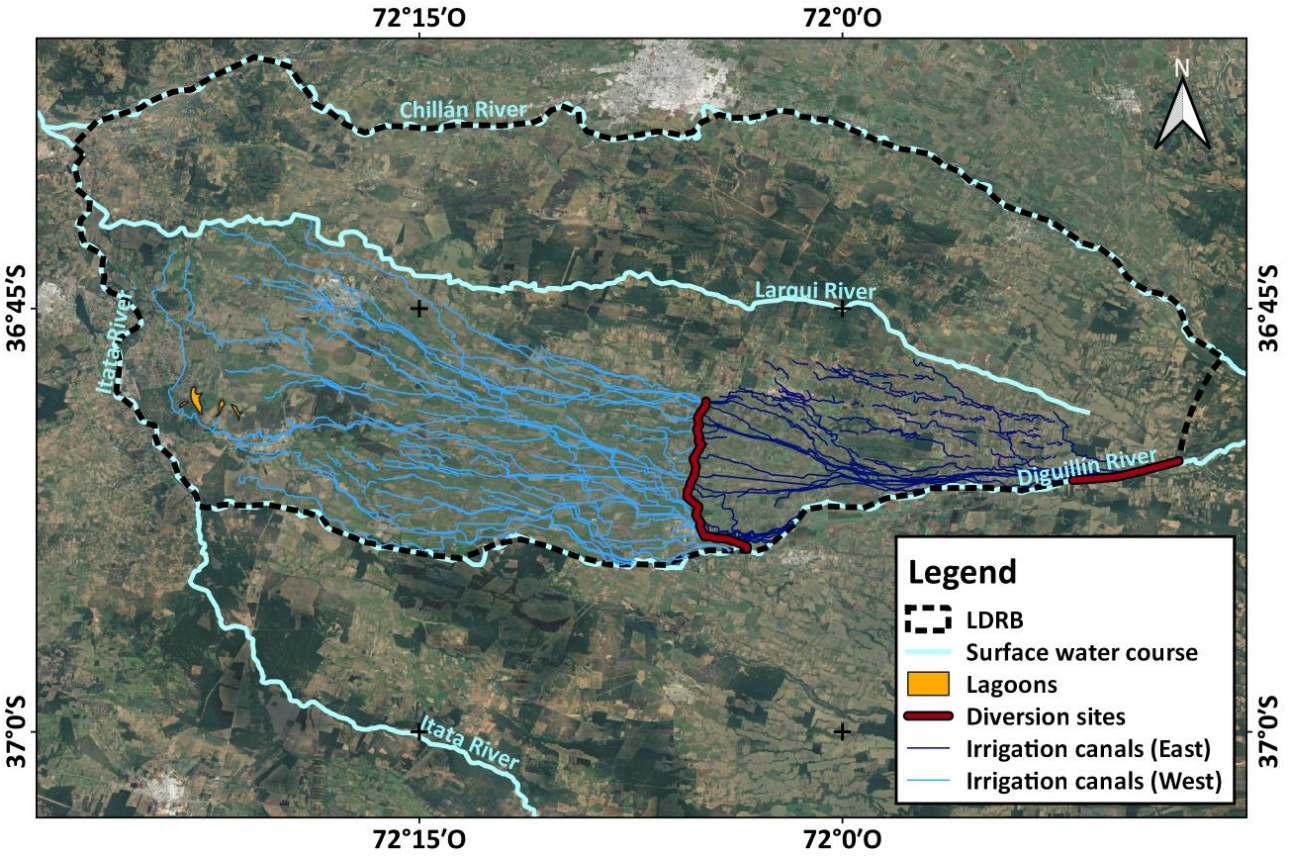

Figure 5-20 Surface water bodies (natural and artificial)

5.4.9.1 Rivers

The 3 main rivers bounding the area (Diguillín, Chillán and Itata rivers) originate in the high Andes Mountain range, mainly to the east of the study area, receiving contributions from rainfall in winter and snowmelt during summer. Their interaction with groundwater is highly variable and is mainly due to the morphological and geological characteristics of the site where it flows, as well as the level of the water table in the shallow aquifer. In addition, since the area is heavily exploited, mainly for agricultural use, groundwater hydraulic gradients tend to vary seasonally and influence the interaction between rivers and the shallow aquifer.

The Larqui River does not originate in the eastern mountain range but rises within the study area acting as a gaining river, and as it flows downhill, it presents variations in the type of interaction with local groundwater depending on the topographic conditions and the depth at which these are located.

5.4.9.2 Lagoons

These water bodies are distributed in the westernmost part of the study area, where the topography is slightly lower and there is not much slope. The overall input from these lagoons is conditioned by surface water courses, either naturally or artificially occurring, especially during winter months. There is not much evidence of whether these water bodies are interacting with the shallow unconfined aquifer and if these are gaining or losing water.

5.4.9.3 Irrigation Canals

There is a high level of agricultural activity in the LDRB, which is supported by groundwater consumption through wells and surface water distributed through irrigation canals over a large part of the land. These canals receive flow mainly from two diversion sites, the Diguillín-Coltón Matrix Canal located in the centre of the LDRB and the upper Diguillín river reaches in the eastern side of the study area (Figure 5-20).

About 90% of these canals are not lined with waterproofing, so freshwater flowing through them infiltrates into the unconfined shallow aquifer at varying rates depending on the soil permeability.

Given that the LDRB is characterised by a high concentration of precipitation in winter season, these canals are closed for half of the year to prevent flooding of surrounding agricultural and urban areas and thus avoid a potential damage to crops or towns. On the other hand, in the summer season, these canals are constantly opened to distribute freshwater coming from rivers, allowing farmers located far from the main rivers to receive surface water for irrigation during months of low rainfall.

Since most of the time, during summer season, these canals are kept with water flowing through them, there is an unknown fraction of these that evaporates due to climate conditions and another that infiltrates towards the unconfined aquifer, depending on whether these canals are lined or not.

5.4.10 Groundwater Discharge

As already mentioned in section 5.4.6 and visualized in Figure 5-11, most of groundwater flow converges towards the northwest corner of the LDRB, specifically at the confluence of the Chillán and Itata rivers. This flow can be discharged into main rivers or secondary streams, depending on if these are gaining or losing groundwater, and it can be discharged into smaller lagoons located in the lower part of the basin. In general, given the distribution of the basin, the local geology of the area and the main direction of groundwater flow, the largest discharge of the local aquifer system is towards the Itata river, to the west of the LDRB.

6 MODEL SET-UP AND CALIBRATION

6.1 Code description

The construction of the hydrogeological numerical model of the LDRB was developed with the MODFLOW 6 code in conjunction with the FloPy package (Bakker et al., 2016), which consist of a Python based package capable of construct, run and postprocess models that are part of the MODFLOW family of codes, by writing scripts directly.

The approach of using scripts to develop groundwater models is clearly different from using a GUI. Some might argue that it is antiquated because it requires the user to write syntactically correct computer code, but in the end, it provides a robust and multifunctional modelling alternative, which in turn allows the adjustment of construction and processing details for the user's needs.

6.2 Modelling domain

The modelling domain is defined based on the hydrologic and hydrogeologic processes in evaluation and the appropriate simplification of the system so that boundaries can be represented by known or very low-complexity boundary conditions. In this sense, the modelling domain includes the entire LDRB with a complete extension of 1402 km^2, simulating an area of about 60 km by 30 km.

The established domain, indicated in Figure 6-1, is largely surrounded by rivers that carry freshwater throughout the year. The only part where the domain is not limited by a river is in the eastern edge, where hydrogeologically speaking there is no physical limit, but it can be easily defined with a boundary condition.

The upper boundary of the model is defined on the topographic surface of the area, while the lower boundary is defined at the base of the deep confined aquifer, approximately at 230 meters depth.

6.3 Grid discretization

MODFLOW is a finite difference flow modeler, thus it uses rectangles of different sizes to discretise the modelling domain. The software allows the refinement of the grid in places where it is desired to evaluate groundwater flow at greater detail, without altering the grid spacing of the overall domain. In this case, the mesh is made up of regular squares with a level 1 refinement in cells where irrigation canals are present. These cells represent areas where it is intended to assess in more detail infiltration coming from subsoil and its movement into the shallow unconfined aquifer. The representation of the grid used in the model is shown in Figure 6-1, which also illustrate the distribution of irrigation canals and the refinement of the grid established based on these canals.

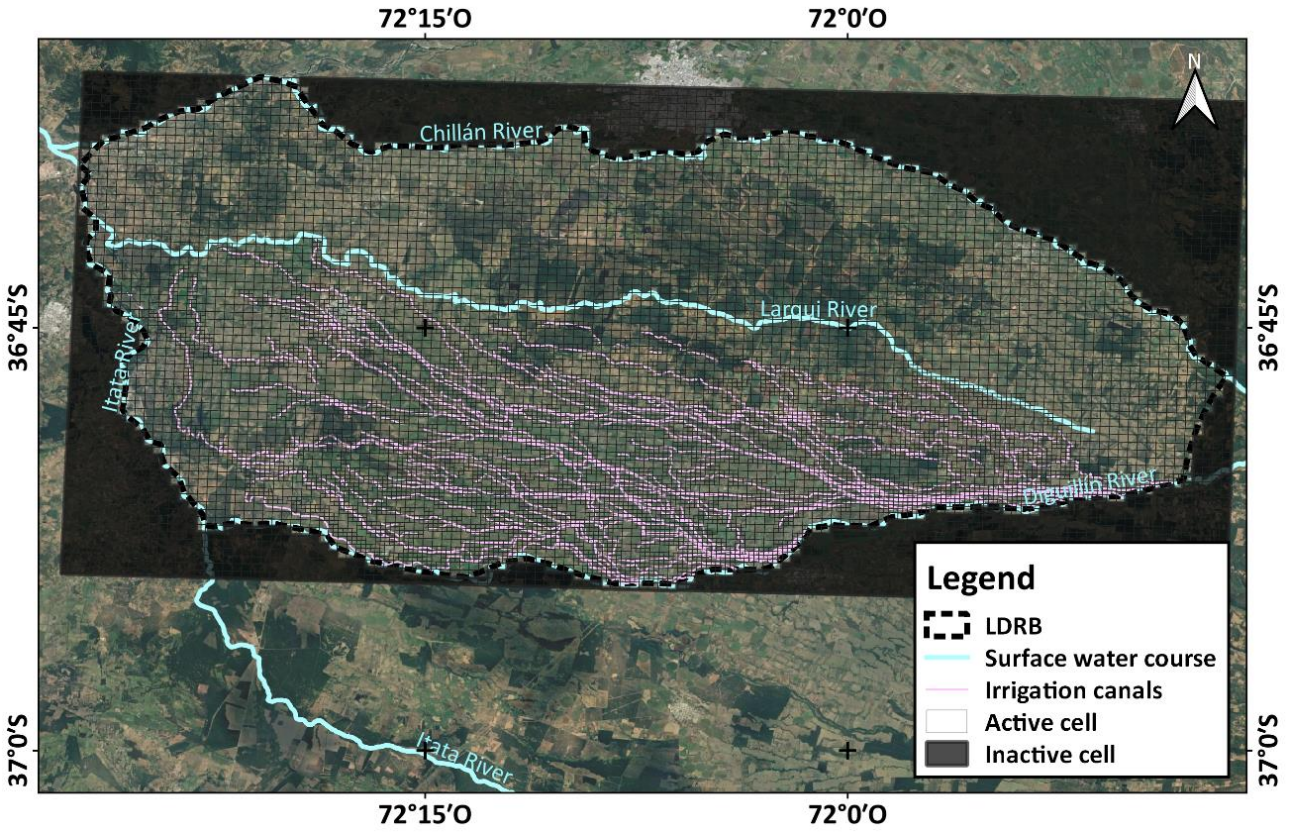

Figure 6-1 Modeling domain and horizontal grid discretization.

The unit of length in the model is "metres", the minimum X-coordinate and Y-coordinate within the model is 191194 and 5911112, respectively. The hydrogeological units of the LDRB are represented in 4 layers of 13176 cells and 14200 vertices each, where there is a total of 6432 normal cells of 500 metres wide and 6744 refined cells half the width of a normal cell.

Regarding the vertical discretisation of the model, the first layer represents the shallow unconfined aquifer with a total thickness of about 30 metres in all its extension, taking the geographical surface of the area as the top limit of this layer and an irregular Leapfrog 3D made surface as the bottom of the layer. The second layer of the model is represented with a thickness of 5 metres and correlates to the very low permeability unit considered as an aquitard in the system. The following two layers are associated with the deep confined aquifer, where it is represented in 2 layers so as not to force the numerical model to abrupt changes in thickness and hydraulic properties. These two consist of a first 75 meters thickness layer and a second deepest 120 meters thickness layer. Figure 6-2 details the vertical discretization of the model.

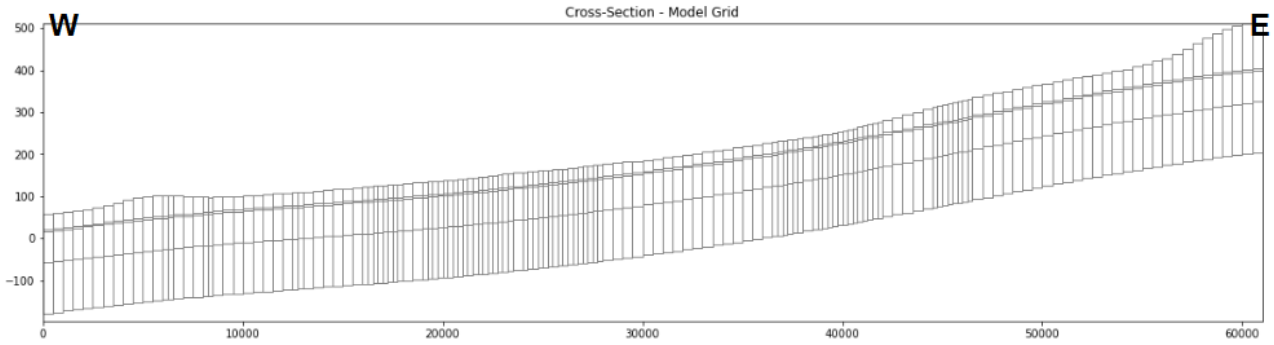

Figure 6-2 Vertical model grid discretization.

6.4 Temporal discretization

Groundwater flow in the study area was simulated from January 2011 to December 2020. The 10-year historical simulation period allowed calibrating 10 years of observed historical records in the LDRB. Two types of flow states were evaluated to simulate the local hydrogeological system, a preliminary steady state, followed by a transient state.

Since MODFLOW allows the definition of stress periods with different time extensions and boundary conditions, first, the steady state model simulates the average static conditions previously described for year 2011, implementing them directly to the model as the first stress period. Based on the outcomes of this simulation, the model runs in a transient state from January 2012 to December 2020, including the steady state hydraulic heads results as initial conditions.

The model is discretised on a monthly basis, with 2-time steps for each stress period to smooth the variation of hydraulic heads produced between each month.

6.5 Boundary conditions

Boundary conditions used in the construction of the numerical model are acquired mainly from the LDRB hydrogeological water balance. These conditions allow defining the physical limits of the modelling domain and allow establishing determining criteria affecting the groundwater flow to be simulated.

The conditions imposed in the numerical model are defined below and some of them are shown in Figure 6-3, representing the input and output conditions of the water system under evaluation:

- Groundwater inflow from upstream
- Direct recharge from precipitation
- Discharge through evapotranspiration
- Groundwater and surface water interaction
- Groundwater extractions from wells.
- No flow condition in inactive zones of the model.

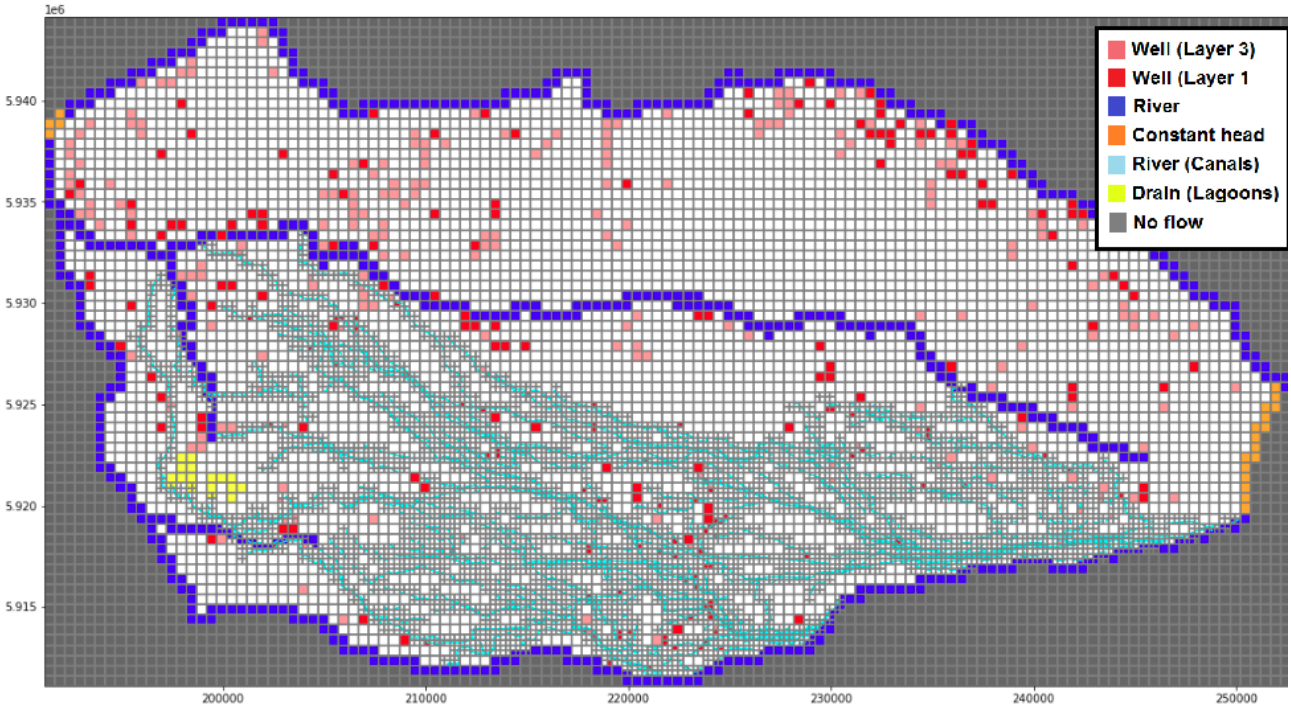

Figure 6-3 General boundary conditions.

A detailed description of these boundary conditions is given below.

6.5.1 Groundwater inflow from upstream

According to the conceptual model, the groundwater inflow from the east is unknown; however, from the potentiometric surface elaborated by Aquaterra (2011) (Figure 5-11), it is possible to define this edge as a first type Dirichlet boundary condition, represented in the model with the CHD (Constant Head) package. A total of 40 cells per layer were assigned to represent the groundwater inflow coming from the foothills on the eastern side of the modelling area. The hydraulic head established for these layers is 440 masl.

6.5.2 Distributed recharge from precipitation

As mentioned in chapter 5.4.4, distributed recharge is represented by a monthly series estimated from precipitation and crop evapotranspiration in the study area. This condition is added to the model through the RCH (Recharge) package, where a monthly varying recharge rate is assigned in units of metres per day. The cells used to represent this condition are almost all the cells in the upper layer, excluding those where rivers or lagoons exist. In total there are 10130 cells assigned for distributed recharge.

6.5.3 Discharge through evapotranspiration

The actual evapotranspiration estimated through the methodology proposed by the FAO Irrigation and Drainage document 56 (Allen et al., 1998), detailed in chapter 5.4.3.2, is implemented in the numerical model by means of a characteristic monthly varying series, via the EVT (Evapotranspiration) package. A total of 10827 grids cells are allocated for this package.

Apart from adding the actual evapotranspiration rate in metres per day to each cell, an extinction depth of 3 metres is assigned, which refers to the maximum depth to which groundwater in the shallow aquifer could be affected by this natural process.

6.5.4 Groundwater and surface water interaction

As mentioned in section 5.4.9, there are three types of surface water bodies interacting with groundwater at different ways, naturally there are rivers and small lagoons, while artificially there are irrigation canals.

In the case of rivers and streams, these are incorporated into the numerical model through the River package using a monthly time series for the stage factor variation obtained from the available data, shown in Figure 5-14. Irrigation canals were constructed using the same River package; however, these did not include the estimated stage fluctuations, but kept this value fixed to 0,5 meters above the bottom of the canals.

As for the lagoons, these were imposed on the model through the Drain package, limiting the interaction of these bodies to only capture groundwater during the simulation period.

6.5.5 Groundwater extractions from wells

The representation of groundwater consumption through pumping was appointed using the Well package, allocating all recorded abstraction flows rates from 2011 to the end of 2020. Considering the DGA information, the sum of the respective flow rates was determined for each active cell, incorporating in addition the usage factor time series and the annual increase in groundwater exploitation through pumping defined in section 5.4.8.

6.5.6 No flow condition in inactive zones of the model

Cells that are located outside the study area are considered as no-flow cells. These are associated with impermeable limits established for the LDRB basin according to the geological and hydrogeological characteristics defined in the conceptual model.

6.6 Initial conditions

6.6.1 Initial hydraulic head surface

The initial hydraulic head conditions imposed to the model are intended to facilitate the processing of information and the correct convergence of the model. First, for the steady-state model run, initial hydraulic heads are stated equal to the topographic surface. After that, the resulting hydraulic heads obtained from the steady state model run are directly addressed as initial conditions for the further transient model run.

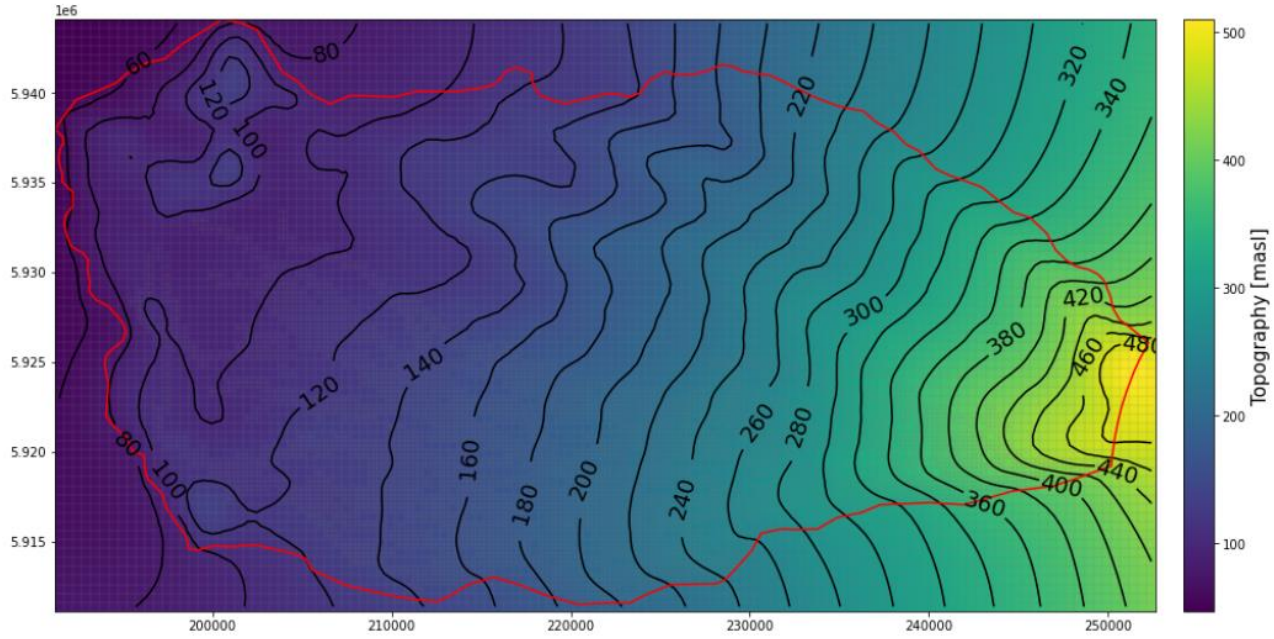

Figure 6-4 Topographic surface [masl] as initial hydraulic heads for the model.

6.6.2 Hydraulic parameters for the model

The ranges of hydraulic parameters derived from previous studies are described in chapter 5.4.5. Considering the information provided in Table 5-2 and previous literature review, the hydraulic conductivity allocated firstly to each of the numerical model layers were determined based on the geometric mean estimates and the characteristics of the aquifer system, representing the hydrogeological units established in the study area in accordance with the vertical discretisation of the model mentioned in chapter 6.3.

These initial values of hydraulic conductivity and specific storage or yield assigned to the model were subsequently modified within the general ranges established for each hydrogeological unit during steady-state and transient model calibration, to ensure the best fit of the groundwater flow model to measured field data. The ranges of hydraulic parameter values imposed in the model are presented in Table 6-1.

Table 6-1 Ranges of hydraulic parameters for the model.

Hydrogeological Unit	Layer	Hydraulic Conductivity [m/d]	Specific Storage	Specific Yield
Unconfined Aquifer	1	10^{-1} - 10^{2}	-	10^{-2} – 10^{-1}
Aquitard	2		10^{-5} – 10^{-3}	-
Confined Aquifer	3 - 4	10^{-2} – 10^{2}	10^{-5} – 10^{-3}	-

6.7 Definition of permeability zones

Considering the general groundwater flow pattern, the general lithological descriptions of each unit and the analysis of permeability tests performed in the study area, a subdivision of the modelling domain into specific zones with different hydraulic conductivities and storage parameters is carried out. As a simplification, these zones are defined as “permeability zones”. In each of these, the hydraulic conductivity is considered isotropic (Kx=Ky). Figure 6-5 shows the subdivision made by using the available information in the LDRB.

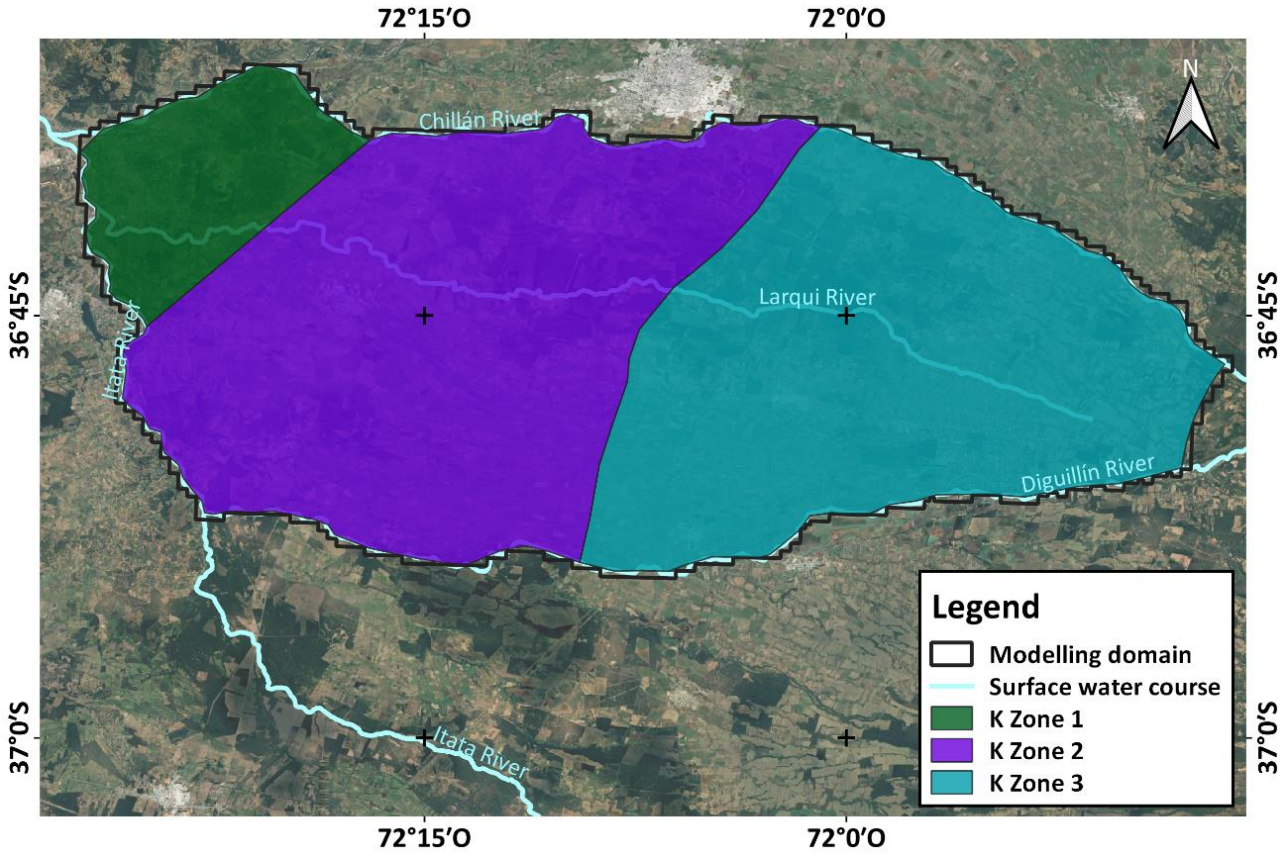

Figure 6-5 Permeability zones in the LDRB.

From this, it is possible to evaluate different combinations of input parameters provided to the numerical model to finally establish the one that most accurately reproduces the historical groundwater level observed along the LDRB.

6.8 Calibration process

Based on the available data at the LDRB, the calibration process was divided into 2 phases. First, a steady-state calibration considering hydrogeological conditions recognised during 2011, followed by a transient calibration including transitional variables and processes for period 2012 - 2020.

6.8.1 Calibration sites

In total, there are 60 calibration sites (observation wells) with head measurements throughout the modelling domain, monitoring the deeper confined aquifer. Just one of these sites contains periodic water level information covering the period 2014 - 2019, while the remaining 59 sites only provide one level measurement for year 2011. The location of these sites is presented in Figure 6-6, also indicating the observed heads during 2011.

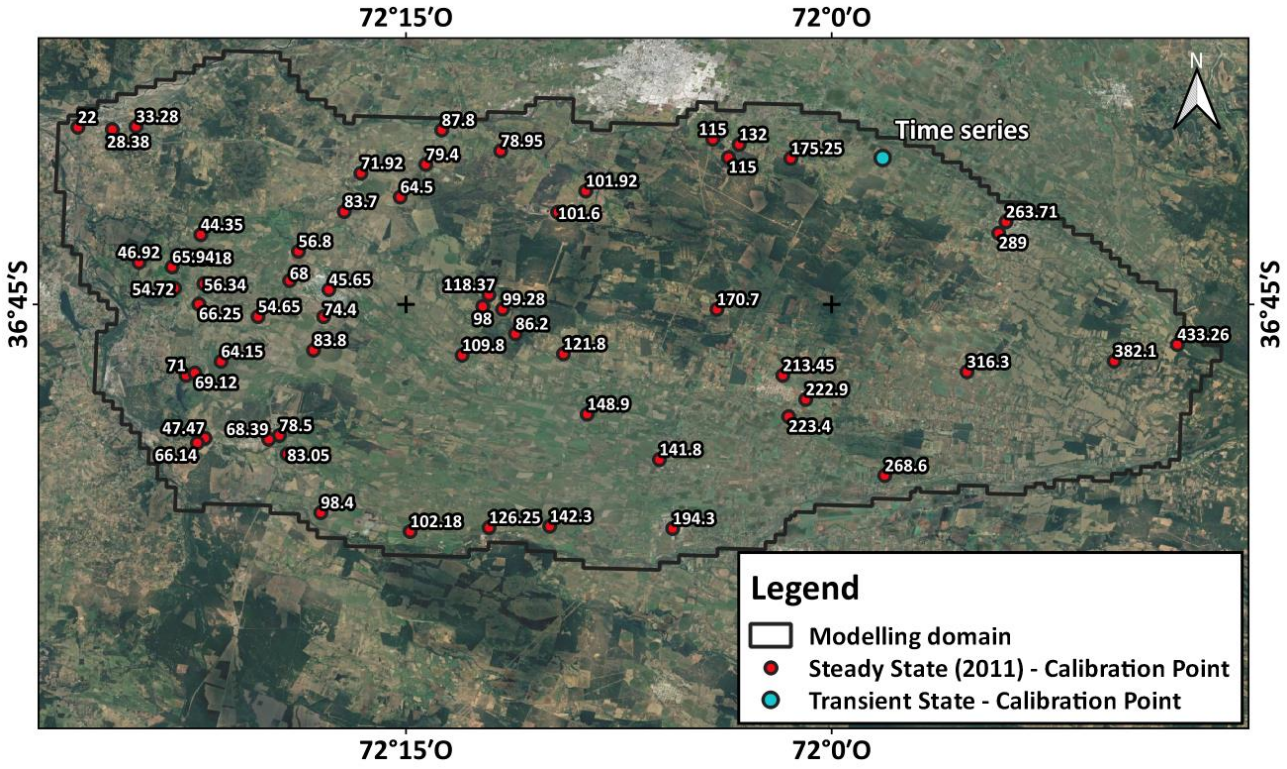

Figure 6-6 Calibration sites and observed heads during 2011.

6.8.2 Steady state calibration

The steady state model was calibrated using the standard trial and error method. Initially, applying the principle of simplicity defined by Barnet (2012), hydraulic conductivity and other hydrogeological parameters were assigned uniformly in each layer to evaluate the model response. Following the calibration process, these parameters, specially hydraulic conductivity values in each permeability zone, were adjusted, within the reasonable limits stated in the conceptual model, to enhance the model output and accurately represent the flow conditions established for year 2011 (Figure 5-11) and match the hydraulic heads observed during that period (Figure 6-6).

In summary, the complexity of the model was increased during the calibration process as the results were consistent with historical observations. To evaluate the most optimal combination of parameters and quantify predicted flow accuracy of the model, 5 commonly used error metrics were compared, the Root Mean Square Error (RMSE), normalized Root Mean Square Error (nRMSE), Mean Absolute Error (MAE), normalized Mean Absolute Error (nMAE) and the The Nash–Sutcliffe efficiency coefficient (NSE). These metrics consists of scaled errors based on an absolute or squared error term (MAE and RMSE, respectively); percentage errors that scale the error term by the observed data in different ways (nRMSE and nMAE); or scaled forecast errors which compare the ratio between the forecast error and an error obtained with a naive forecasting method (NSE) (Jackson et al., 2019).

The resulting calibrated hydraulic conductivity obtained through the trail an error process is detailed in Table 6-2. Also, Figure 6-7 presents a comparative scatter plot between observed and simulated water levels, allowing to verify how close the points are to the diagonal and thus evaluate whether the model accurately predicts the observed heads or not.

Table 6-2 Calibrated hydraulic conductivity [m/d] values.

Model Layer	Aquifer	Permeability Zone	Calibrated Horizontal K [m/d]	Calibrated Vertical K [m/d]
Layer 1	Unconfined	Zone 1	4×10^{1}	4×10^{0}
		Zone 2	4×10^{1}	4×10^{0}
		Zone 3	4×10^{1}	4×10^{0}
Layer 2	Aquitard	Zone 1	1×10^{-3}	1×10^{-4}
		Zone 2	1×10^{-3}	1×10^{-4}
		Zone 3	1×10^{-3}	1×10^{-4}
Layer 3	Confined	Zone 1	4×10^{1}	4×10^{0}
		Zone 2	2×10^{1}	2×10^{0}
		Zone 3	1×10^{1}	1×10^{0}
Layer 4	Confined	Zone 1	4×10^{1}	4×10^{0}
		Zone 2	2×10^{1}	2×10^{0}
		Zone 3	1×10^{1}	1×10^{0}

Table 6-3 Steady state calibration statistics

Count	59
RMSE =	12.8
nRMSE =	3.1
MAE =	9.7
nMAE =	2.3
NSE =	0.98

Considering the graph in Figure 6-7 and the calculated error metrics presented in Table 6-3, it is implied that the steady state model accurately simulates the observed water level during 2011. However, if we look at the results in more detail, we can see that there are some places where the model overestimates or underestimates the observed water level.

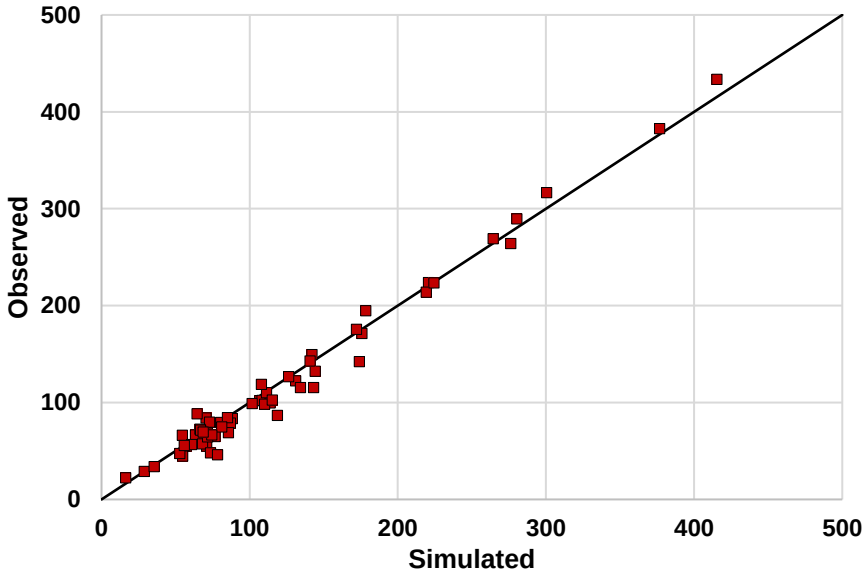

Figure 6-7 Steady state calibration results along 1:1 correlation line.

6.8.3 Transient state calibration

For the transient model calibration, the time series of piezometric levels (Figure 5-13) measured at 'School of Pinto' observation well during period 2014 - 2019 was included. This model was extended to year 2020. The variation in water level is mainly due to the extraction of groundwater through pumping wells located in the LDRB and because of seasonal recharge series over the study area. The calibration of the model in transient state was performed manually, using the previously calibrated hydraulic conductivity, and varying the storage coefficient and specific yield in each hydrogeological unit until the simulation was able to represent the variation of levels observed in time. The resulting calibrated aquifer storage and specific yield at this stage are shown in Table 6-4. A specific yield of 0.1 was used uniformly for the unconfined aquifer and a specific storage of 0.0008 1/m was used for the confined aquifer and the local aquitard.

Table 6-4 Calibrated specific yield and specific storage [1/m] values.

Model Layer	Aquifer	Permeability Zone	Calibrated Sy	Calibrated Ss [1/m]
Layer 1	Unconfined	Zone 1	0.1	-
		Zone 2	0.1	-
		Zone 3	0.1	-
Layer 2	Aquitard	Zone 1	-	0.0008
		Zone 2	-	0.0008
		Zone 3	-	0.0008
Layer 3	Confined	Zone 1	-	0.0008
		Zone 2	-	0.0008

Model Layer	Aquifer	Permeability Zone	Calibrated Sy	Calibrated Ss [1/m]
		Zone 3	-	0.0008
Layer 4	Confined	Zone 1	-	0.0008
		Zone 2	-	0.0008
		Zone 3	-	0.0008

6.8.4 Calibrated water budget

Since this study focuses on the evaluation of the shallow unconfined aquifer, this section presents the results related to the top layer of the numerical model. The water budget for layer 1 was divided into two separate graphs. The first one (Figure 6-8) displays the following processes: inflows and outflows through groundwater flow, groundwater, and surface water (rivers and streams) interactions, discharge to lagoons, recharge by irrigation canals, evapotranspiration and the extraction flows related to pumping. The second graph (Figure 6-9) shows rainfall recharge and groundwater storage variations within the unconfined aquifer. These last two variables were separated from the rest because of their high flows, either negative (GW storage loss) or positive (Recharge/GW Storage gain), allowing a better visualization and understanding of the water budget chart.

These two processes (recharge and storage variation), despite being the largest flows observed in the system, are highly correlated with each other, i.e., when recharge flows increase during winter, groundwater outflow coming from aquifer storage increases simultaneously. On the contrary, when recharge from precipitation decreases, it is noted that groundwater storage gains are greater than losses (Figure 6-9). During these same months of scarce rainfall, the greatest outflow from layer 1 is through evapotranspiration (Figure 6-8).

Another important aspect to note regarding evapotranspiration is that the calibrated numerical model result differs from the estimated evapotranspiration time-series established in the conceptual model (**Figure 5-6**). This is mainly because of the availability of groundwater in the system to be evapotranspired and the way this condition is computed in the model. Since there is a defined extinction depth (3 meters) within the model, the evapotranspiration time-series mentioned conceptually does not reach its maximum expected discharge value through this process, mainly because water levels in certain areas are below 3 metres from the topographic surface, reducing the maximum evapotranspiration capacity.

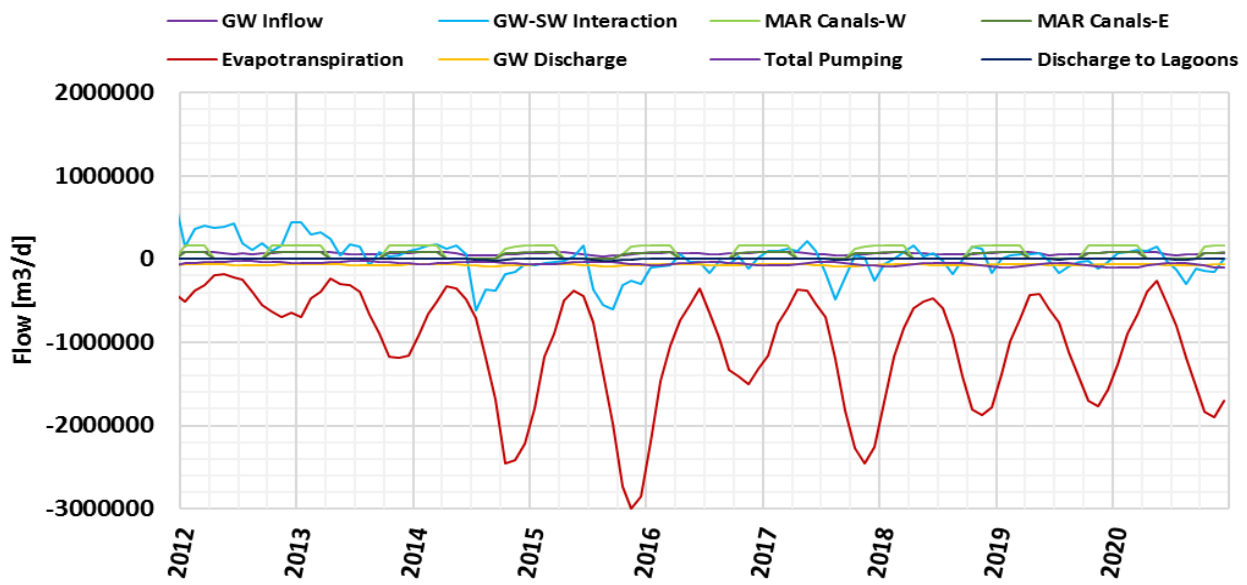

Figure 6-8 Water budget for Layer 1. (1)

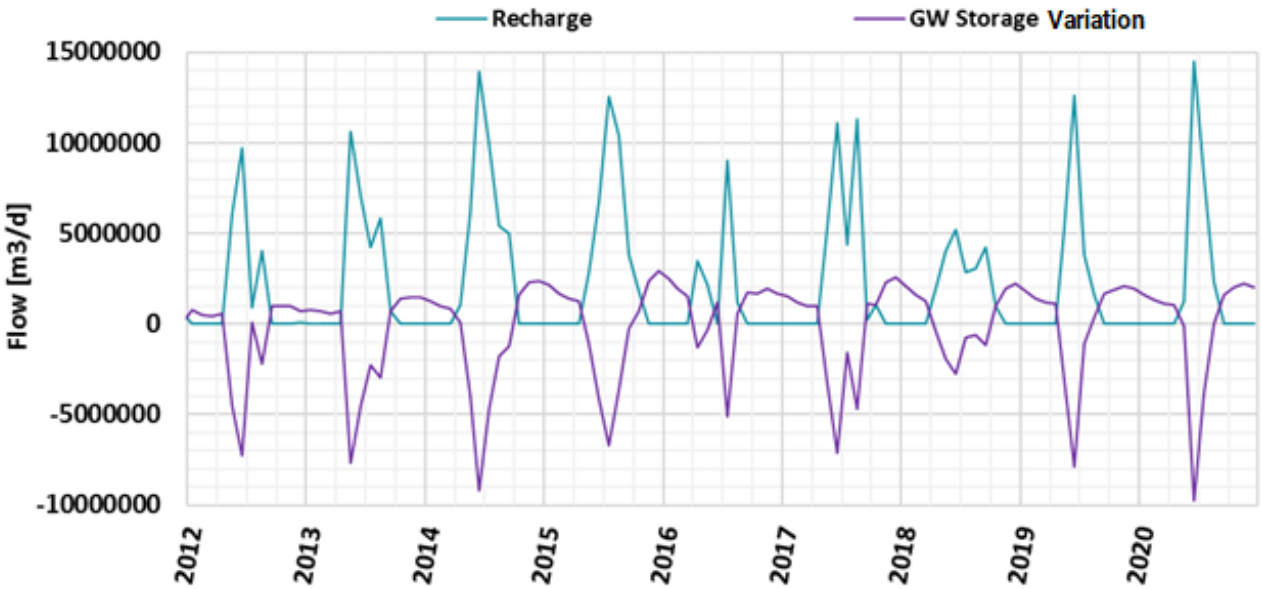

Figure 6-9 Water budget for Layer 1. (2)

6.9 Base Case results

Considering all natural and anthropogenic processes involved in the groundwater system within the LDRB, the calibrated transient state model output is established as the Base Case for the purposes of this study. It should be emphasized that this case considers the opening of irrigation canals for 6 consecutive months, from October to March, during the period 2012 – 2020. This relates to the fact that these months have limited or null rainfall and, in addition, crops require more water, so irrigation plays a fundamental role.

Based on the results of the base case, the main findings and observations related to the unconfined aquifer system are described below.

6.9.1 Recharge flow through canals

As mentioned above, recharge through irrigation canals corresponds to a limited fraction of the total recharge of the system, either directly from precipitation or laterally from upstream as groundwater flow. On average, the amount of recharge occurring through irrigation canals is about 5% of the total recharge calculated for the unconfined aquifer. This recharge is distributed as 3.4% and 1.7% in the western and eastern irrigation canals, respectively.

The maximum percentage of this recharge is reached in 2016 with about 8% of total recharge between both canals' sites, while the minimum percentage is placed between 2014 and 2015. The way this recharge is imposed in the model, it does not depend on the amount of precipitation available, but rather acts as a constant hydraulic load. Therefore, the percentage with respect to total recharge is inversely proportional, i.e., when there is less total recharge, the percentage of recharge provided by irrigation canals increases.

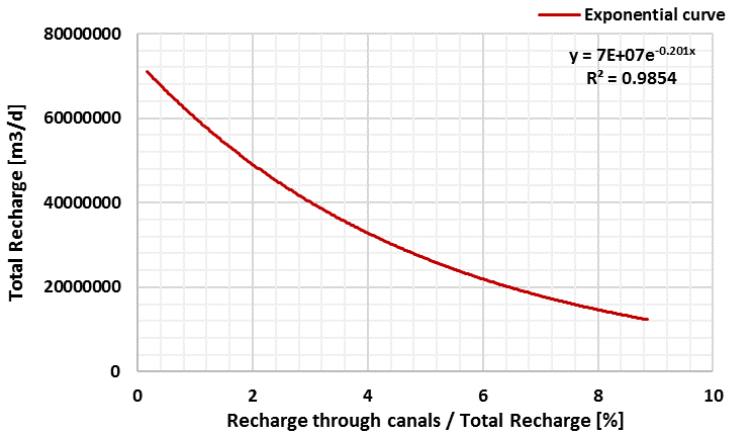

Figure 6-10 Percentage of recharge through channels with respect to total recharge

6.9.2 Groundwater storage variation

According to baseline outcomes, it is noted that the shallow aquifer storage is highly influenced by direct recharge from precipitation, not allowing to clearly establish the influence of recharge through canals on groundwater storage. What can be identified is that during months with null rainfall and active irrigation canals, the aquifer's capacity to incorporate water into storage increases. This performance might be related to other involved processes rather than canal induced recharge itself, but it is important to note the difference in aquifer storage between stations (Figure 6-8 and Figure 6-9).

6.9.3 Discharge to surface water bodies

Another important process occurring in the upper layer is the interaction between groundwater and surface water bodies, specifically with lagoons and rivers that are present in the basin. In this case, there are a few lagoons located at the lower site of the LDRB towards the west acting as “gaining surface water bodies”, so it is important to see if there is significant flow going to these small reservoirs.

As for discharge to rivers, since this study focuses on the effects of varying recharge through irrigation canals, the water body desired to evaluate is the one located directly downstream in the same direction of groundwater flow, which is the Itata River. Based on this, this analysis is limited to the interaction that occurs between the shallow aquifer and the Itata River only. In Figure 6-11 we can see the temporal evolution of the outflows to both water bodies described above.

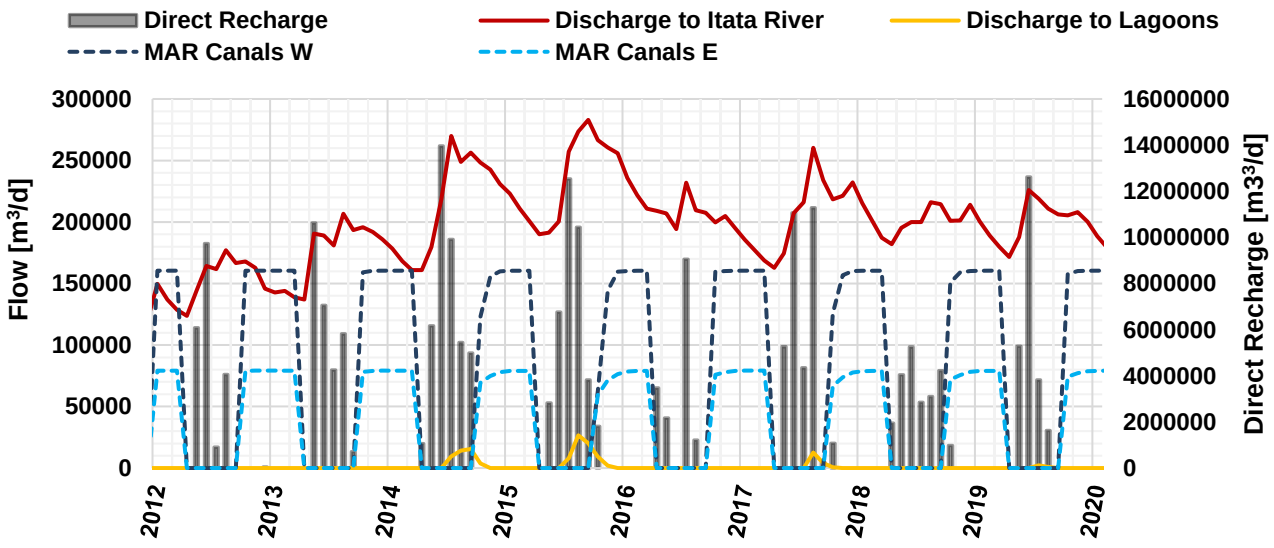

Figure 6-11 Groundwater discharge towards surface water bodies.

The flow that escapes to the lagoons is minimal compared to the discharge to the Itata River, being negligible during most of the time. On average, discharge towards lagoons reaches about 3% of the total discharge to the Itata River.

The relationship observed between recharge produced through irrigation canals and discharge into the Itata River is similar to that observed with rainfall; however, it is difficult to differentiate precisely what are the causes of these variations, taking into account only one particular case. I can be inferred that the increase in groundwater levels resulting from recharge through canals would generate an increase in discharge towards the river and lagoons.

In general, discharge to the Itata River begins to increase at the beginning of winter and reaches a peak amount between June and September. After that, it begins to gradually fall during dry season. It should also be noted that the highest discharges towards the Itata River occur between 2014 and 2016, which in turn, correspond to years with highest precipitation. This same 2-year period is where the greatest discharge to the lagoons occurs.

6.9.4 Groundwater level variation

Another crucial factor that must be analysed in order to characterize a site where a managed aquifer recharge is being carried out, is the potentiometric level and how it varies over time while additional water is infiltrating into the system. The baseline hydraulic heads computed with the model, as well as the depth at which the water level would be found within the study basin are detailed below.

6.9.4.1 Hydraulic heads

The main output of a numerical model is the distribution of hydraulic heads for all defined stress periods. In the base case, we can see that the values vary between 20 to 450 m asl., showing a general groundwater flow in an east-west direction, mainly discharging to the Itata river, but also yielding water to the rest of the rivers in the basin.

Figure 6-12 shows the representative head distribution for summer and winter season, where in the first state recharge through irrigation canals is taking place, while in the second is not, but there is a larger amount of recharge generated from precipitation. It is noted that along the irrigated sites there is a notorious excess of groundwater, possibly caused by the effect of these canals or by the geometry of the shallow aquifer and the limiting rivers placed at lower heights.

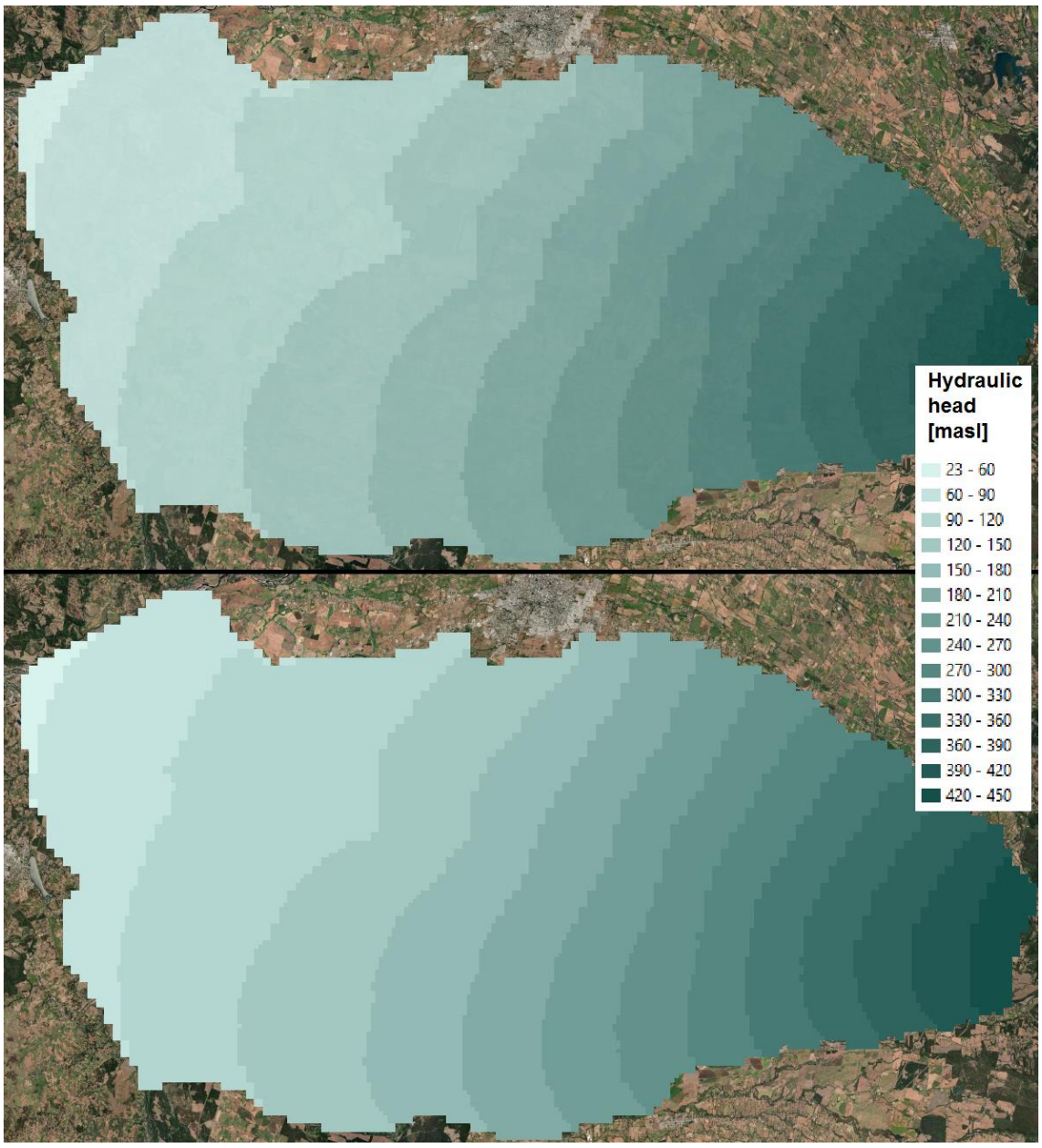

Figure 6-12 Head distribution in January (Top) and September (Bottom) for Base Case during 2020.

The difference between the summer season and the winter season is best appreciated in Figure 6-13, where it is possible to identify specific sites along the LDRB that have larger increases in simulated water level between January 2020 and September 2020 for the base case conditions.

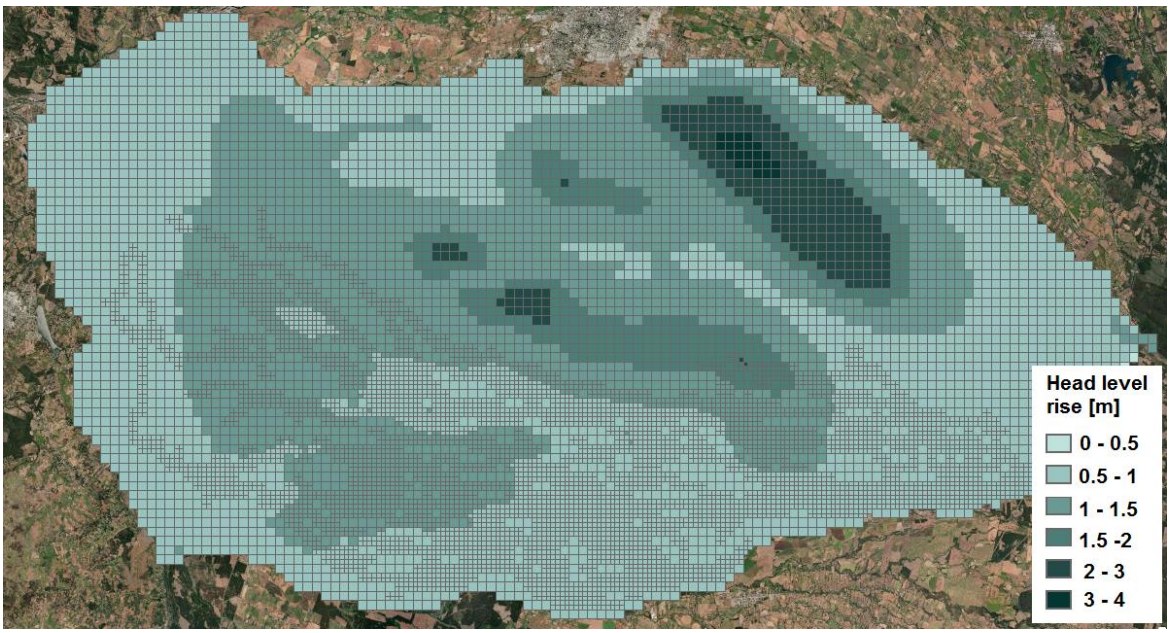

Figure 6-13 Hydraulic head level rise between summer and winter season.

6.9.4.2 Depth to water table

The depth at which the water table is encountered varies from near 0 to 75 meters along the LDRB basin, with the greatest depths located towards the eastern and western edge of the modelled domain and the shallowest depth located at the centre of the basin. Specifically, on the land through which the irrigation canals pass, the water level is at a maximum depth of 10 meters.

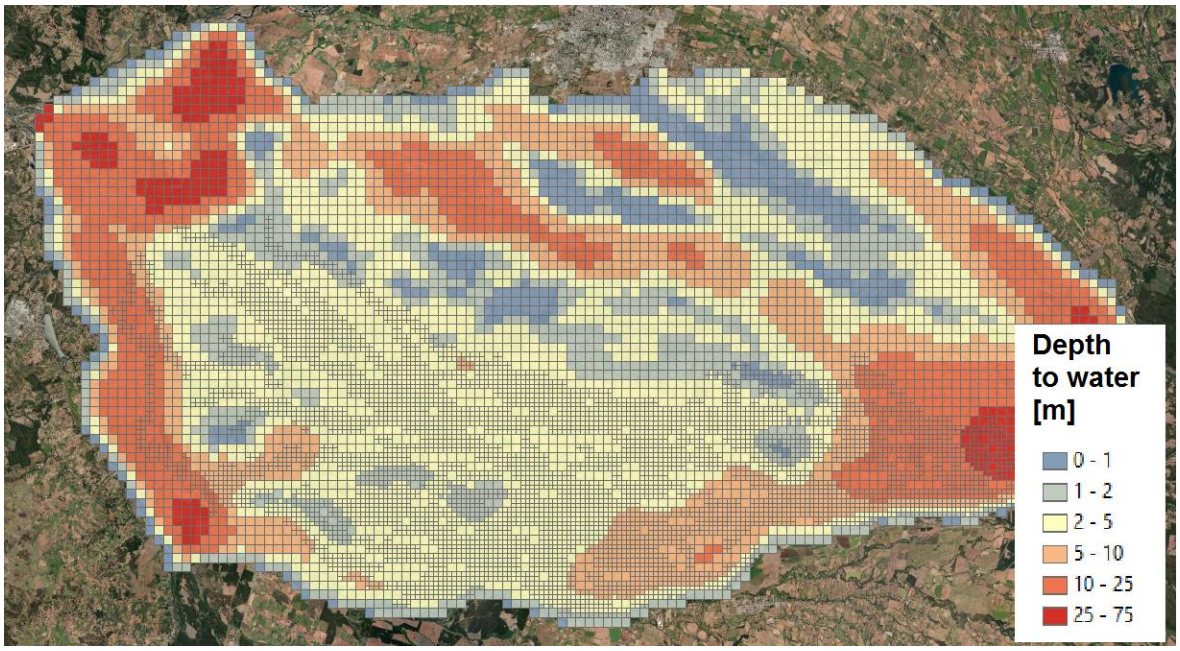

Figure 6-14 Computed groundwater depth in January 2020 for Base Case.

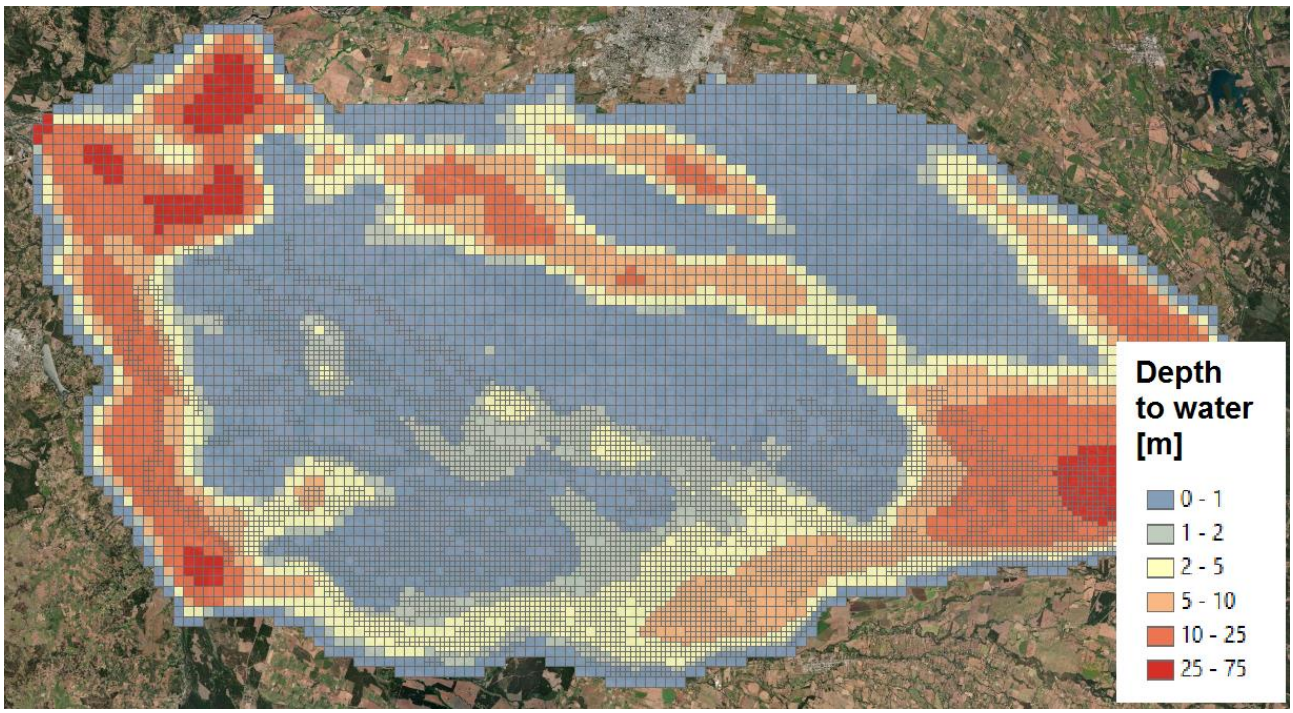

Figure 6-15 Computed groundwater depth in September 2020 for Base Case.

Figure 6-14 and Figure 6-15 show the difference in water level depths between one date and another, specifically between January 2020 and September 2020. The first graph shown refers to the season with little to no rainfall, also representing the period of active irrigation canals for the Base Case simulation. At this time, the water level around irrigation canals is mostly between 2 to 5 meters deep, with specific sites where the water level could be at depths lower than 1 meter. Also, towards the southeast of the zone of interest, there is an increase in the depth of the water level, which may be related to the topography of the sector, as well as the edges of the LDRB.

By September 2020, a different depth distribution is expected, due to the excess of water falling on top of the basin and recharging the shallow aquifer. During this period, groundwater level is closer to the surface, with a notorious decrease of localized water level depths around irrigation land sites.

On average, the depth of the water table for the entire LDRB is 6.5 and 4.3 meters for February and September, respectively, which means that between summer and winter season, groundwater level of the shallow aquifer rises a little more than two meters in some sites, and more than 10 meters in critical areas.

6.9.5 Seasonal water budget variations

As can be inferred, the impact of precipitation over the aquifer system is high, therefore, in a focused manner, the variation that occurs in the water budget between rainy and dry years must be analysed. To evaluate this, 2014 was chosen because of its high rate of fallen water into the LDRB, while year 2016 represents the conditions of a drier year.

The flows analysed were groundwater and surface water interaction with rivers, recharge through irrigation canals, evapotranspiration, and total pumping.

Of the mentioned flows, the main difference observed between 2014 and 2016 is that during winter months (June to August) and early spring (September to October), there is a greater discharge occurring towards the main rivers during the rainy year (2014), possibly caused by the excess of direct recharge over the basin and the rise of potentiometric heads that this entails.

Connected to this, there is also a greater evapotranspiration observed during the rainy year, which is consistent with the increased amount of water to be evaporated and transpired, as well as there is a higher probability that the extinction depth associated with evapotranspiration (defined for the model at 3 meters below the topography) is bigger than the depth of the water level during a rainy year, which in turn translates into a higher yield for evapotranspiration occurring over the LDRB surface.

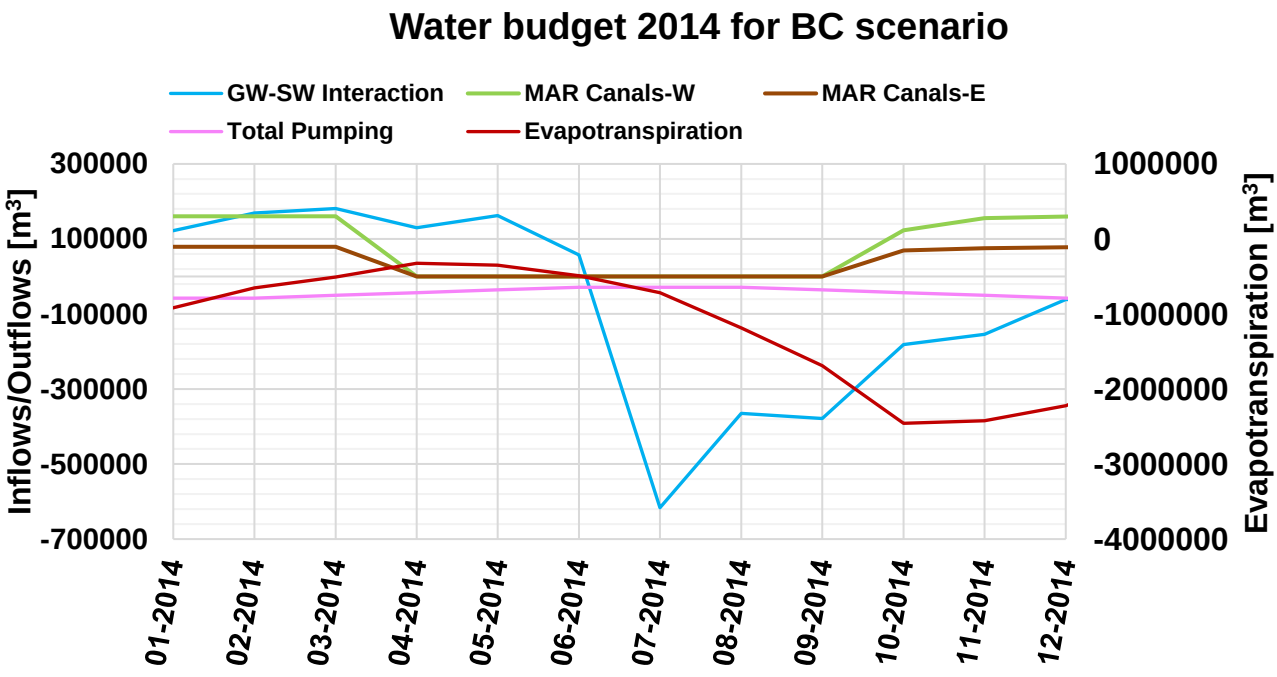

Figure 6-16 Water budget of 2014 for BC scenario.

Another important point inferred from the water budget graphs is that the recharge induced through irrigation canals shows a slight variation in the initial months of activation post winter season, where for the rainy year (2014) the gradual increase in recharge has a slightly lower slope than the observed for the dry year (2016).

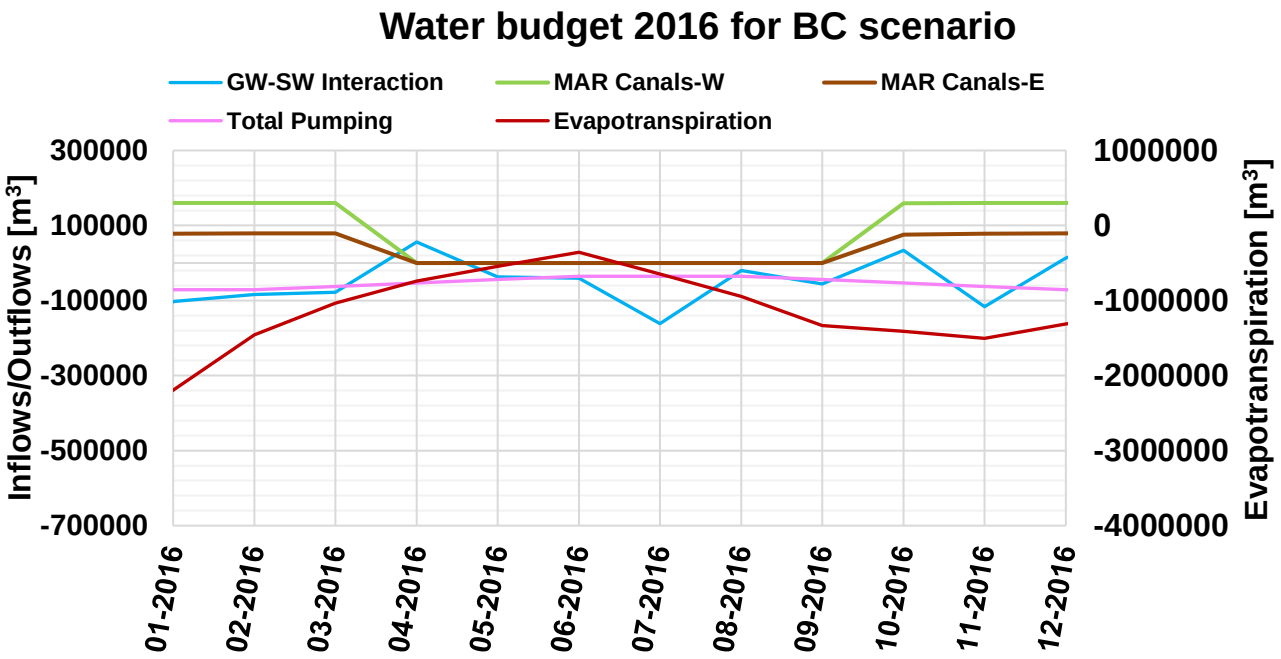

Figure 6-17 Water budget of 2016 for BC scenario.

This difference, although small, is important when evaluating the efficiency of managed aquifer recharge, since it indicates that after extreme rainfall events during winter, there is a lower rate of initial recharge through irrigation canals.

7 PREDICTIVE SCENARIOS ANALYSIS

This section includes a series of predictive scenarios built over the same period of the calibrated transient model. Considering the input parameters and conditions imposed to the base case, different settings were prepared to evaluate various managed aquifer recharge designs using irrigation canals. Among the factors under evaluation are the opening time of these canals and their spatial distribution along the LDRB irrigation sites.

These two factors are extremely important for evaluating the efficiency of managed aquifer recharge, as well as other relevant factors such as the volume of water discharged into the canals or the proximity of MAR sites to surface water diversion points. However, due to the lack of information available and the scope of this study, only the first two factors mentioned above are being considered in this chapter.

7.1 Recharge timing variation

The relationship between the time over which a managed aquifer recharge technique is developed and the effective volume of water that is supplied to the aquifer system, is an extremely important variable when evaluating the efficiency of a MAR method.

In this case study, the aim is to evaluate how the efficiency of the MAR through irrigation canals varies when the opening time of these canals is increased beyond the opening season established for the base case and, in turn, to define whether increasing the opening time of these canals has a positive, negative, or simply no impact on the shallow aquifer storage.

When we talk about positive or negative impact on the aquifer, we are referring to the ability of the aquifer to incorporate the amount of infiltrated water into its storage, minimizing losses occurring towards downstream surface water bodies such as rivers and lagoons. Considering the distribution of the LDRB, the main surface water bodies that could receive groundwater in case of losses, would be the Itata River and small lagoons located just to the east of the Itata River, directly downstream of irrigation sites under evaluation.

Taking into account the months of activation for the base case, 6 activation configurations were established to evaluate the aquifer response.

7.2 Recharge location distribution

The second factor being assessed has to do with the spatial distribution of the land where irrigation canals are considered active and the impact this has on the efficiency of the MAR technique.

In this case, only 2 distributions of irrigation canals have been selected, which were mentioned in 5.4.9.3. This distribution is related to the diversion points that exist within the LDRB, specifically located at the Diguillín river, allowing the flux of surface water to be supplied into different canals depending on their location. Based on the distribution of existing canals (Figure 5-20), 3 predictive scenarios are designed to evaluate how recharge efficiency varies: total activation of irrigation canals, activation of the eastern canals and activation of the western canals. What defines whether a canal is located to the east or to the west is the Diguillín-Coltón Matrix Canal, which crosses the basin very close to the centre. This matrix canal is not considered in the evaluation because it is lined with an impervious material.

Table 7-1 describes all 20 scenarios constructed to evaluate the aquifer response and compare it to the base case. These scenarios were designed considering the two influencing factors mentioned above (activation time and spatial distribution of activated irrigation canals).

Table 7-1 Description of each computed scenarios.

Scenario	Description
BC	Canals W & E activated from Oct - Mar
Sc1	Canals W & E activated from Oct - Apr
Sc2	Canals W & E activated from Oct - May
Sc3	Canals W & E activated from Oct - Jun
Sc4	Canals W & E activated from Oct - Jul
Sc5	Canals W & E activated from Oct - Aug
Sc6	Canals W & E activated from Oct - Sep
Sc7	Canals W activated from Oct - Mar
Sc8	Canals W activated from Oct - Apr
Sc9	Canals W activated from Oct - May
Sc10	Canals W activated from Oct - Jun
Sc11	Canals W activated from Oct - Jul
Sc12	Canals W activated from Oct - Aug
Sc13	Canals W activated from Oct - Sep
Sc14	Canals E activated from Oct - Mar
Sc15	Canals E activated from Oct - Apr
Sc16	Canals E activated from Oct - May
Sc17	Canals E activated from Oct - Jun
Sc18	Canals E activated from Oct - Jul
Sc19	Canals E activated from Oct - Aug
Sc20	Canals E activated from Oct - Sep
Sc21	Canals W & E activated from Sept - Apr
Sc22	Canals W & E activated from Aug- May

7.3 Main outcomes from predictive scenarios

Based on the different combinations of activation time and irrigation canals distribution, the resulting water budgets were compared between each one of these scenarios and the base case to subsequently establish correlations and identify potential impacts on the aquifer. The main outcomes of this analysis are presented below.

7.3.1 Recharge amounts

Taking the overall numbers into account, the amount of water injected to the aquifer through irrigation canals for each predictive scenario was compared to the stablished baseline. Figure 7-1 compares the volume of water induced by MAR entering the shallow aquifer system for each scenario. From this it is noted that there is a clear increase in the amount of water recharged as the periods of canals activation are prolonged. Also, the graph differentiates between scenarios that include the entire distribution of canals (in shades of red and purple), only those in the west (blue tones) and those that include only the eastern canals activated (yellow tones).

From the latter, there is also a directly proportional relationship between the distribution of canals and the amount of water infiltrating the aquifer. As the surface area with activated canals is wider, the recharged volume is also higher.

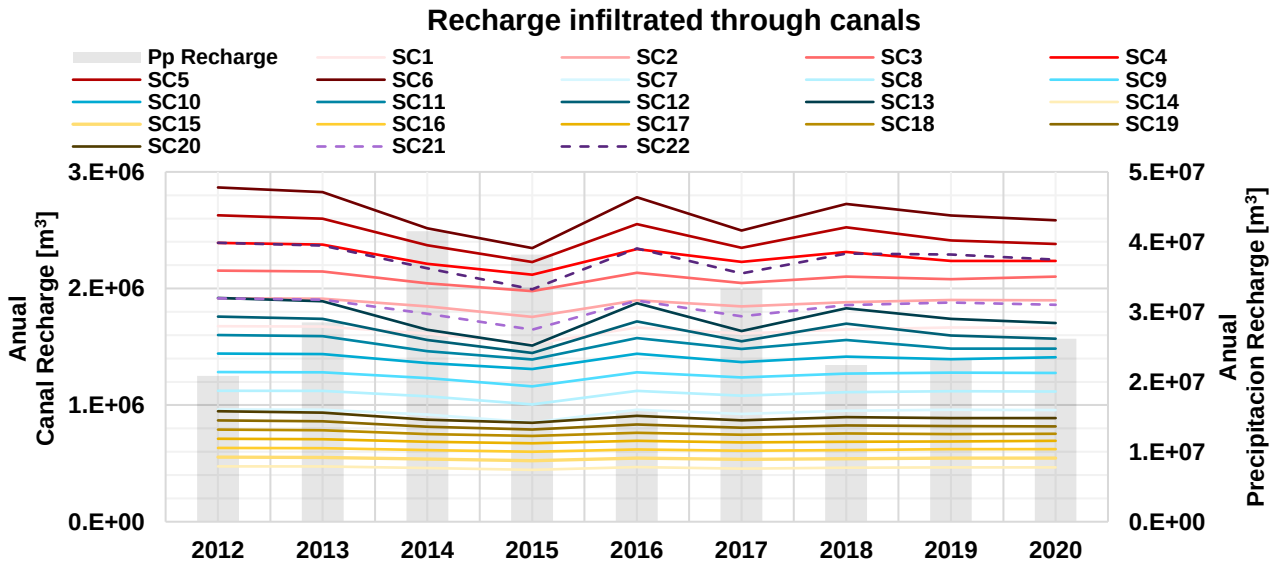

Figure 7-1 Total amount of recharge infiltrated through irrigation canals.

It is important to note the difference between Sc2 and Sc21 and between Sc4 and Sc22 scenarios, where the first two have 8 consecutive months of activation and the other two have 10, with the entire distribution of active canals for the four scenarios. The difference between the two pairs of scenarios is that Sc2 and Sc4 had months of activation added immediately after the canals are closed in the base case, i.e., from April onwards, while Sc21 and Sc22 had months of canals

activation added proportionally before the opening period and after the closing period according to the base case, i.e., from March onwards and from October backwards.

This detail in the canal activation setting is observed in Figure 7-1, where during years with less annual precipitation, the volume of recharge induced through canals is similar between Sc2 and Sc21 and between Sc4 and Sc22, but during years of higher annual precipitation (2014, 2015 and 2017), there is a slight increase in the total recharge volume induced by irrigation canals at scenarios that have a proportional activation distribution forward and backwards of the stated baseline closure and opening dates, respectively.

This is consistent with the variations observed in the base case water budget analysis for rainy and dry years, described in section 6.9.5 above. In this, it is stated that for rainy years, the observed initial amount of recharge through irrigation canals is lower because of excess direct recharge caused by precipitation during the winter. Given that Sc21 and Sc22 scenarios start canal recharge 1 and 2 months earlier than the base case scenario, their calculated total annual recharge is expected to be lower than the scenarios where only pre-winter activation months are added.

7.3.2 GW storage gain

When we look at the total storage volumes, there is no major impact generated by the different managed aquifer recharge design scenarios, i.e., the amount of water stored in the shallow aquifer is much higher than the volumes of water being introduced through irrigation canals. Even so, it is possible to observe some variations in terms of the distribution of active canals within the basin. For example, the scenarios that include only active eastern canals present a higher groundwater storage gain during most of the time compared to the rest, especially during the first years of evaluation (Figure 7-2).

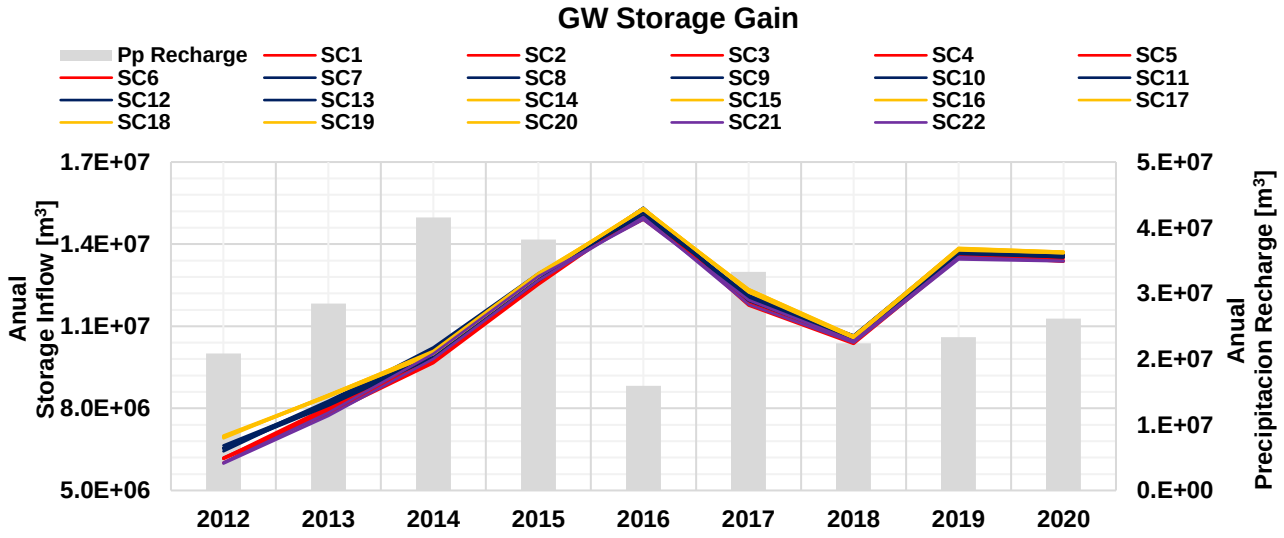

Figure 7-2 Total amount of groundwater storage gain per scenario.

On average, the percentage increase in storage evaluated for the entire modelling period between the predicted scenarios and the base case, lies between -1.0% and 3.9%, with a maximum annual variation of 10.8 % achieved with the Sc14 scenario. Consequently, the highest percentage increases in groundwater storage gain are obtained with scenarios where only eastern canals are active along the LDRB basin (Figure 7-5).

The following figures show graphically the groundwater storage gain increase achieved for all predictive scenarios compared to the baseline condition.

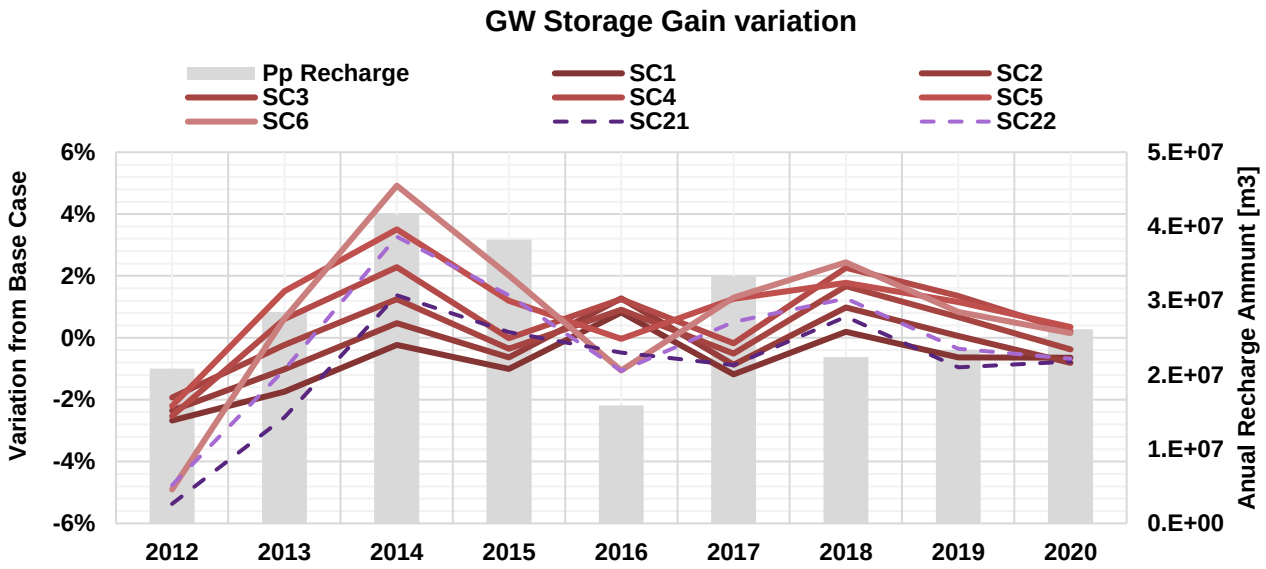

Figure 7-3 Groundwater storage gain variation (1).

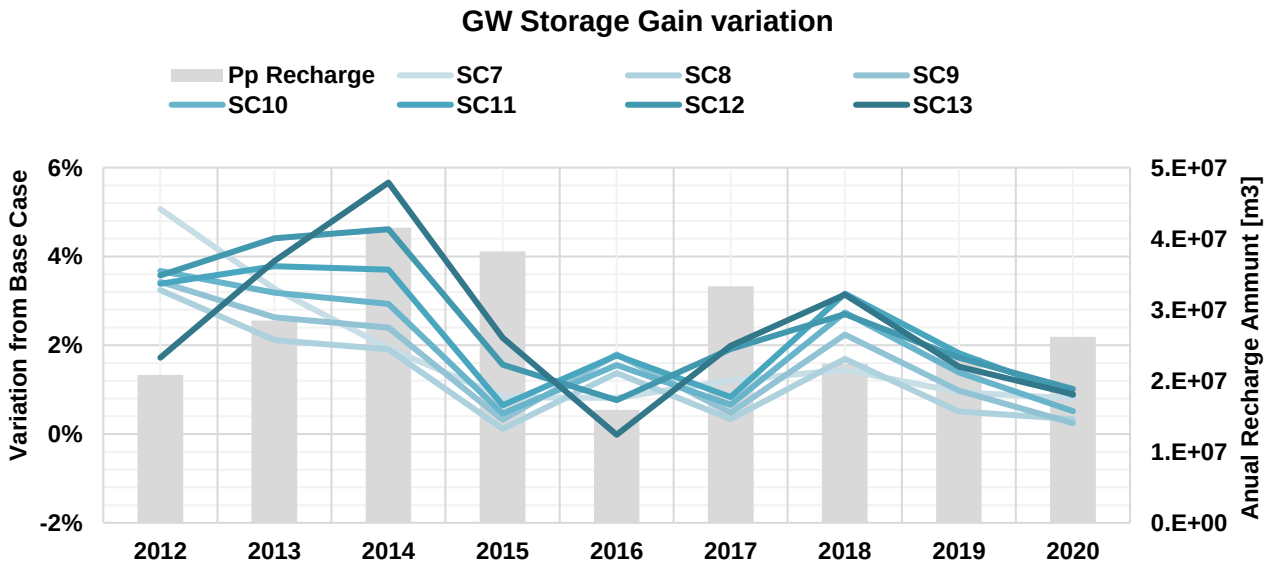

Figure 7-4 Groundwater storage gain variation (2).

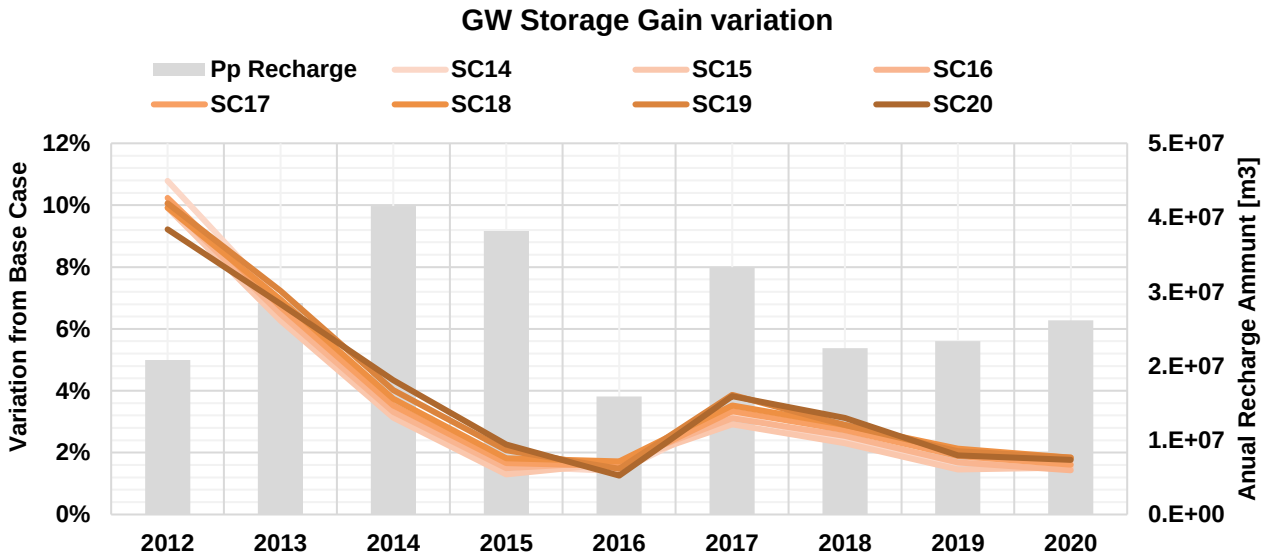

Figure 7-5 Groundwater storage gain variation (3).

7.3.3 GW discharge to surface water bodies

Groundwater discharges variations towards surface water bodies are negligible compared to the total discharge amounts computed with the base case. As with the storage gain analysis, if we visualize the total discharge amounts, variations from one scenario to another are not well appreciated because the orders of magnitude of these changes are much smaller than the total amount of outflows.

In addition, Figure 7-6 shows the difference between the discharge flows to the Itata River compared to the discharge flows to the lagoons. The latter are very low compared to the discharge to the river but show a similar upward behaviour during the first 4 years of simulation, and then decrease and stabilize until 2020.

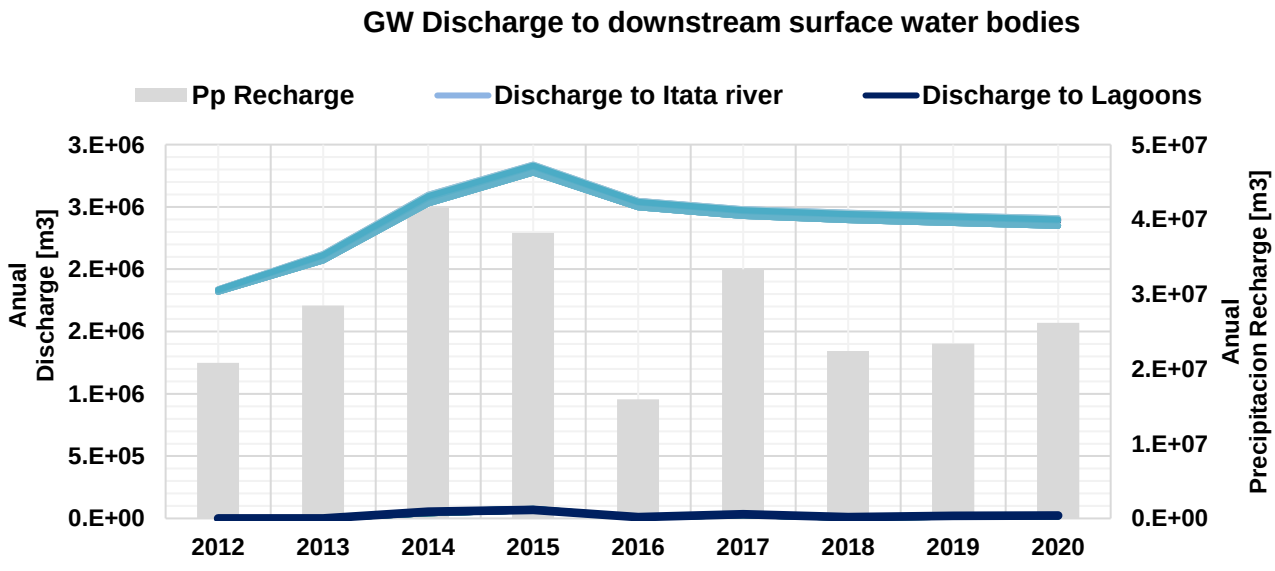

Figure 7-6 Groundwater downstream discharge towards surface water bodies.

In detail, the average annual variations in discharge to the Itata River, considering all scenarios compared to the base case scenario, lies between -1.2% and 1.0%, while the range for variations in discharge towards the western lagoons lies between -16.0% and 8.5%.

The variation in discharge to the Itata River and to the lagoons in all predictive scenarios with respect to the baseline is shown below.

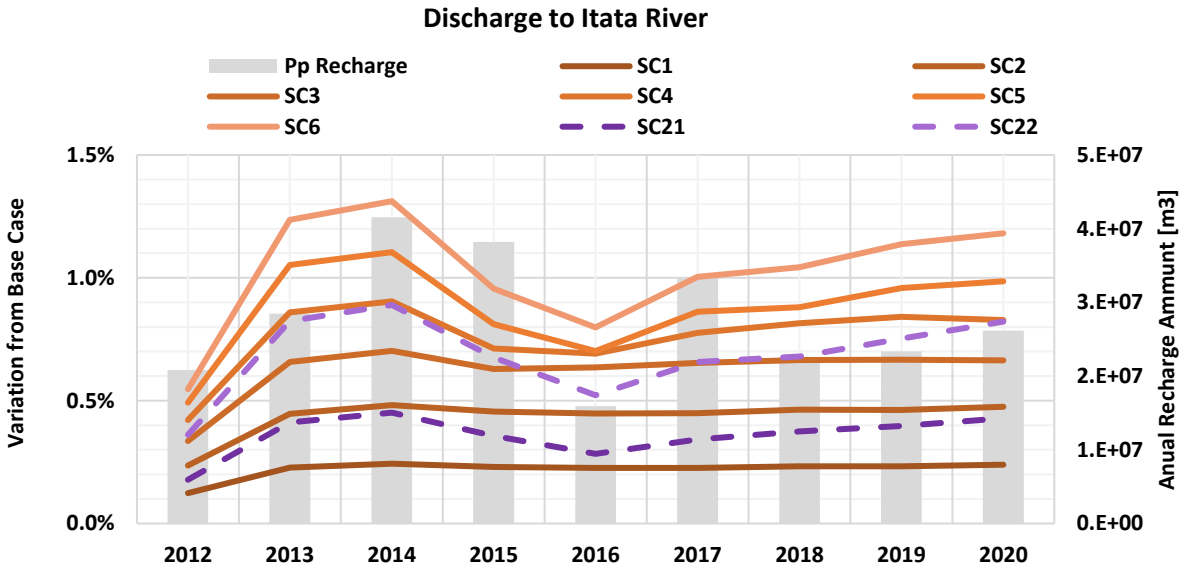

Figure 7-7 Groundwater discharge towards Itata river (1).

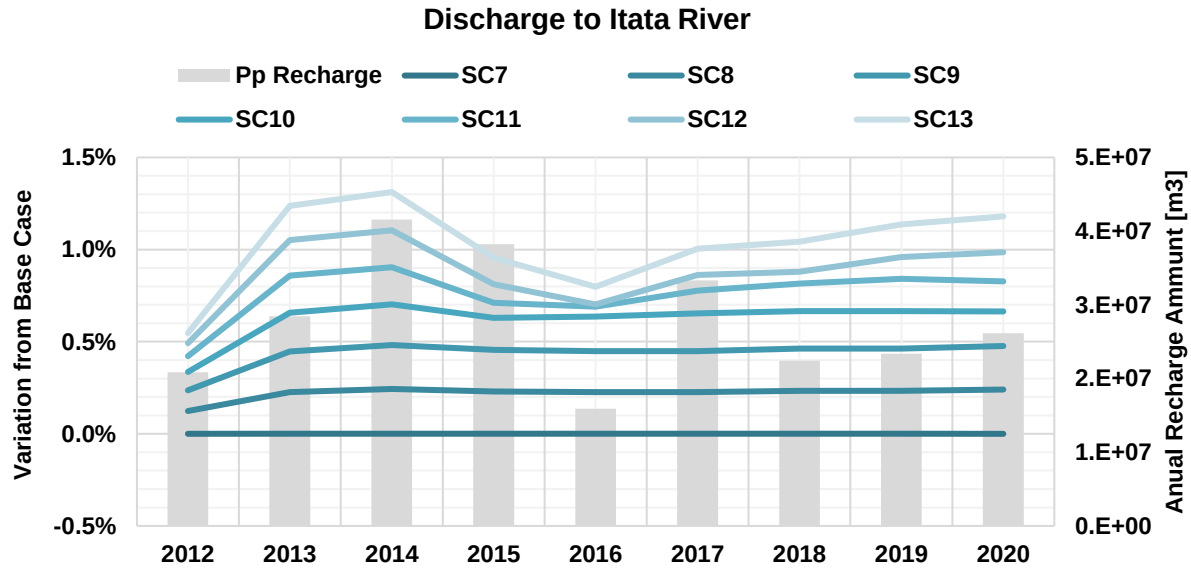

Figure 7-8 Groundwater discharge towards Itata river (2).

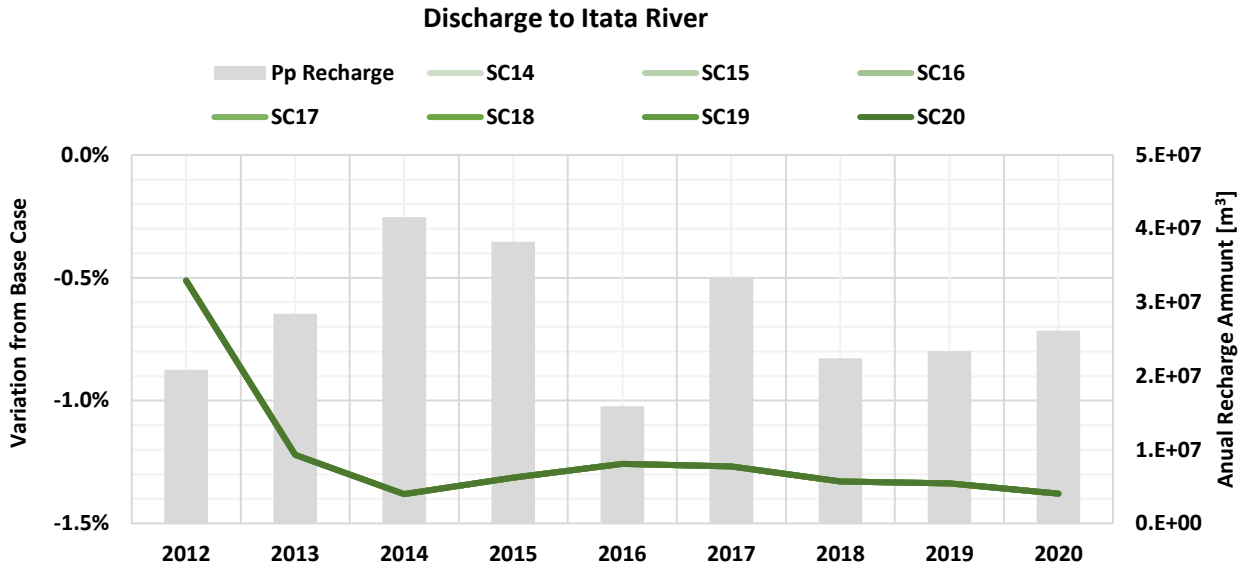

Figure 7-9 Groundwater discharge towards Itata river (3).

It should be noted that the percentages of variation are much higher when we evaluate the discharge to the lagoons because the discharge flow of the base case is low, therefore, a small variation in the inflow or outflow of the system generates disturbance to these values. Even so, the high percentages of variability in discharges towards the lagoons are related to the fact that they are located directly downstream of the irrigation canals in the western sector, before the groundwater flow meets the Itata River.

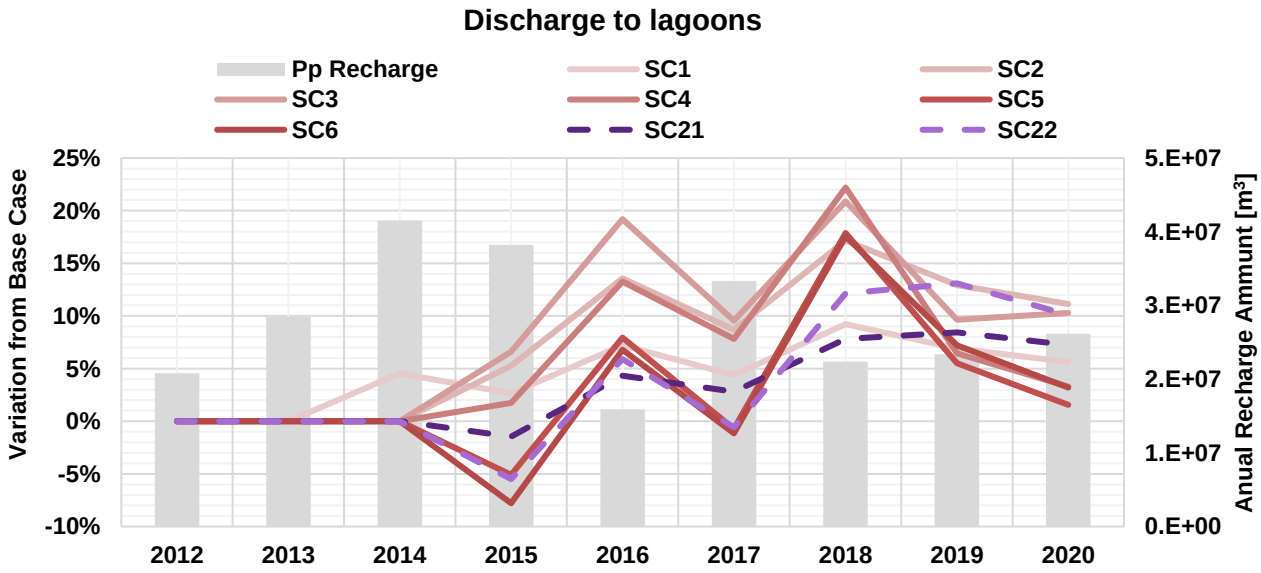

Figure 7-10 Groundwater discharge towards small lagoons (1).

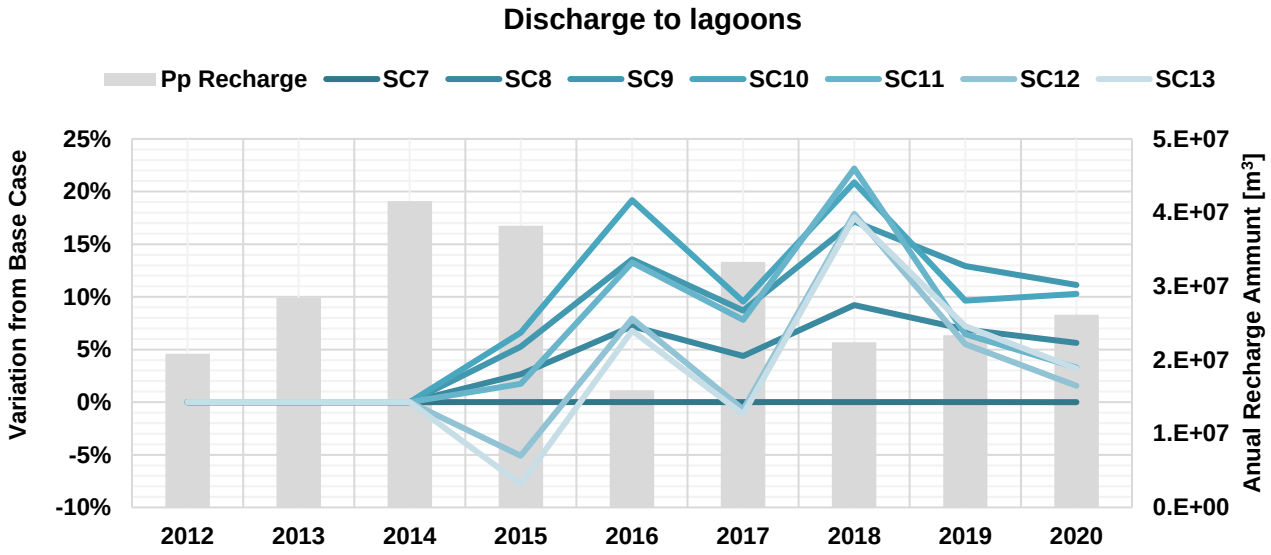

Figure 7-11 Groundwater discharge towards small lagoons (2).

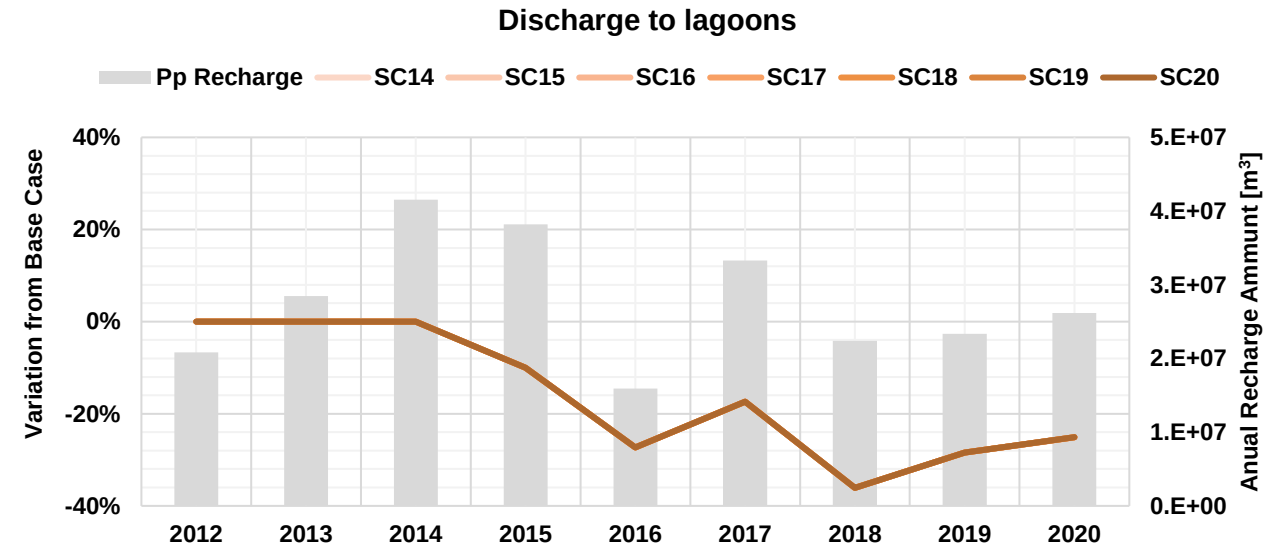

Figure 7-12 Groundwater discharge towards small lagoons (3).

7.3.4 Depth to water table

Once the predictive models were run, the simulated depths to groundwater for January and September 2020 were compared to the base case results. The range of minimum and maximum variations obtained for all model cells in January lies between -1.0 m to 1.3 m, while in September it lies between -1.3 m and 3.0 m. It is important to remember that we are talking about depths, therefore, a negative value corresponds to a rise in level.

The scenarios with the highest water level rise are Sc5, Sc6, Sc19 and Sc20, while those with the highest water level deepening are Sc6, Sc20 and Sc22. It is understandable that the scenarios that present the highest-level rises may also present the highest-level deepening, since the system

must be balanced in some way, and the recharge that is being added to the system is focused only on the irrigation canals area.

Considering the mentioned critical scenarios, the following paragraphs analyse the potential areas where crops could be damaged as a result of rising levels into the rootzone or eventual groundwater outcrops at specific agricultural sites or urban areas. In this case,

The scenarios identified as the most critical were those shown in Figure 7-13, where for the months of January only the scenarios with canal activation limited to the east are affected, while for September simulations, all the shown scenarios present potential critical zones where the level increases up to 3 meters above the base case.

The zone with the greatest increase in water level is located to the east, in the centre of the basin, which can be directly attributed to the recharge induced by canals of the east sector. Increases are also observed in the site of western irrigation canals and downstream. In this, there are smaller but widely distributed increases, reaching level increments of up to 1 meter.

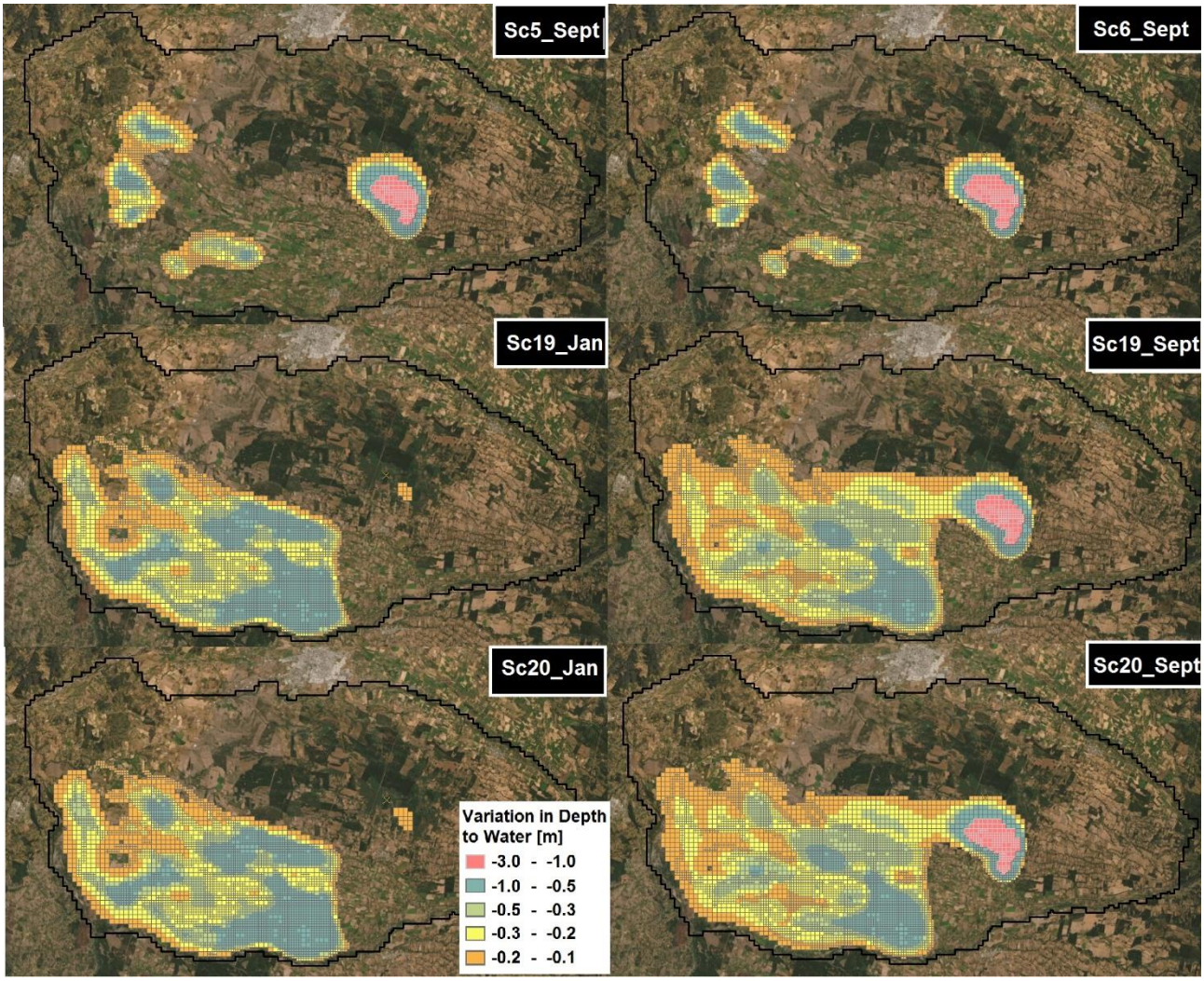

Figure 7-13 Variation of depth to water table in critical scenarios.

7.3.5 Recharge efficiency

In general, the objective of implementing managed aquifer recharge in any location is to find the best design that allows maximizing groundwater storage and minimizing groundwater losses towards surface water bodies located downstream of the MAR site.

Another way to assess whether one method is better than another, or whether one type of design is more effective than others, is by maximizing groundwater storage and minimizing the total amount of recharge injected into the aquifer. On the other hand, it is also possible to define the efficiency through the times it takes for the induced recharge to become effective. In short, there are many methodologies that allow evaluating and comparing MAR efficiencies.

In this section, efficiency is evaluated using two statistics that allow comparing the results between the predictive scenarios and the conditions established as the base case. The first considers the definition of maximizing storage over minimizing downward outflows. This statistic is a simple ratio between the flows that enter the groundwater storage of the shallow aquifer, over the flows that are discharged towards the Itata River and towards the small lagoons, both located downstream of the irrigation canals site.

Table 7-2 MAR efficiency statistics for predictive scenarios.

Scenario	GW storage gain / discharges	GW Storage gain / recharge
SC1	4.654	6.8
SC2	4.665	6.0
SC3	4.675	5.4
SC4	4.691	5.0
SC6	4.699	4.3
SC5	4.685	4.6
SC8	4.764	10.4
SC9	4.735	9.0
SC7	4.739	12.1
SC10	4.742	8.2
SC11	4.751	7.6
SC12	4.755	7.0
SC13	4.744	6.5
SC14	4.896	**24.9**
SC15	4.886	21.3
SC16	4.893	18.7
SC17	4.900	16.7
SC18	4.907	15.2
SC19	**4.911**	14.0
SC20	4.908	12.9
SC21	4.643	6.1
SC22	4.661	5.0

As a result, we have that the scenarios with the best efficiency statistics are those that only have active canals in the eastern area of the LDRB. Specifically, the most efficient scenarios according to these results would be the Sc14 and Sc19 scenarios. On the other hand, the scenarios with the worst efficiency statistics would be, in general, those that keep all canals active for the MAR operation.

Considering the results of the simulated scenarios that present the highest recharge efficiencies, the maximum annual volume of water recharged through irrigation canals would lie between $5x10^5$ m^3 and $9x10^5$ m^3, representing between 2.5% and 11.2% of the total annual inflows for the same period.

8 DISCUSSION

8.1 Conceptualization uncertainty

The hydrogeological conceptualization of an aquifer system is one of the most influential stages in the development of a hydrogeological model due to the high degree of uncertainty that it can hold (Gupta et al., 2012) if there is not enough information about the aquifer system or if it has a high degree of complexity and heterogeneity.

It is vitally important to have a good understanding of the hydrogeological system from the outset if the idea is to design a predictive groundwater flow model capable of accurately reproduce the natural conditions of a specific basin.

In this case, the conceptualization stage included at first a literature review of a series of reports that present a high content of information that could be rescued, however, most of these documents and the information included in them describes a hydrogeological system in a more regional way or, also, in a local detail but in surrounding sites rather than in the current study area.

From this, the degree of uncertainty contained in some variables is quite high, while others have been estimated in a convincing and precise manner to reduce their level of uncertainty. Among the variables for which little or no information is available is the base of the unconfined shallow aquifer, which is of crucial importance due to the scope of this study. Since there is not enough information to define the lower boundaries of the shallow aquifer, some assumptions were made based on background information that allow at least defining the depth at which this is located. This factor may be influencing the groundwater flow depending on how it has been defined.

Another fundamental aspect in the elaboration of this conceptual model is the behaviour of the local rivers. Since the basin is limited by a series of non-minor rivers, it is advisable to have a high degree of knowledge regarding the seasonal stage variations of these rivers, their morphology, and the hydraulic characteristics of the river bottom. Only some of these parameters actually present robust estimates, while others possess a high degree of uncertainty.

Finally, after specifying and indicating that this model indeed has a high level of uncertainty in some fundamental aspects, it is important to detail that the final hydrogeological conceptualization was carried out through the consensus model approach, where a single representation of the system's behaviour is established based on collected information and personal knowledge, but during the process of designing and construction of the numerical model through Flopy, a series of adjustments and conditions were adapted as the groundwater system of the site was better understood. These slight variations in the initial conceptual model could be considered as a kind of

multi-model approach (Enemark et al., 2019) without evaluating the uncertainty that this approach implies but making the related observations of the outcomes visually.

8.2 Model limitations

Since this model is built with a relatively low level of confidence, it has limitations with respect to its potential use for real life assessment and applications. Here we present the main limitations found, which are directly related to the use of the numerical model in managing aquifer recharge through irrigation canals.

The constructed model does not simulate the flow conditions in unsaturated porous media, there is a bias related to the movement of the flow from the moment the canals are activated, and surface water starts to infiltrate the soil, until it reaches the saturated zone. This time can vary depending on how deep the unconfined aquifer is, but if it is deep enough, the effect of not simulating the unsaturated zone will induce on a greater impact. The problem related to this has direct connexion with the speed at which the recharge technique is being performed and therefore its efficiency.

The model does not allow limiting the recharge volumes in a direct way or establishing diversion points to connect different canals so that groundwater flows can be simulated together with surface flows. By simulating both flows equally, the availability of water to apply managed aquifer recharge is included, thus establishing a more realistic version of the technique, allowing a more detailed evaluation of the most appropriate periods that maximize the efficiency of the MAR practice.

Despite the limitations encountered, the model allows us to quantify and evaluate the feasibility of implementing various designs of managed aquifer recharge through unlined irrigation canals.

8.3 Calibration and sensitivity analysis

To assess the uncertainties related to the model input parameters, a sensitivity analysis was performed on some of these that were previously identified as critical parameters during the steady state calibration process. By carrying out a sensitivity analysis, we can quantify the impact generated on the model outcomes by varying selected input parameters on a one-by-one basis and analyse how much does the predictive error varies, allowing to identify which of these parameters are the drivers of the system.

This analysis was performed manually, evaluating the parameters that have the greatest influence on the result of the numerical model. Specifically, this process was carried out to define the horizontal hydraulic conductivity values that allow the best-fit for the model, resulting in the model being highly sensitive to the settings of this parameter in the system.

Other secondary parameters that were sensitized during the construction stage were specific yield and storage capacity of each hydrogeological unit and defined homogeneous zones, but also, some specific parameters related to different modelling packages.

Regarding the calibration carried out in steady state, it was evaluated using a series of statistics that allow calculating how accurate the model is. These statistics, or so-called error metrics, are generally used automatically, without any questioning or reasoning, however, there are several criteria that should be considered when we want to calibrate a hydrogeological model and characterize their skill (Jackson et al. 2019), for example, the specific use to which the groundwater flow model will be designed for, the flow regime over which the error metric is being applied, and also the way the historical data is distributed.

8.4 Predictive MAR outcomes

According to Table 7-2 there is a great similarity in the efficiency results obtained with the coefficient that includes the downstream discharge. This is consistent with what was mentioned above, where it is highlighted that the total discharge volume of the system is several orders of magnitude greater than the recharge injected by MAR. Even so, it is possible to observe small variations from one scenario to another.

In general, a rising water table is always welcomed and well received when there are over exploited sites, but it could happen that the change in water table reaches the root zone and cause severe crop damage in the area. One way to overcome this dilemma is to first identify the areas where there is indeed a simulated water level increase that becomes detrimental, and then to evaluate the conditions that cause this to happen to subsequently design a recharge plan that does not substantially affect the different stakeholders within the basin. Al this was performed in this study in a simplified manner, identifying those sectors most likely to damage crops because of aquifer recharge.

The results obtained through the numerical modelling of predictive scenarios indicate that the efficiency of managed aquifer recharge through the irrigation canals of the LDRB is highly influenced by climate conditions and hydraulic parameters imposed to the system. In this regard, the analysis of the scenarios shows that precipitation recharge is the variable that most affects the outcome efficiency of the MAR practice. Since groundwater levels are highly sensitive to extreme precipitation event, when this happens, there is less storage capacity available for gaining water within the shallow aquifer.

On the other hand, the distribution of irrigation canals also represents a variable of interest when designing a MAR mechanism, due to the large number of canals registered at the LDRB. The best combination of canal distribution along the basin, based on the outcomes of the modelling runs, is

achieved by activating only those located to the east of the Diguillín-Coltón Matrix Canal. With this, it is possible to increase the gaining in groundwater storage for the upper aquifer and also decline the losses of the system towards downstream water bodies.

The methodology used to estimate the maximum feasible volume of water to be recharged through irrigation canals is based on previously defined recharge efficiency factors. Using both factors it is possible to compare different MAR designs, and finally determine which of all minimizes losses and maximizes profits with the least amount of recharge added to the system. In this case, the estimated maximum annual volume for efficient recharge is around 10 m^6, as long as the external conditions exist to be able to execute this in reality, that is, if there is sufficient availability of surface water to distribute through the activated canals of the eastern sector and that those canals maintain the estimated hydraulic behaviour entered into this numerical model.

9 CONCLUSIONS AND RECOMMENDATIONS

This study presents the evaluation of different designs of Managed Aquifer Recharge (MAR) through unlined irrigation canals, to identify whether or not it is feasible to implement this technique in the Lower Diguillín River Basin (LDRB) and define the most efficient design to conduct the MAR practice.

First, a numerical hydrogeological model was built to simulate the different predictive scenarios of MAR and evaluate the benefits and consequences generated on the basin in the short term. Once the numerical model was built and went through a calibration process, it was established as capable to adequately simulate the potentiometric levels historically observed and, in turn, to predict different variations induced by implementing a MAR technique at the LDRB.

Among the main results, it was found that the amount of recharge injected through irrigation canals is notoriously lower than the total recharge of the system; therefore, the impacts generated in the shallow aquifer are rather local and limited to the canals surrounding area or downstream, and do not generate disturbances in more distant sites along the basin.

There is a lower recharge rate through canals when they are activated during post-winter months following extreme rainfall events. In contrast, the highest canal recharge volumes are achieved during summer months, when the water level is still low.

Longer recharge periods implies higher amounts of recharge inflows, however, they also generate greater discharges to surface water bodies.

Greater aquifer storage gain is achieved while only the eastern canals at the LDRB are active and, the largest volumes of discharge to surface water bodies occur towards the Itata River rather than to lagoons.

The water level can rise up to 3 meters during MAR's operation, with the greatest variations in water level occurring during the winter months. The sectors most prone to water level rise are those located directly downstream of the canals and to the north of the eastern canals.

The highest recharge efficiency is observed in scenarios including only the eastern active canals. In these, there is a greater gain in storage over time and, in addition, losses to downstream surface water bodies are lower. From this, the estimated maximum annual recharge volume for efficient recharge is in the order of 10^6 m3.

Considering the above and the results reflected in this thesis, it is verified that the implementation of a managed aquifer recharge (MAR) through irrigation canals in the LDRB basin is feasible, as long as there is complete control over the distribution and opening time of these canals, as well as continuous monitoring of the shallow aquifer in the surrounding areas.

Finally, I strongly recommend that studies of this type continue to be carried out in order to keep searching for highly sustainable solutions focused on the management of water resources.

10 BIBLIOGRAPHY

Allen, R. G., Pereira, L. S., Raes, D., & Smith, M., 1998. Crop evapotranspiration-Guidelines for computing crop water requirements-FAO Irrigation and drainage paper 56. Fao, Rome, 300(9), D05109.

Alves, M. E. B., Mantovani, E. C., Sediyama, G. C., & Neves, J. C. L., 2013. Estimate of the crop coefficient for Eucalyptus cultivated under irrigation during initial growth. Cerne, 19, 247-253.

Arumí, J., 2014. Caracterización de dos grupos de manantiales en el río Diguillín, Chile. Tecnología y ciencias del agua /, 5(6), p.151.

Bakker, M et al., 2016. Scripting MODFLOW Model Development Using Python and FloPy. Ground water, 54(5), pp.733–739.

Barnett, T P, Adam, J C & Lettenmaier, D P, 2005. Potential impacts of a warming climate on water availability in snow-dominated regions. Nature., 438(7066), pp.303–309.

Boisier, Juan P et al., 2016. Anthropogenic and natural contributions to the Southeast Pacific precipitation decline and recent megadrought in central Chile. Geophysical research letters, 43(1), pp.413–421.

Bonilla Valverde, José P et al., 2018. Inventory of managed aquifer recharge schemes in Latin America and the Caribbean. Sustainable water resources management., 4(2), pp.163–178.

DGA (Dirección General de Aguas), 2016. DGA Atlas del Agua, in: Atlas Del Agua Chile 2016 Chile (2016), p. 141.

Dillon, P., 2005. Future management of aquifer recharge. Hydrogeology journal., 13(1), pp.313–316.

Dillon, Peter et al., 2020. Managed Aquifer Recharge for Water Resilience. Water., 12(7), p.1846.

Donoso, G., 2006. Water markets: case study of Chile's 1981 Water Code. Cien. Inv. Agr. 33 (2): 157-171. International Journal of Agriculture and Natural Resources, 33(2), 131-146.

Enemark, T., Peeters, L., Mallants, D., & Batelaan, O., 2019. Hydrogeological conceptual model building and testing: A review. Journal of Hydrology (Amsterdam), 569, 310-329.

Gajardo, A., 1981. Hoja de Concepción-Chillan, Región del Bío-Bío. Instituto de Investigaciones Geológicas, Mapas Geológicos Preliminares 4: 32 p., escala 1:250.000.

Garreaud, René D et al., 2017. The 2010–2015 megadrought in central Chile: impacts on regional hydroclimate and vegetation. Hydrology and earth system sciences., 21(12), pp.6307–6327.

Garreaud, René D et al., 2020. The Central Chile Mega Drought (2010–2018): A climate dynamics perspective. International journal of climatology., 40(1), pp.421–439.

Gupta, H., Clark, M., Vrugt, J., Abramowitz, G., & Ye, M., 2012. Towards a comprehensive assessment of model structural adequacy. Water Resources Research, 48(8), Np-N/a.

Harbaugh, A. 2005. MODFLOW-2005, the U.S. Geological Survey Modular Ground-Water Model—The Ground-Water Flow Process. U.S. Geological Survey Techniques and Methods, Book 6, Chapter A16, variously paged. Reston, Virginia: USGS.

Hervé, M., 1977. Geología del área de Liquiñe, Provincia de Valdivia, Xa. Región, Chile. Memoria de Título (Inédito), Universidad de Chile, Departamento de Geología.

Howden, S.M. et al., 2007. Adapting agriculture to climate change. Proceedings of the National Academy of Sciences of the United States of America., 104(50), pp.19691–19696.

Jackson, E. K., Roberts, W., Nelsen, B., Williams, G. P., Nelson, E. J., & Ames, D. P., 2019. Introductory overview: Error metrics for hydrologic modelling–A review of common practices and an open-source library to facilitate use and adoption. Environmental modelling & software, 119, 32-48.

Markovich, K.H., Manning, A.H., Condon, L.E., McIntosh, J.C., 2019. Mountain-block recharge: a review of current understanding. Water Resour. Res. 55. https://doi.org/ 10.1029/2019WR025676.

Muñoz, Enrique et al., 2016. Unraveling complex hydrogeological processes in Andean basins in south-central Chile: An integrated assessment to understand hydrological dissimilarity. Hydrological processes., 30(26), pp.4934–4943.

ODEPA/INE, 2019. Estadísticas productivas agrícolas. Cultivos anuales históricos. Available in https://www.odepa.gob.cl/estadisticas-del-sector/estadisticasproductivas. Oficina de Estudios y Políticas Agrarias (ODEPA)/Instituto Nacional de Estadísticas (INE), Santiago, Chile.

Page, Declan et al., 2020. Progress in the development of risk-based guidelines to support managed aquifer recharge for agriculture in Chile. Water Cycle, 1, pp.136–145.

Pfeiffer, Lisa & Lin, C-Y Cynthia, 2014. Does efficient irrigation technology lead to reduced groundwater extraction? Empirical evidence. Journal of environmental economics and management., 67(2), pp.189–208.

Prudhomme, C. et al., Hydrological droughts in the 21st century, hotspots, and uncertainties from a global multimodel ensemble experiment. Proceedings of the National Academy of Sciences of the United States of America., 111(9), pp.3262–3267.

Sprenger, C et al., 2017. Inventory of managed aquifer recharge sites in Europe: historical development, current situation and perspectives. Hydrogeology journal, 25(6), pp.1909–1922.

Vicuña, Sebastian, Garreaud, René D & McPhee, James, 2011. Climate change impacts on the hydrology of a snowmelt driven basin in semiarid Chile. Climatic change, 105(3), pp.469–488.

Zúñiga, René Muñoz, Enrique & Arumí, José Luis, 2012. Estudio de los procesos hidrológicos de la cuenca del Río Diguillín. Obras y proyectos., (11), pp.69–78.